

Can solar PV reliably reduce loading on distribution networks?

Jeremy F Keen¹ and Jay Apt^{1,2}

¹ Department of Engineering and Public Policy, Carnegie Mellon University, Pittsburgh, PA 15213, USA

² Tepper School of Business, Carnegie Mellon University, Pittsburgh, PA 15213, USA

E-mail: jkeen@andrew.cmu.edu

Keywords: value of solar, distribution network, effective load carrying capability, energy storage, transformer aging, capacity deferral

Supplementary material for this article is available online.

Abstract

Utility managers and solar photovoltaic (PV) advocates often disagree about whether rooftop solar can reliably reduce loading on distribution network feeders. We examined 23 prototypical feeders for 6 locations in the United States and two real feeders in eastern Pennsylvania. Using 19 years of weather data, we simulated 30 minute resolution substation loading and solar output for hypothetical solar penetrations. A positive correlation between peak loading and solar generation improves the effective capacity of solar (i.e. the net load reduction relative to solar system AC capacity). In our quantitative analysis, the effective PV capacity under worst-case loading conditions was above 40% at low penetrations for 19 of the 23 feeders examined. For all feeders, the effective capacity of solar decreases with penetration. Utility engineers often use statistical weather normalization and transformer aging criteria to plan for capacity, both of which allow a small amount of overloading risk. When these planning criteria are used with solar and transformer aging is fixed at pre-solar levels, we find that the effective capacity of solar is consistently higher than found under worst-case loading conditions. Alternatively, relatively small amounts of energy storage used with solar can achieve high effective capacities without any overloading events. We found that pairing solar PV with a one hour duration battery rated at 5% of the feeder peak loads could achieve an effective capacity of 50% or more for all feeders when the peak load penetration of solar is at or below 20%.

Introduction

Rooftop solar capacity has been growing rapidly in the United States, leading policymakers to reevaluate net energy metering (NEM) and other regulatory policies. Many states have studied Value of Solar (VOS) tariffs as an alternative to NEM (Rocky Mountain Institute, 2013). VOS studies are avoided cost studies for solar. Typical avoided cost categories are energy, transmission capacity, generation capacity, and environmental damages. Despite solar often being located on distribution networks, the value of solar on distribution networks has been treated with less rigor than transmission and generation value of solar components or omitted altogether. The Rocky Mountain Institute (RMI) describes the distribution value of solar as a “significant methodological gap” due to the inherent complexity and heterogeneity of distribution networks (2013). In a review of VOS methods for the National Renewable Energy Lab (NREL), Denholm *et al* write “Further research is required to develop and validate such ELCC [Transmission Effective Load Carrying Capability]-like approaches to distribution capacity value. Until

such calculation approaches are validated, utilities may be reluctant to reduce feeder capacity with solar PV because of concerns about high loads during periods of low solar output” (2014).

In this chapter, we focus on characterizing a fundamental metric for estimating the capacity value of solar on distribution networks. To be consistent with power systems standards, we call this metric the Distribution Effective Load Carrying Capability (D-ELCC), which we define generally as the net load reduction relative to solar PV AC capacity. The D-ELCC values in this chapter can be used by policy makers to understand how solar might reduce large capital investments on distribution networks and produce value for all ratepayers. ELCC estimates for the bulk electric grid may differ from the D-ELCC because:

1. **Distribution feeders may be more vulnerable to variability in loading and solar generation.** The small geographic footprint of distribution feeders means that solar will not benefit much from geographic smoothing of the effects of intermittent cloud cover.
2. **The risk of overloading is managed differently on distribution feeders than on the bulk power grid.** While both sectors of the electric grid are risk averse, the bulk power grid manages risk through a combination of planning (e.g. a 1-in-10 year loss of load expectation) and operational (e.g. demand response, spinning reserve, under frequency load shedding) standards. On distribution feeders, engineers may be highly risk-averse and plan for capacity based on worst-case scenarios. Or, depending on the feeder and utility, engineers may allow some risk of overloads. Transformers, for example, are designed to operate above their nameplate capacity for short durations.

We next review analogous Effective Load Carrying Capability (ELCC) studies for the bulk power grid and D-ELCC estimates in consultant reports since there appears to be no peer-reviewed literature.

Comparison with Previous Research

Perez *et al* estimated the ELCC of solar for 39 utilities and all states excluding Alaska using 2 years of hourly weather and loading data. They found ELCCs on the transmission network from 11%-60% at low PV penetrations and 4-40% at a 20% penetration for fixed axis solar installations with a 30° tilt (Perez *et al* 2006). Furthermore, they found that ELCCs could be increased to 100% with small amounts of storage. They did not account for the contingency analysis typically included in ELCC studies, which ensure that the loss of load expectation (i.e. the risk of shedding load) remains constant under different grid constraints and generator failures (e.g. Denholm *et al* 2014, Madaeni *et al* 2013). We also exclude any form of contingency analysis from our estimates. We assume that the highly distributed nature of solar will make individual solar system failures and distribution line outages unimportant or that solar will be placed directly at substations.

The Peak Capacity Allocation Factor (PCAF) is another method used to estimate the effective capacity of solar on distribution networks. In the PCAF method, hours with load within one standard deviation of the maximum peak are estimated, and distributed energy resources are compensated if they generate energy during those hours. The PCAF method is described in many value of solar studies by the consulting firm E3 (Energy and Environmental Economics), such as for New York (E3 2016). The PCAF method is similar to the D-ELCC metric we describe in this chapter, and it could probably be adapted to include the utility planning practices that we use in our Method section to define the D-ELCC. Current implementations could equally benefit from more years of weather, solar, and loading data, which are a key part of our analysis. Overall, the PCAF method is useful for estimating the hourly capacity value of solar. The D-ELCC is better for visualizing the effect of varying solar penetrations on solar PV's capacity value.

Distribution network utilities have also published estimates of the effective capacity of solar. In their 2016 Preferred Resources Pilot Portfolio Design Report, Southern California Edison (2017) define a “dependable” output curve that is approximately 20% of nominal solar AC capacity at noon and rapidly declining for their commercial, residential, and system peak. Southern California Edison’s method appears to base this “dependable” output only on the performance of solar during a cloudy day. They do not appear to account for any possible relationship between peak load conditions and better solar performance.

EPRI (2017) performed a study on several distribution feeders in Spain and despite using a fairly high “probable” D-ELCC for solar (around 60% in the early afternoon) they found that late peaking feeders in the region made solar’s effective capacity negligible. A low D-ELCC for evening peaking feeders is an undeniable short-coming of solar. While most of our analysis is on prototypical feeders that tend to peak in the afternoon, we also estimate the D-ELCC for two real feeders from an eastern Pennsylvania utility that peak in the evening.

In the remainder of the chapter, we describe our method, results, and policy conclusions. We first describe our load, feeder, and solar modeling; these primarily use GridLab-D (PNNL 2018) and the NREL Physical Solar Model (PSM) dataset (NREL, 2018). Next, we define two D-ELCC metrics based on typical utility planning practices. Our first estimate, D-ELCC_{worst} is based on the worst-case loading associated with several solar penetrations and aims to prevent any overloading associated with solar. Our second estimate, D-ELCC_{age}, does allow overloading associated with solar but the aggregate deterioration of the transformer insulation condition (commonly referred to as transformer aging) cannot exceed the deterioration caused by weather normalization. Each method is based on 19 years of weather and loading data to reflect the long investment horizons faced by utility engineers. Overall, we find that a positive correlation between peak loading days and solar generation appears to improve solar’s D-ELCC_{worst}. It is typically above 40% at low penetrations but decreases with penetration. When small amounts of overloading are allowed, D-ELCC_{age} is consistently above 50%. Alternatively, small amounts of energy storage can be used to achieve a 50% D-ELCC if solar peak penetrations are at or below 20%.

Method

Feeder and Load Modeling

We use the U.S. Department of Energy’s Pacific Northwest National Laboratory (PNNL) feeder taxonomy (K. P. Schneider *et al* 2008) to capture some of the heterogeneity in US distribution networks. The PNNL feeder taxonomy is a set of 23 distribution network feeders selected through clustering for use as representative feeders for the United States. They are based on 575 real feeders from 17 separate investor owned, rural electric, and municipal utilities but with changes made by PNNL to remove proprietary information. A description of the feeder taxonomy is in Table 1.

To create time-varying loads, the feeder taxonomy was populated with temperature and humidity dependent building models and made available to the public by Fuller *et al* (2012). Residential buildings parameters were based on the Energy Information Administration’s (EIA) Residential Energy Consumption Survey (EIA 2018). Non-weather-dependent load profiles were based on the Bonneville Power Administration’s End-Use Load and Consumer Assessment Program (Prat *et al* 1989), and show the characteristic morning and evening peak typical for most residential customers. Commercial buildings were modeled using building codes and end-use metering studies (Fuller *et al* 2012). All commercial buildings are modeled as office buildings, big box stores, and strip malls.

We also used two PECO feeders. PECO is the electric and gas utility for the Philadelphia area, and uses CYMDIST, a popular distribution powerflow solver, with static spot loads that do not vary with time. We

converted the CYMDIST feeders to the GridLab-D format using the National Rural Electric Cooperative Association (NRECA)'s Open Modeling Framework (OMF) (NRECA 2018) and populated the spot loads with secondary systems and weather-dependent customer loads. Our objective was to ensure that both substation loading and simulated peak load hours were close to the values observed in SCADA readings.

We used a genetic algorithm to adjust residential and commercial building parameters so that the simulated feeder load time-series matched hourly SCADA readings. Our objective function minimized the difference between the simulated and SCADA load profiles from May-September 2016. The decision variables were the air conditioning coefficient of performance, insulation R values, cooling set points, floor areas, scaling factors for predefined temperature independent load profiles with constant power loads, the proportion of commercial buildings modeled as strip malls, office buildings, and big box stores, the percentage of residential homes with air conditioners, and the percentage of residential homes with hot water heaters. Further details of our genetic algorithm implementation can be found in the Supplementary Materials (Section 1).

Figure 1 compares our simulated load with SCADA loading in the year 2016 for both PECO feeders. Simulated loads and SCADA readings are close on Feeder #1. On Feeder #2, the simulated load underestimates the peak load, but the peak hour, which is important for estimating solar's effective capacity, is still close to the observed hour. Feeder #2 is an industrial feeder and the error is likely caused by exogenous effects, such as shifting factory production schedules. These exogenous effects are difficult to include in GridLab-D's weather-dependent models.

Table 1: Taxonomy Feeder Descriptions. Customer class types are abbreviated as R(Residential), C(Commercial), A(Agricultural), and I(Industrial). Agricultural and industrial time-series loads are modeled with residential and commercial load models. The PECO feeders are not shown. Feeder #1 and Feeder #2 have peak loads of 6MW and 17 MW, and peak hours at 5pm and 6pm, respectively.

Climate Region	Feeder ID	Peak	Development	Customer Class Type	Peak Hour
Temperate California	R1-12-1	7 MW	suburban/rural	96% R, 2% C, 2% A	1 pm
	R1-12-2	3 MW	suburban/rural	95% R, 5% C	4 pm
	R1-12-3	1 MW	urban	5% R, 95% C	3 pm
	R1-12-4	5 MW	suburban	95% R, 5% C	4 pm
	R1-25-1	2 MW	rural	22% R, 18% C, 56% A, 4% I	3 pm
Cold New York	R2-12-1	6 MW	urban	50% R, 49% C, 1% A	2 pm
	R2-12-2	6 MW	suburban	95% R, 5% C	12 pm
	R2-12-3	1 MW	suburban	91% R, 1% C, 8% A	12 pm
	R2-25-1	17 MW	suburban	72% R, 18% C, 10% A	2 pm
	R2-35-1	9 MW	rural	18% R, 1% C, 79% A	12 pm
Hot/Arid Arizona	R3-12-1	8 MW	urban	87% R, 13% C	4 pm
	R3-12-2	4 MW	urban	92% C, 8% I	4 pm
	R3-12-3	7 MW	suburban	93% R, 7% A	12 pm
Hot/Cold North Carolina	R4-12-1	6 MW	urban/rural	89% R, 11% C	12 pm
	R4-12-2	2 MW	suburban/urban	88% R, 12% C	12 pm
	R4-25-3	1 MW	rural	99% R, 1% C	12 pm
Hot/Humid Texas	R5-12-1	9 MW	suburban/urban	85% R, 15% C	2 pm
	R5-12-2	4 MW	suburban/urban	66% R, 34% C	2 pm

	R5-12-3	9 MW	rural	94% R, 6% C	2 pm
	R5-12-4	7 MW	suburban/urban	85% R, 15% C	2 pm
	R5-12-5	9 MW	suburban/urban	93% R, 7% C	2 pm
	R5-25-1	12 MW	suburban/urban	95% R, 5% C	2 pm
	R5-35-1	12 MW	suburban/urban	88% R, 12% C	2 pm

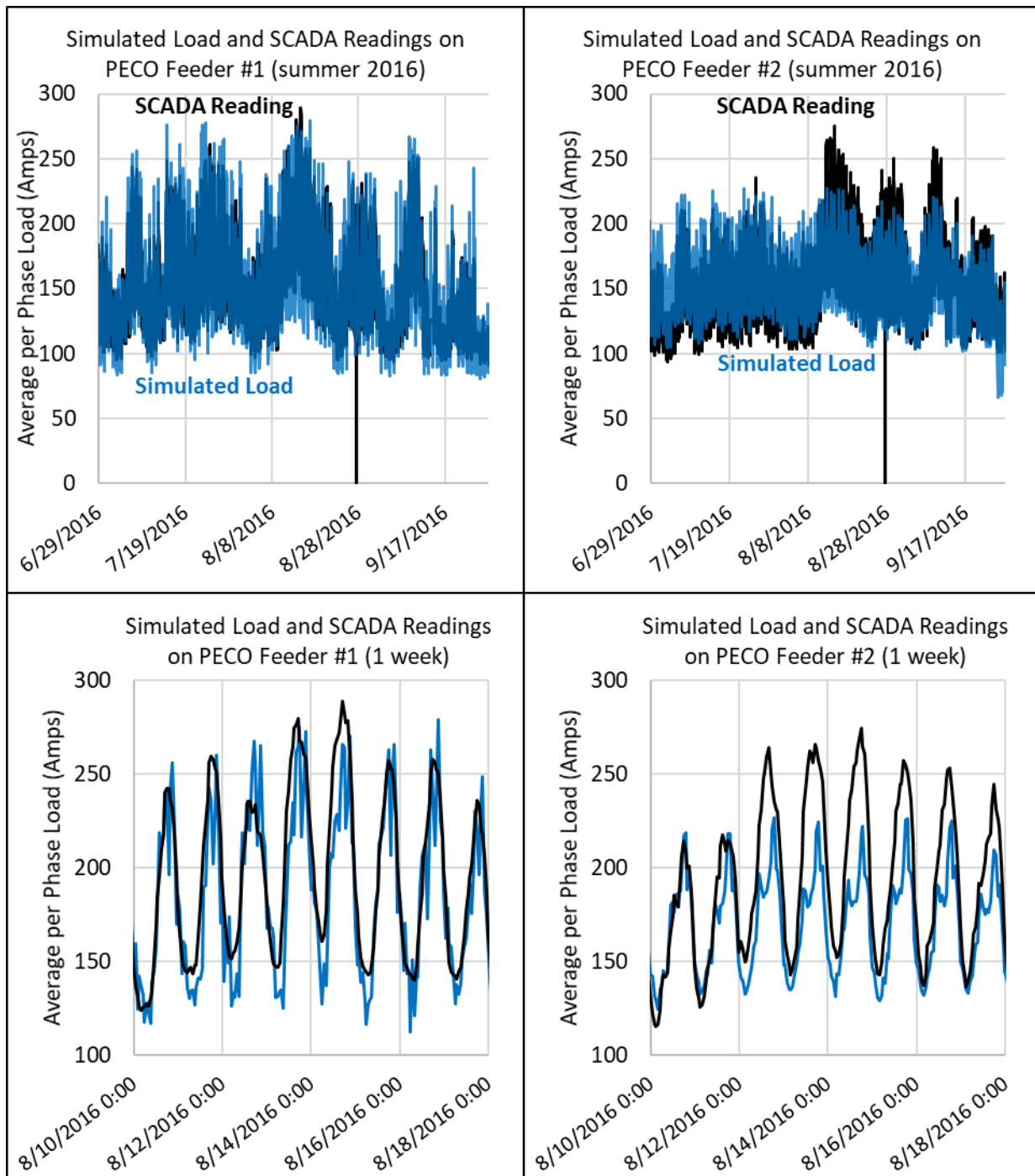


Figure 1: Comparison of SCADA substation loading from eastern utility and modeled loading using GridLab-D. GridLab-D building models were tuned to capture the weather dependence of the feeder load. The simulated peak hours closely matched SCADA readings. On Feeder #2, non-weather exogenous effects cause the simulated peak to underestimate several peaks.

Solar Modeling

We used solar radiation and weather data from NREL's National Solar Radiation Database, Physical Solar Model-Version 3 (PSM-V3) (NREL 2018). PSM-V3 estimates solar irradiance from satellite data from 1998-2016 with a geographic resolution of 4-km by 4-km and a 30-minute time resolution (Habte *et al* 2017). Compared to ground measurements, mean bias errors are approximately $\pm 5\%$ for GHI and $\pm 10\%$ for DNI. RMS errors are as high as 20% for GHI and 40% for DNI. Our results also include 1 year of data from Vibrant Clean Energy, which provides 5-minute resolution solar irradiance data (Vibrant Clean Energy 2018). Vibrant reports correlations with ground measurements of 93% for GHI and 82% for DNI. The Vibrant and PSM-V3 irradiance correlations range from 94-98% for each location studied.

Developing good solar radiation datasets is an area of active research, and comparisons between satellite models and ground-based measurements are imperfect. For example, several authors have found typical uncertainties of 3-5% even in well-maintained ground-based radiometers (Reda 2011, Myers *et al* 2001, Habte *et al* 2014).

Solar generation was modeled using GridLab-D's solar panel and inverter objects (PNNL 2018). GridLab-D uses the same solar modeling as NREL's System Advisory Model (SAM) (Tuffner *et al* 2012), a widely used engineering-economic tool (NREL 2018). For all solar panels and locations, we assumed a solar panel tilt of 30 degrees, a solar multiplier of 1.20, an inverter efficiency of 96%, a panel efficiency of 17% and a constant power factor of 1.0. A south facing panel orientation was used for all feeders. West facing panels were also used for the two evening peaking Pennsylvania feeders. Solar AC capacity factors were 18-20%.

Distribution-Effective Load Carrying Capability Definition

We define the Distribution-Effective Load Carrying Capability generally as the change in substation peak demand relative to the total solar system AC capacity. We report the average D-ELCC in the main body of the chapter; the marginal D-ELCC (the additional D-ELCC when an additional increment of PV is added) is provided in the Supplementary Materials (Section 6).

Worst Case D-ELCC

We use two metrics to estimate the D-ELCC with 19 years of available data. We define the worst-case D-ELCC at solar penetration p as

$$D - ELCC(p)_{\text{worst}} = \frac{\text{Max Peak}(at p = 0) \text{ over all years} - \text{Max Peak}(at p) \text{ over all years}}{\text{Rooftop Solar Capacity}(at p)} \quad (1)$$

The penetration, p , is defined as the AC solar capacity relative to the peak feeder load.

This metric describes how much solar can reduce the largest net peak load over all 19 years for each penetration. A low D-ELCC occurs if solar performs very poorly (e.g. due to cloudy conditions) on the largest peak over all years for each penetration. In contrast, this metric ignores the D-ELCC in any year when solar is performing poorly if the peak load in that year is relatively low. Thus, $D-ELCC_{\text{worst}}$ should reflect any positive correlation between solar performance and larger peaks due to hot weather. In our results, we also show the D-ELCC for individual years.

Transformer Aging D-ELCC

Often, transformers are the main capacity constraint in capacity expansion projects. We calculate the transformer aging D-ELCC ($D-ELCC_{\text{age}}$) using PJM weather normalization and both IEEE and IEC transforming aging estimation procedures. $D-ELCC_{\text{age}}$ allows overloading associated with solar, but the

aggregate deterioration of the transformer insulation condition (commonly referred to as transformer aging) cannot exceed the deterioration caused by weather normalization without solar.

The PJM weather normalization procedure, described in PJM Manual 19 (2017), performs ordinary least squares regression with summertime peak daily loads as the dependent variable and weighted temperature humidity indices (WTHI) as the independent variable. It then solves the regression equation at a weather standard associated with extreme weather. The WTHI is based on the dry bulb temperature and humidity with a 20% weight based on previous days to account for the thermal inertia of buildings. PJM defines the weather standard as the 50th percentile of past yearly peak WTHI's. Details of PJM's weather normalization procedure are in the Supplementary Materials (Section 2).

A problem with weather normalization is that it does not guarantee similar levels of overloading at different solar penetrations. So, we modify PJM's weather normalization procedure in our estimate of the $D - ELCC_{age}$. Our modification is summarized by Equation 2 and Figure 2. First, we define overloading as transformer aging. While overloading could be expressed in terms of the maximum overload (kW) or the total overload (kWh), we use transformer aging because it can estimate how both high loading from a loss of solar output on a cloudy day and low loading from solar on typical days affect transformer insulation condition. To correct for increased or decreased transformer aging, we use quantile regression and iteratively search for the quantile (q^*) resulting in the same aging as the 50th percentile quantile regression without solar. We use the IEC Standard 60076-7 (2005) "exponential model" to estimate the increased aging of transformers caused by overloading. Our estimates are based on a medium power transformer (2.5-100MVA) with ONAF cooling (Oil Natural Air Forced, i.e. the oil circulates naturally but air is forced over the cooling fins) and non-thermally upgraded paper insulation. Additionally, we follow the IEEE Standard C57.91™ (2012) normal life expectancy loading which limits the transformer hotspot temperature to a 130°C. Details of our transformer aging procedure can be found in the Supplementary Materials (Section 3). Figure S1 in the Supplementary Materials shows how a 50% penetration of solar affects transformer loading and hotspot temperatures over time.

$$D - ELCC(p)_{age} = \frac{W/N \text{ Peak}(at p = 0, q = 50\%) - W/N \text{ Peak}(at p, q = q^*)}{\text{Rooftop Solar Capacity at penetration } p} \quad (2)$$

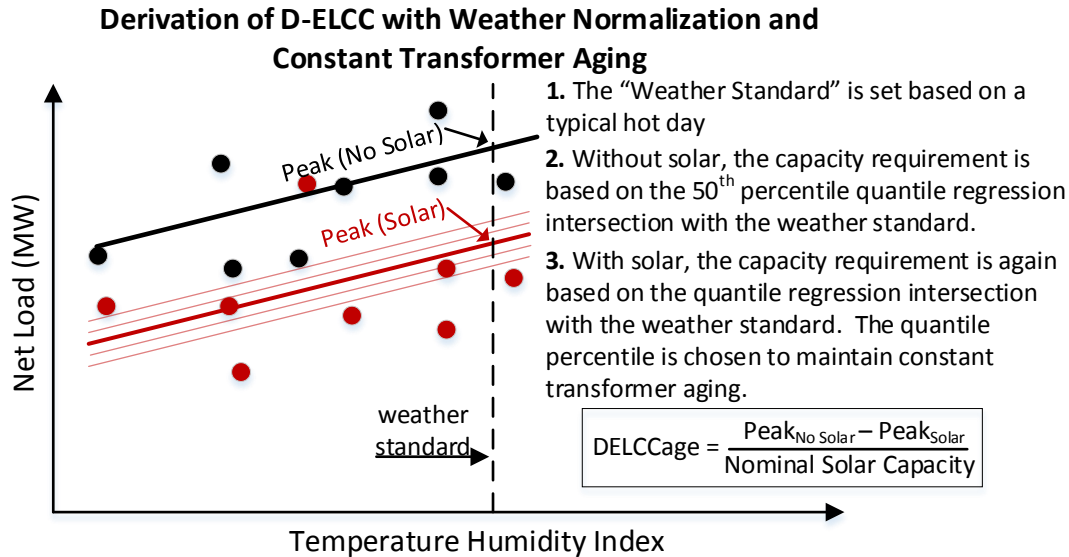


Figure 2: Method for estimating the D-ELCC with Weather Normalization (D-ELCC_{age}) and maintaining transformer condition. D-ELCC_{age} allows overloading associated with solar but the aggregate deterioration of the transformer insulation condition (commonly referred to as transformer aging) cannot exceed the deterioration caused by weather normalization without solar. Peak loads with solar are shown in red. Peak loads without solar are shown in black.

Results

Figure 3 demonstrates how solar performs on peak loading days at very low PV penetrations for the PG&E and PECO service territories. Real loading data are used for all scatterplots and real solar generation data from SoCore Energy (2016) is used for the California scatterplots. Each point shows a daily peak event as a fraction of the maximum peak and the solar output at the hour of the daily load peak as a fraction of maximum solar output.

There are two important features of the plots in Figure 3. First, we never observed a complete loss of solar generation during a peak loading event. Second, there is a trend towards greater solar output as loads increase. This trend is caused by the high correlation between temperature and load and between temperature and solar insolation. Solar output is worst on peak events on the two PECO feeders that peak in the evening. When west facing panels are used, solar output during the peak load events is higher, as discussed below. An exhaustive set of solar performance scatterplots is shown in the Supplementary Materials (Section 7) for all taxonomy feeders and the two PECO feeders using every year of simulated loading.

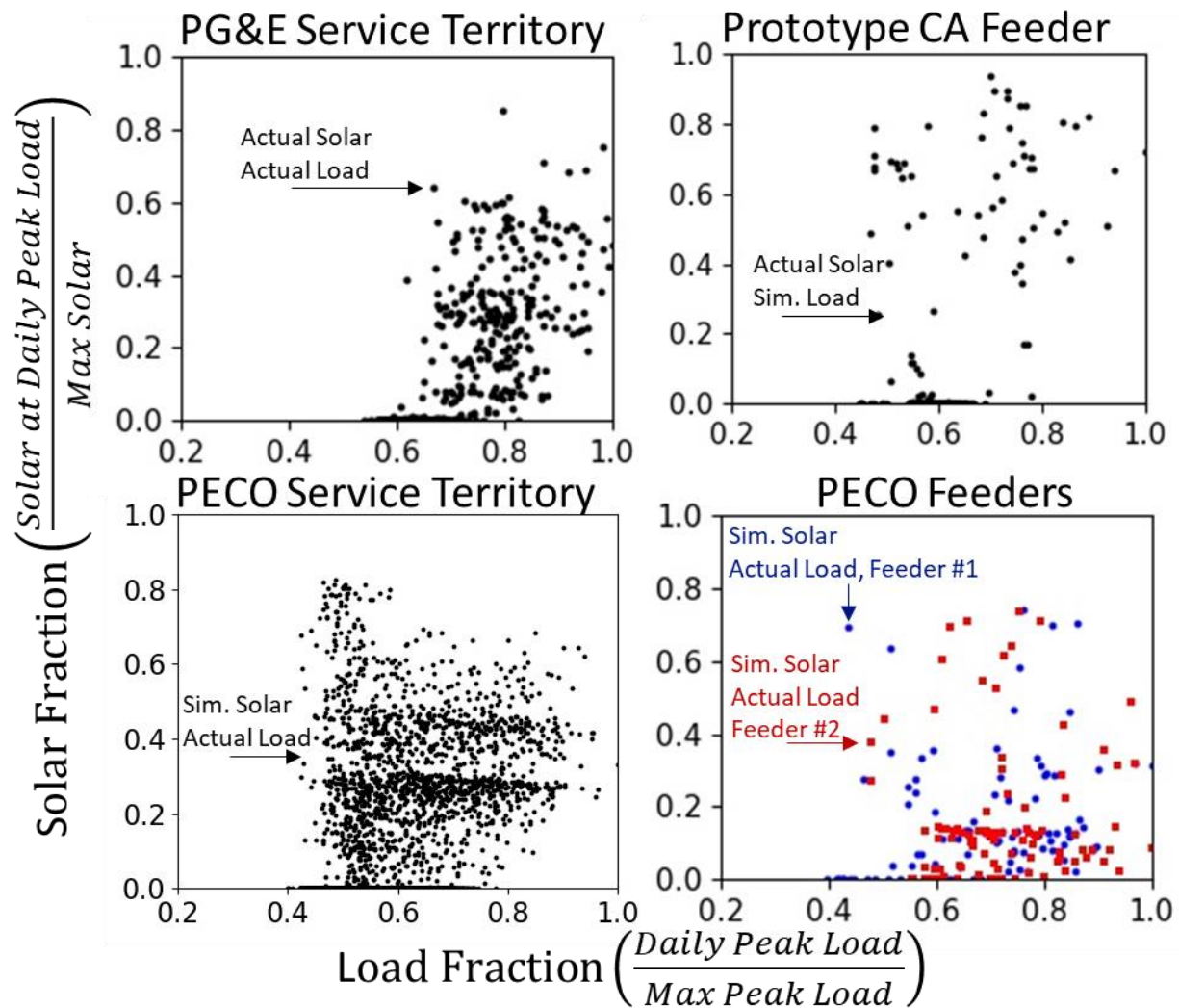


Figure 3: Solar performance is higher during peak loading times in California and eastern Pennsylvania. Solar performance for PECO and PG&E service territories are shown on the left. Solar performance for feeders are shown on the right. PG&E service territory (top left): the solar profile is based on a solar installation near Sacramento and the load is taken from CAISO market data. Prototype California feeder (top right): the solar profile is based on the Sacramento installation and the load is simulated using feeder R1-12.47-1. PECO Service Territory (bottom left): the solar profile is simulated using GridLab-D and NREL's Physical Solar Model, and the load is taken from PJM data. PECO Feeders (bottom right): solar profiles are simulated for summer months using GridLab-D and NREL's Physical Solar model with south facing panels, and the summer load profiles are from 2016 SCADA readings.

Figure 4 shows the average D-ELCC for both feeders in eastern Pennsylvania for south facing and west facing orientations. Figure 5 shows the average D-ELCC for five locations and sixteen of the PNNL taxonomy feeders. Each figure includes the yearly D-ELCC, $D\text{-ELCC}_{\text{worst}}$, $D\text{-ELCC}_{\text{age}}$, and the D-ELCC using a 5-minute time resolution with the 2014 Vibrant Clean Energy weather data. A worst-case D-ELCC based on SCADA measurements and simulated solar is also shown for the year 2016 for the PECO feeders. The marginal D-ELCC values are shown in the Supplementary Materials (Figure S3, Figure S5, Figure S6). Features of these results are discussed below.

D-ELCC estimates are strongly affected by the peak hour. In Table S2 of the Supplementary Materials (Section 5), the peak hour for each feeder is shown. Both PECO feeders peak in the evening and exhibit a lower effective capacity than most of the taxonomy feeders which peak in the afternoon. The evening peaking feeders benefit from the west facing solar panel orientation.

D-ELCC_{worst}, shown in black, is strongly affected by regional climate. In California, Arizona, and Texas, the D-ELCC_{worst} is always over 40% at low penetrations. Even in climates with a weaker solar resource, effective capacity estimates were typically above 40% at low penetrations. Every Minnesota feeder (see Figure S4 of the Supplementary Materials) had a D-ELCC_{worst} greater than 40% at low penetrations. However, several exceptions exist where solar performs poorly. On feeder R4-25.00-1 in North Carolina, an abnormally high morning peak in the late winter causes the effective capacity of solar to be very low. Additionally, two feeders in New York (R2-12.47-3 and R2-25.00-1) are dominated by cloud events and have a low D-ELCC_{worst}. The Texas feeders, with D-ELCC_{worst} values around 40%, are lower than expected for a region with a high solar resource and remain very flat at higher penetrations. Details can be found in Figure S8 of the Supplementary Materials, which shows the loading and solar profile on the peak load days that are used in the estimate for D-ELCC_{worst}.

The transformer aging D-ELCC with an allowance for “planned loading beyond nameplate capacity”, as described by IEEE C57.91™ (2012) is shown with black dashed lines. The D-ELCC_{age} maintains a constant level of transformer aging but by allowing occasional overload events, solar on each feeder achieves a capacity value of 60% at low penetrations. The decline in D-ELCC_{age} is relatively small as the solar penetration increases.

On all feeders, small amounts of energy storage used with solar can achieve high effective capacities without any overloading events. To find the energy storage requirement, we assume a target D-ELCC, and size the energy storage to the maximum overload event. Figure 6 shows the full set of energy storage capacity requirements and duration for each feeder. Energy capacity requirements are provided relative to peak feeder load in %-hour units for conversion to kWh. For all feeders, a one hour energy storage duration rated at 5% of the feeder peak loads could achieve an effective capacity of 50% when the peak load penetration of solar is below 20%. The storage duration with solar is shorter than deferral projects using only storage. For example, Lazard (2017) assumes a 6 hour duration and Hledik *et al* (2018) use a 4 hour duration for their energy storage capacity deferral scenarios.

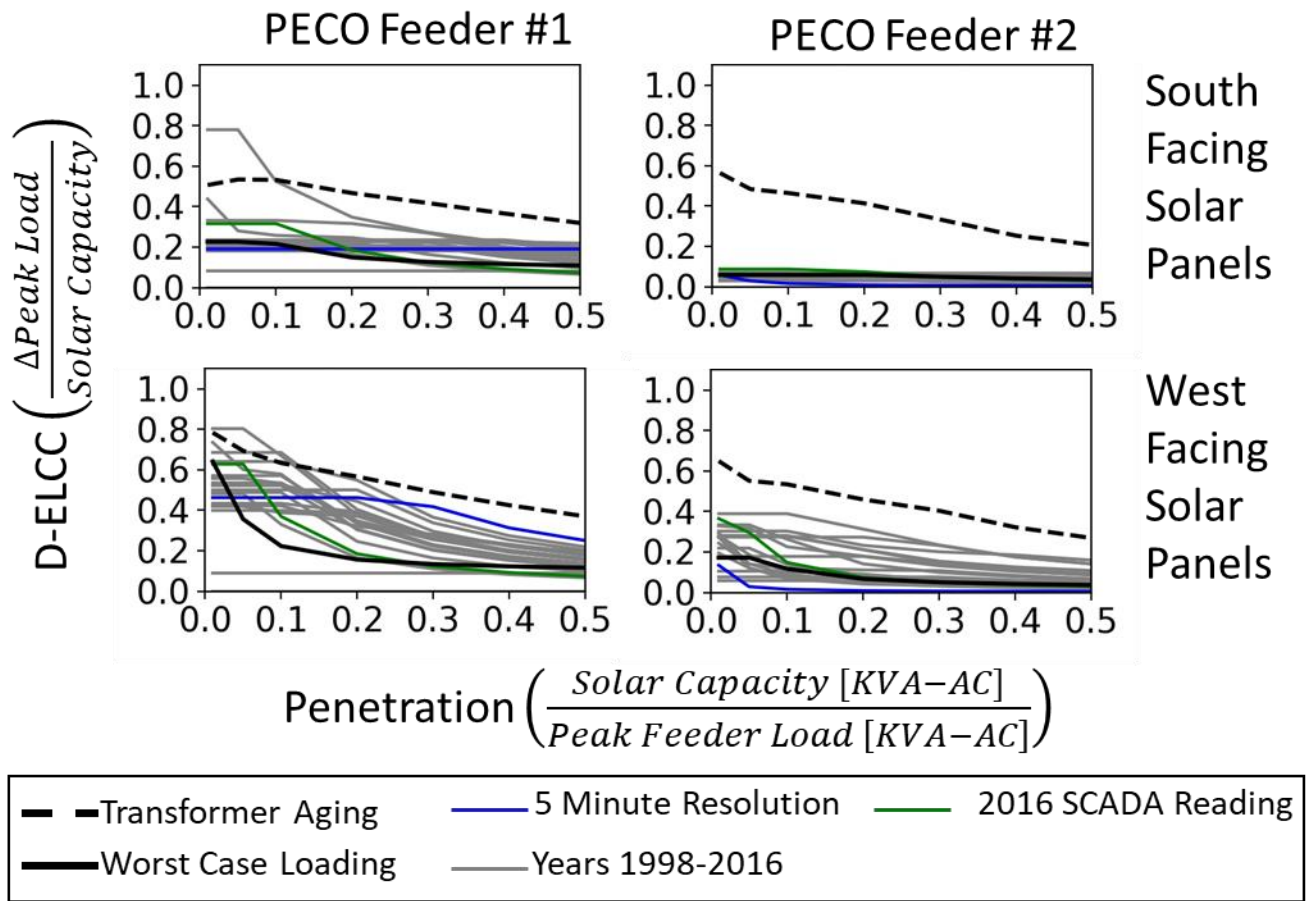


Figure 4: Distribution Effective Load Carrying Capability (D-ELCC) for two evening peaking feeders in the PECO service territory.

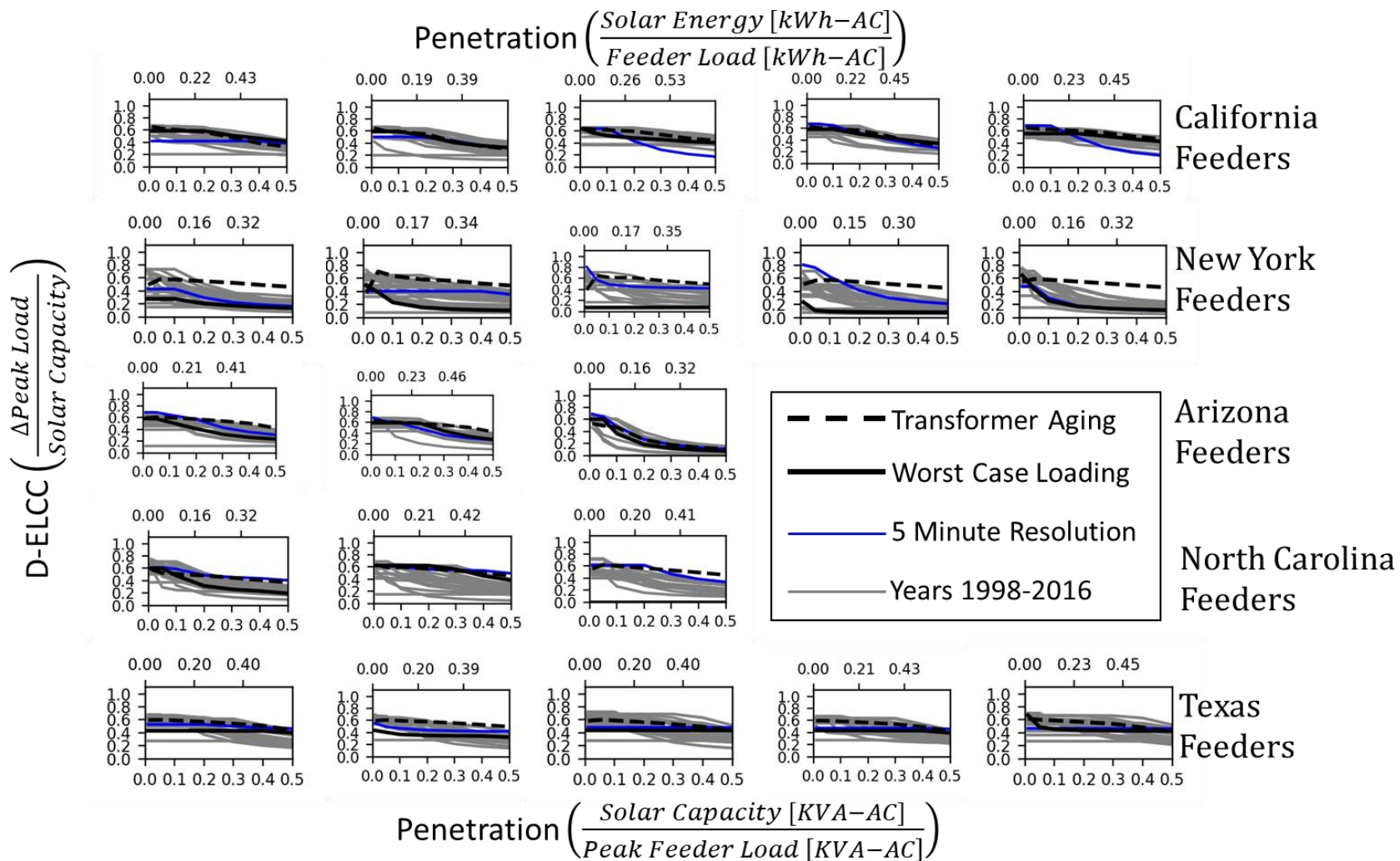


Figure 5: Distribution-Effective Load Carrying Capability (D-ELCC) for representative feeders in major US climate regions. Columns show the taxonomy feeders in order from left to right. California Feeders: R1-12.47-1, R1-12.47-2, R1-12.47-3, R1-12.47-4, R1-25.00-1. New York Feeders: R2-12.47-1, R2-12.47-2, R2-12.47-3, R2-25.00-1, R2-35.00-1. Arizona: R3-12.47-1, R3-12.47-2, R3-12.47-3. North Carolina Feeders: R4-12.47-1, R4-12.47-2, R4-25.00-1. Texas feeders: R5-12.47-1, R5-12.47-2, R5-12.47-3, R5-12.47-4, R5-12.47-5.

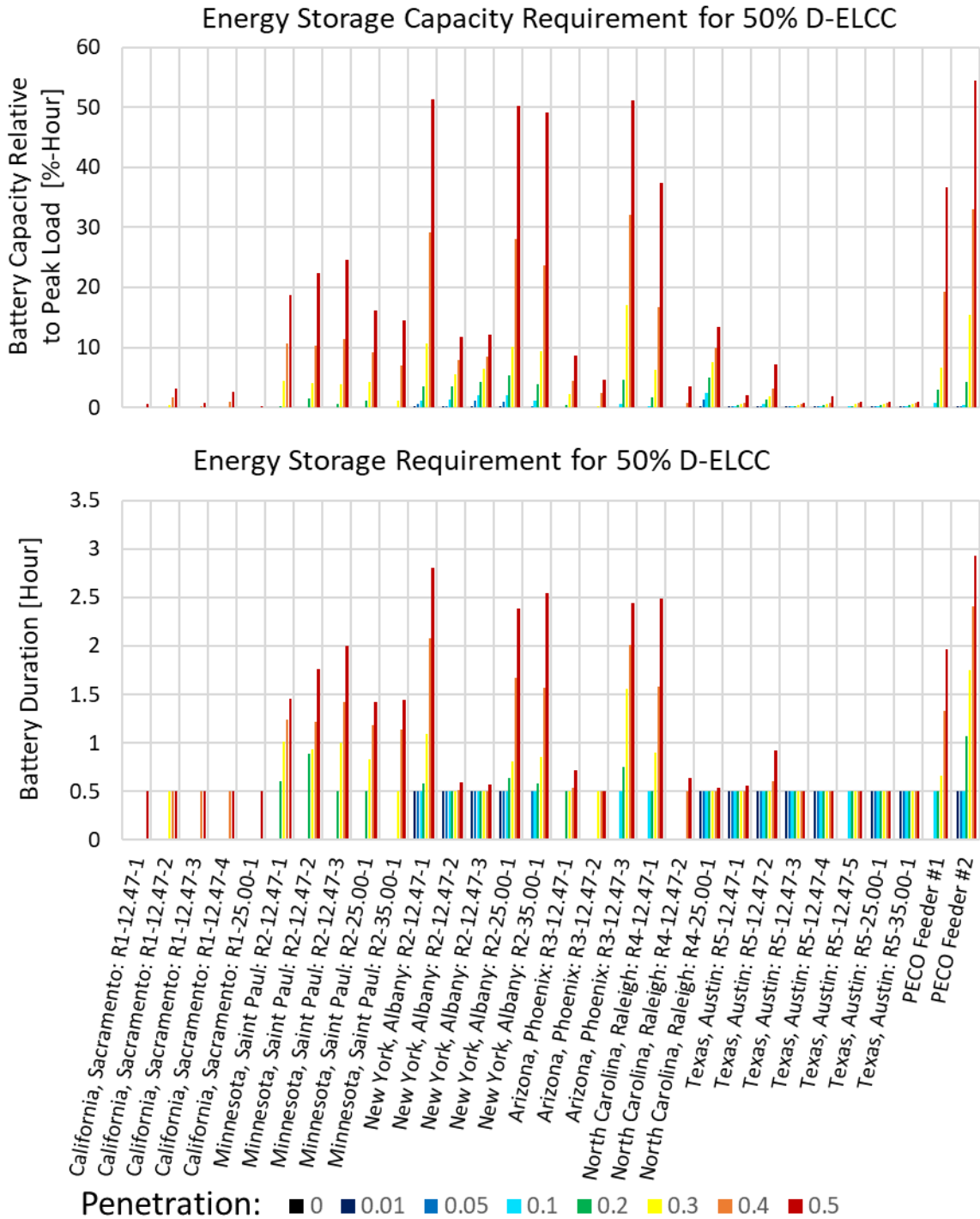


Figure 6: Energy storage capacity and duration requirements for a 50% D-ELCC when used with solar. Storage capacity units are in %-hour of feeder peak (kW) allowing for the conversion to storage capacity units of kWh. For all feeders, a one hour energy storage duration rated at 5% of the feeder peak loads could achieve an effective capacity of 50% when the peak load penetration of solar is below 20%.

Conclusion

We have performed feeder-level analysis based on 19 years of loading and solar profiles. Correlations between solar output and peak loads, flexibility in transformer overloading, and the relatively small amounts of energy storage needed to achieve high D-ELCCs all suggest that solar could act as a valuable capacity resource. As a point of comparison, we found that New York Feeder R2-12.47-3 at a 20% solar peak penetration of its 1 MW peak, had a worst-case D-ELCC of only 10%, due to cloudy conditions in the region, but had a transformer aging D-ELCC of 56% because some overloading was allowed, and could achieve a 50% D-ELCC without any overloading with 50 kWh of energy storage.

Utility managers and public utility commissions (PUCs) should consider strategies to take advantage of the effective capacity of solar. In afternoon peaking feeders in regions with a strong solar resource, solar is sufficient by itself to reduce loading on substations and defer investments. In regions with a weaker solar resource, large gains in the effective capacity of solar with small amounts of energy storage may make solar and energy storage an economic option for capacity deferral projects. The capacity value of solar may be lost if energy storage systems are oversized and overcompensate for the risks associated with solar. Figure 6 offers guidance on energy storage capacity requirements when used with different penetrations of solar.

The greatest opportunity for value creation with solar is in capacity expansion projects where transformers are the primary capacity constraint. In our D-ELCC_{age} method we allow occasional “planned loading beyond nameplate capacity” as described by IEEE C57.91™. Relying on this inherent flexibility of transformers, rather than costly energy storage, will increase the value of solar.

Acknowledgements

This work was funded by the Richard King Mellon Foundation. The findings and conclusions in this material are those of the authors. We are grateful for the Pennsylvania Public Utility Commission, and PECO for providing data, technical expertise, and thoughtful comments. Special thanks to Eric Matheson and George Sey Jr.

References

- Denholm, Paul, Robert Margolis, Bryan Palmintier, Clayton Barrows, Eduardo Ibanez, Lori Bird, and Jarett Zuboy. 2014. *Methods for Analyzing the Benefits and Costs of Distributed Photovoltaic Generation to the U.S. Electric Utility System*. Golden: NREL.
<https://www.nrel.gov/docs/fy14osti/62447.pdf>.
- E3. 2016. *Full Value Tariff Design and Retail Rate Choices*. New York State Energy Research and Development Authority (NYSERDA) and New York State Department of Public Service.
<http://documents.dps.ny.gov/public/Common/ViewDoc.aspx?DocRefId=%7BA0BF2F42-82A1-4ED0-AE6D-D7E38F8D655D%7D>.
- EIA. 2018. *RESIDENTIAL ENERGY CONSUMPTION SURVEY (RECS)*.
<https://www.eia.gov/consumption/residential/>.

- EPRI. 2017. *Time and Locational Value of Photovoltaics (PV) on Distribution Feeders in Spain*. Palo Alto: EPRI. <https://www.epri.com/#/pages/product/3002011694/?lang=en>.
- Fuller, J C, N Pakash Kumar, and C A Bonebrake. 2012. *Evaluation of Representative Smart Grid Investment Grant Project Technologies: Demand Response*. Richland: PNNL. https://www.pnnl.gov/main/publications/external/technical_reports/PNNL-20772.pdf.
- Habte, A, A Lopez, M Sengupta, and S Wilcox. 2014. *Temporal and Spatial Comparison of Gridded TMY, TDY, and TGY Data Sets*. 2014: NREL. <https://www.nrel.gov/docs/fy14osti/60886.pdf>.
- Habte, Aron, Manajit Sengupta, and Anthony Lopez. 2017. *Evaluation of the National Solar Radiation Database (NSRDB): 1998-2015*. Golden: NREL. <https://www.nrel.gov/docs/fy17osti/67722.pdf>.
- Happy, P., and SoCore Energy. 2016. "private communication."
- Hledik, Ryan, Judy Chang, Roger Lueken, Johannes Pfeifenberger, John Pedtke, and Jeremy Vollen. 2018. "The Economic Potential for." Brattle, October 1.
- IEC. 2005. "Power transformers-Part7: Loading guide for oil-immersed power transformers (60076-7:2005)." <https://webstore.iec.ch/publication/605>.
- IEEE. 2012. "IEEE Guide for Loading Mineral-Oil-Immersed Transformers and Step-Voltage Regulators (IEEE Std C57.91™-2011)." March 7. <https://ieeexplore.ieee.org/document/6197686>.
- Lazard. 2017. "Lazard's Levelized Cost of Storage Analysis-Version 3.0." November. <https://www.lazard.com/media/450338/lazard-levelized-cost-of-storage-version-30.pdf>.
- Madaeni, Seyed Hossein, Ramteen Sioshansi, and Paul Denholm. 2013. "Comparing Capacity Value Estimation Techniques for Photovoltaic Solar Power." *IEEE Journal of Photovoltaics* 407-415.
- Myers, Daryl R, Thomas L Stoffel, Ibrahim Reda, Stephen Wilcox, and Afshin Andreas. 2001. "Recent Progress in Reducing the Uncertainty in and Improving Pyranometer Calibrations." *Journal of Solar Engineering* 124 (1): 44-50. <http://solarenergyengineering.asmedigitalcollection.asme.org/article.aspx?articleid=1473618>.
- NRECA. 2018. *Open Modeling Framework*. <https://github.com/dpinney/omf>.
- NREL. 2018. <https://sam.nrel.gov/>.
- . 2018. *NSRDB Data Viewer*. <https://maps.nrel.gov/nsrdb-viewer/>.
- Perez, R., R. Margolis, M. Kmieciak, M. Schwab, and M. Perez. 2006. *Update: Effective Load-Carrying Capability of Photovoltaics in the United States*. NREL. <https://www.nrel.gov/docs/fy06osti/40068.pdf>.
- PJM. 2017. "PJM Manual 19: Load Forecasting and Analysis, Revision 32." <https://www.pjm.com/~media/documents/manuals/m19.ashx>.
- PNNL. 2018. <http://www.gridlabd.org/>.
- Prat, R G, C C Conner, E E Richman, K G Ritland, W F Sandusky, and M E Taylor. 1989. *Description of Electric Energy Use in Single-Family Residences in the Pacific Northwest*. Richland: Bonneville Power Administration. <https://elcap.nwccouncil.org/Documents/Electric%20Energy%20Use%20Single%20Family.pdf>.

- Reda, Ibrahim. 2011. *Method to Calculate Uncertainties in Measuring Shortwave Solar Irradiance Using Thermopile and Semiconductor Solar Radiometers*. Golden: NREL.
<https://www.nrel.gov/docs/fy11osti/52194.pdf>.
- Rocky Mountain Institute. 2013. "A Review of Solar PV Benefit & Cost Studies: 2nd Edition." Boulder.
http://www.rmi.org/Knowledge-Center%2FLibrary%2F2013-13_eLabDERCostValue.
- Schneider, K P, Y Chen, D Chassin, Dave E, and S Thompson. 2008. *Modern Grid Initiative Distribution Taxonomy Final Report*. Pacific Northwest National Laboratory.
http://www.gridlabd.org/models/feeders/taxonomy_of_prototypical_feeders.pdf.
- Southern California Edison. 2017. "2016 Portfolio Design Report: Revision 2."
https://www.sce.com/wps/wcm/connect/d7cb7297-cbc4-4766-a640-e01e9fd0adc1/020317_PRP_PortfolioDesignReport.pdf?MOD=AJPERES.
- Tuffner, F K, J L Hammerstrom, and R Singh. 2012. *Incorporation of NREL Solar Advisor Model Photovoltaic Capabilities with GridLAB-D*. Richland: PNNL.
- Vibrant Clean Energy. 2018. <http://www.vibrantcleanenergy.com/>.

Supplementary Materials for Can solar PV reliably reduce loading on distribution networks?

Jeremy F Keen¹ and Jay Apt^{1,2}

¹Department of Engineering and Public Policy, Carnegie Mellon University, Pittsburgh, PA 15213, USA

²Tepper School of Business, Carnegie Mellon University, Pittsburgh, PA 15213, USA

E-mail: jkeen@andrew.cmu.edu

1. Genetic Algorithm for Substation Load Matching

We used a genetic algorithm to find a global set of building parameters that led to a match between simulated loading and actual SCADA measurements. The decision variables were the air conditioning coefficient of performance, insulation R values, cooling set points, floor areas, scaling factors for predefined temperature independent ZIP load profiles, the proportion of commercial buildings modeled as strip malls, office buildings, and big box stores, the percentage of residential homes with air conditioners, and the percentage of residential homes with hot water heaters.

We used a population of 400 and a parent size of 100. The computation time for a single time-series powerflow run are typically over one hour, so it was important to parallelize all simulation trials and to use good initial conditions with a narrow search space. To determine these parameters, we started with estimates for the northern United States (region 2 of the GridLab-D feeder taxonomy) (K. P. Schneider *et al* 2008). It was necessary to first perform several trials of the genetic algorithm with a wide search space. Altogether, this was a time-consuming process that could benefit from further research.

Unlike typical genetic algorithm implementations, we used real (not integer) decision variables. During each iteration, a new population of 400 was created based on the top 100 best solutions. The top 100 solutions were carried over without change (i.e. Elitism). The remaining 300 were a crossover of the top 100, with mutations. We used an adaptive mutation. A 5% variation was added to a trait if the mutation occurred but the probability of mutation decreased as the objective function improved. The traits for each crossover child were selected from all the solutions (i.e. k-point crossover).

2. Weather Normalization Procedure

We use PJM's weather normalization described in PJM Manual 19 (2017). Weather normalization requires several steps. First, each daily peak in the summer is associated with a weighted temperature humidity index (WTHI). The temperature humidity index is defined as:

$$\begin{aligned} & \text{If } DB \geq 58, \\ & \text{THEN } THI = DB - 0.55 * (1 - HUM) * (DB - 58) \\ & \text{ELSE } THI = DB \end{aligned}$$

Where, THI = Temperature Humidity Index, DB = Dry Bulb Temperature (°F), HUM = Relative Humidity

A 20/80% weight is applied using the current and previous day. Months including March through September are used, but the WTHI must be at least 74 to be included in the regression. The weather normalization regression is fit to all WTHIs and Peak Days (MWs) and solved at the weather standard to find the weather normalized peak. PJM defines the weather standards as the average of the peak WTHIs over the last 20 years. We used the 90th percentile of the peak WTHI's to ensure that we were not overestimating the risk associated with using weather normalization.

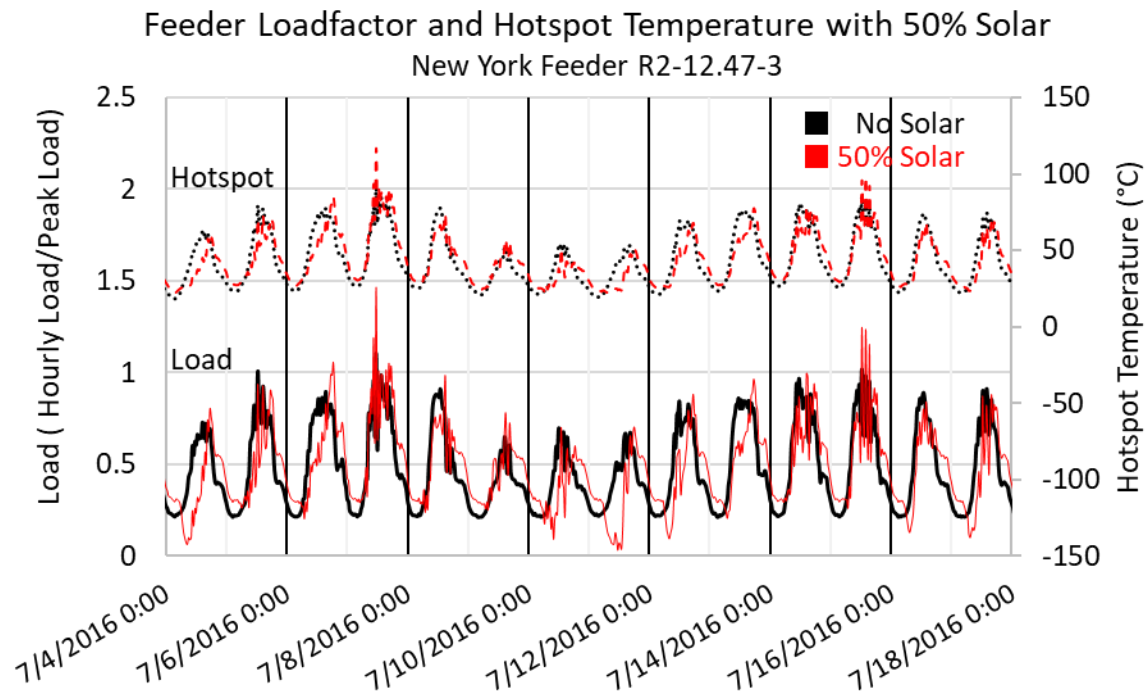
3. Transformer Aging

We use the IEC Standard 60076-7 (2005) "exponential model" to estimate the increased aging of transformers caused by overloading. Transformers that are frequently loaded above nameplate capacity experience high internal temperatures, and their paper insulation deteriorates more quickly. These internal temperatures are modeled as a heat transfer problem based on the "hotspot" (i.e. the hottest temperature in the transformer windings), "top oil" (i.e. the temperature at the top of the oil tank), and ambient temperature. The deterioration of the paper insulation and transformer age is modeled empirically using the Arrhenius equation and the hotspot temperature. Additionally, various transformer cooling parameters and the cooling system are important. Our estimates are based on ONAF cooling (Oil Natural Air Forced, i.e. the oil circulates naturally but air is forced over the cooling fins), non-thermally upgraded insulation paper and parameters for a typical "medium power" transformers, shown in Table S1. Medium power transformers are defined by the IEC as ranging from 2.5-100MVA.

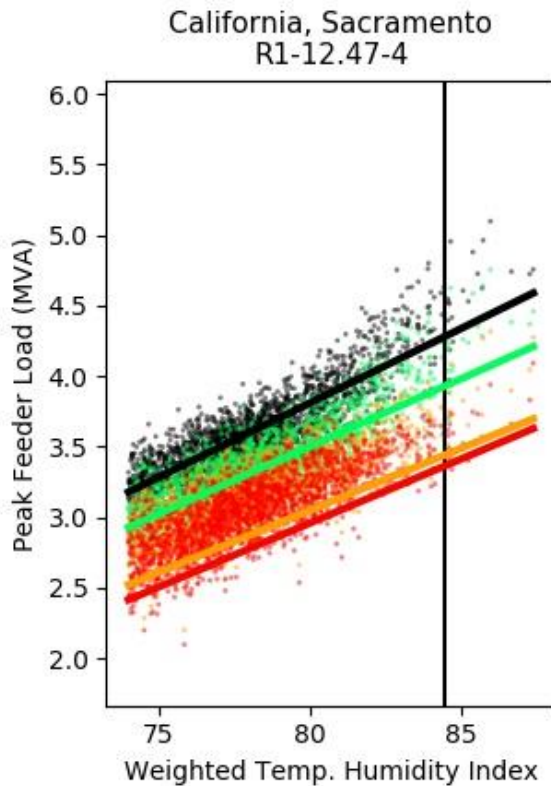
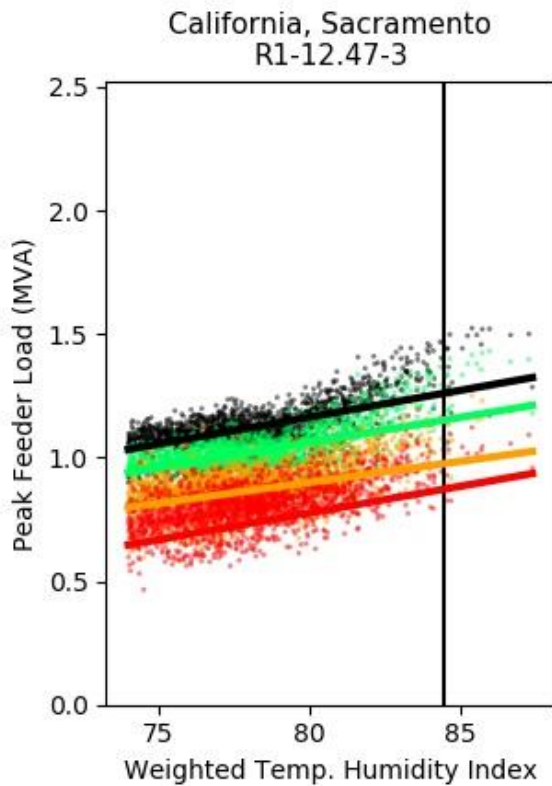
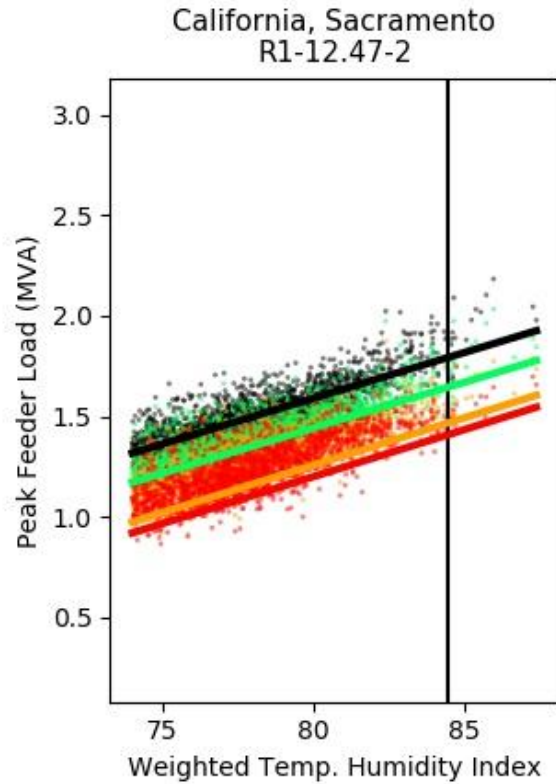
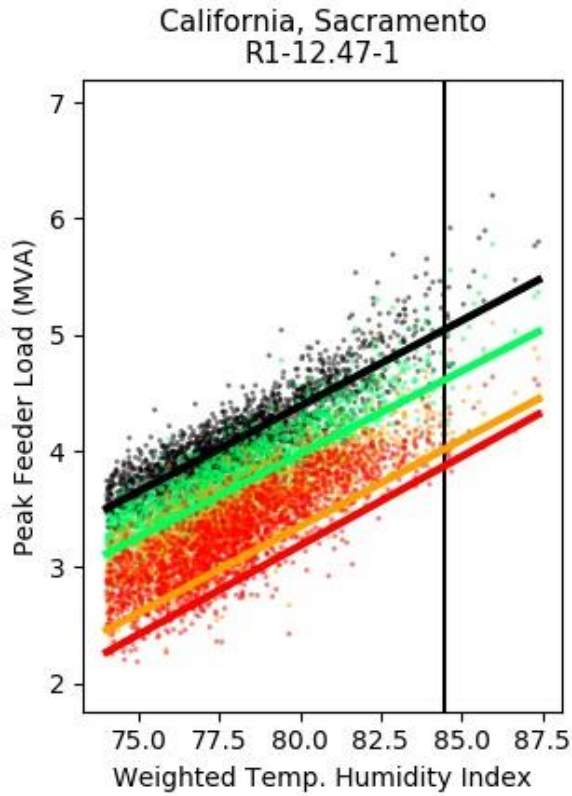
The IEEE Standard C57.91™ (2012) describes several typical "load cycles" for sizing transformers: normal life expectancy loading, planned loading beyond nameplate rating, long-time emergency loading and short-time emergency loading. We use the ratings defined by "planned loading beyond nameplate capacity", which is limited to a 130°C hotspot but can withstand frequent overload occurrences. In contrast, short-time emergency overloading condition can occur infrequently, but the hotspot temperature can be as high as 180°C. Figure S1 shows the transformer load factor for California feeder R1-12.47-1. A quantile was chosen that allows frequent overloads but limits the hotspot temperature to 130°C and results in the same transformer aging with and without solar.

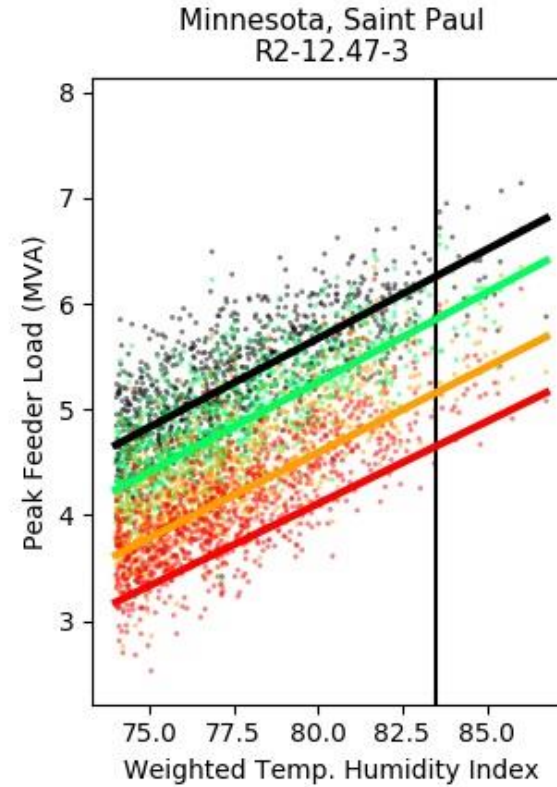
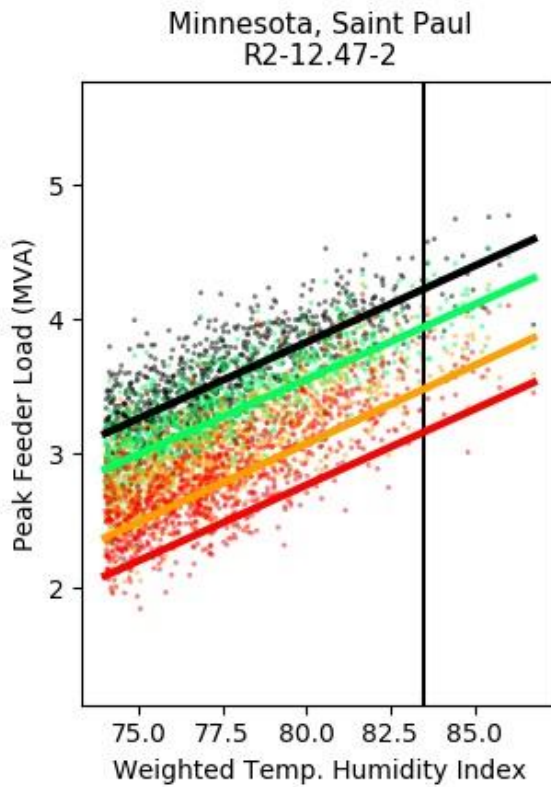
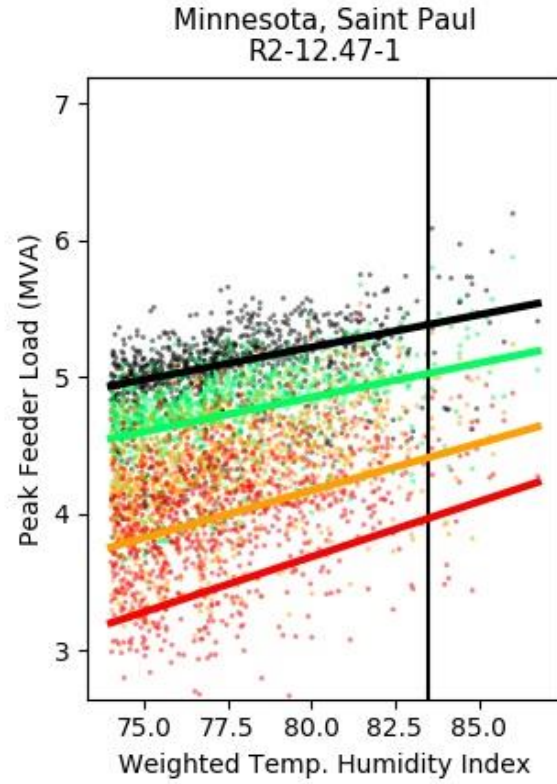
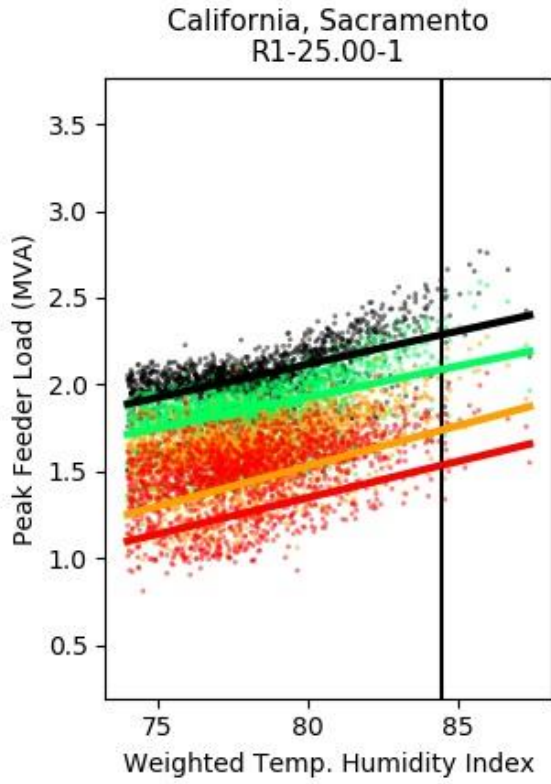
Table S1: IEC Standard 60076-7 transformer aging model parameters.

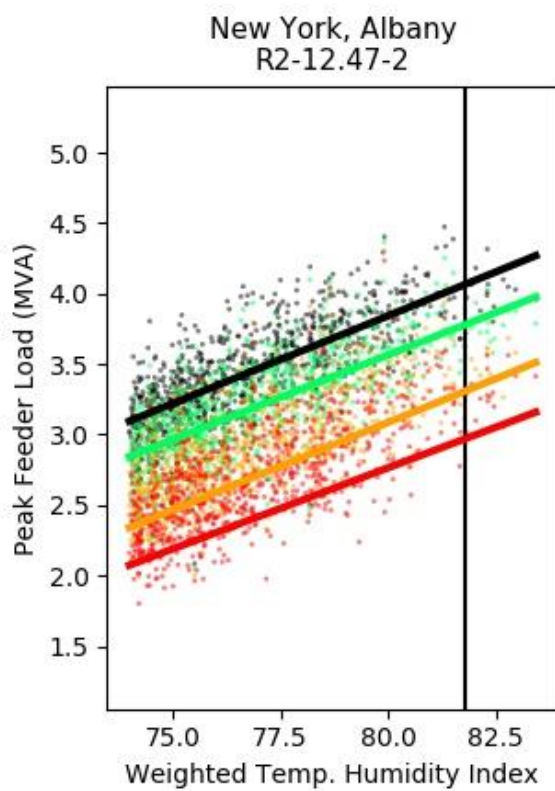
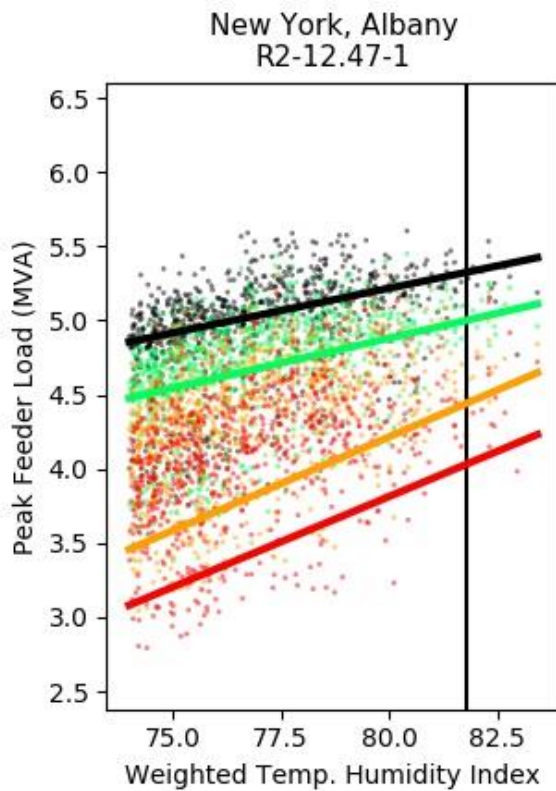
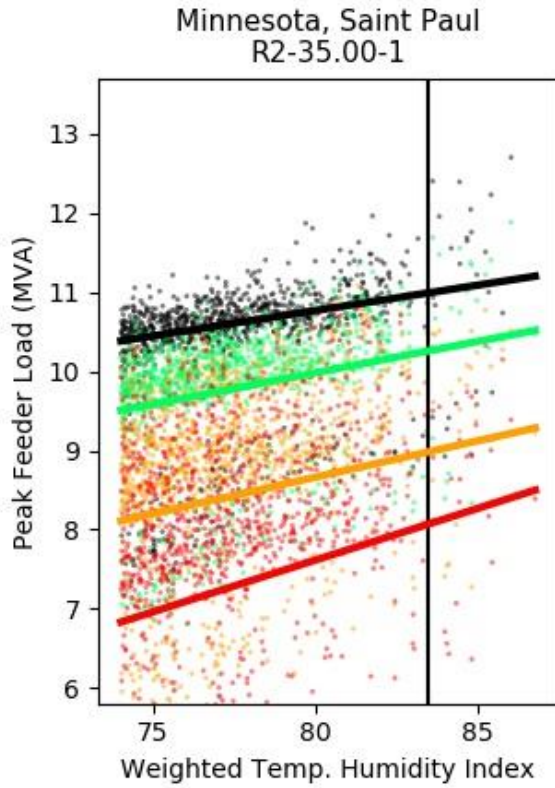
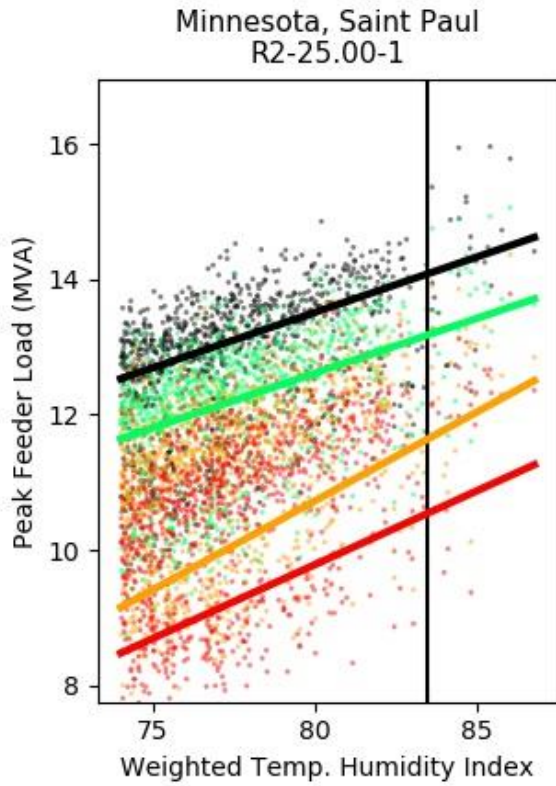
Transformer Aging Parameters	Value
Cooling System	ONAF
Paper Insulation	Not thermally upgraded
Load Cycle	"Planned loading beyond nameplate rating"
Maximum Top Oil Temperature	110°C
Maximum Hot Spot Temperature	130°C
Oil exponent	0.8
Winding exponent	1.3
Loss ratio	6
Hot-spot factor	1.3
Oil time constant	150
Winding time constant	7
Hot-spot to top-oil gradient	26
K11	0.5
K21	2.0
K22	2.0

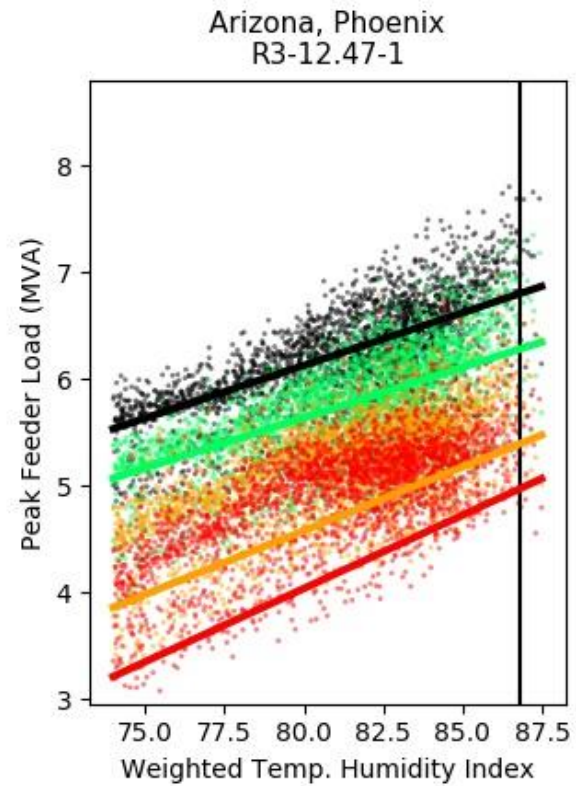
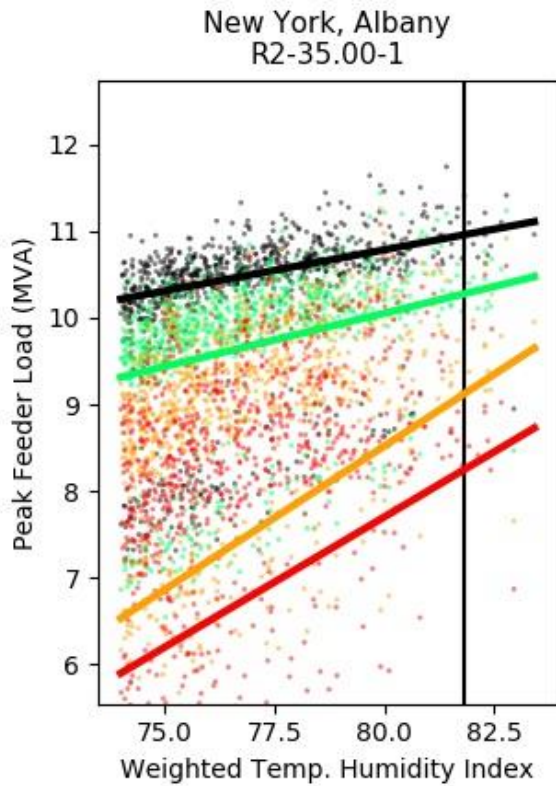
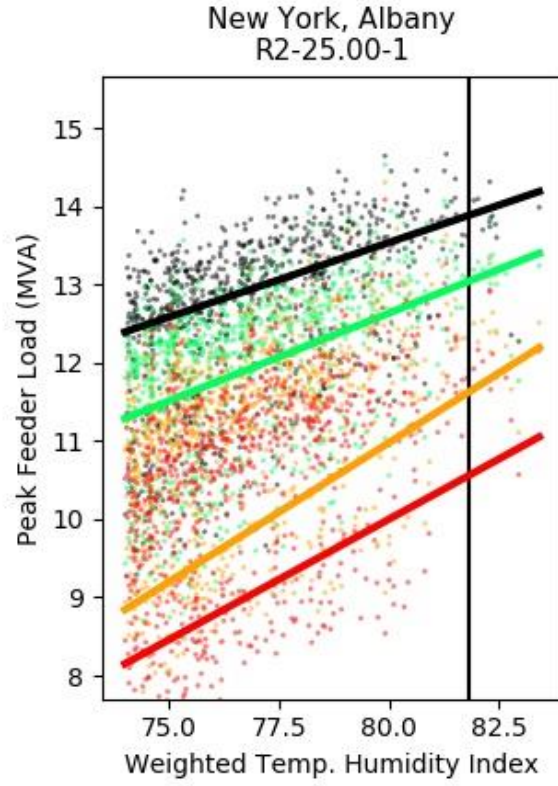
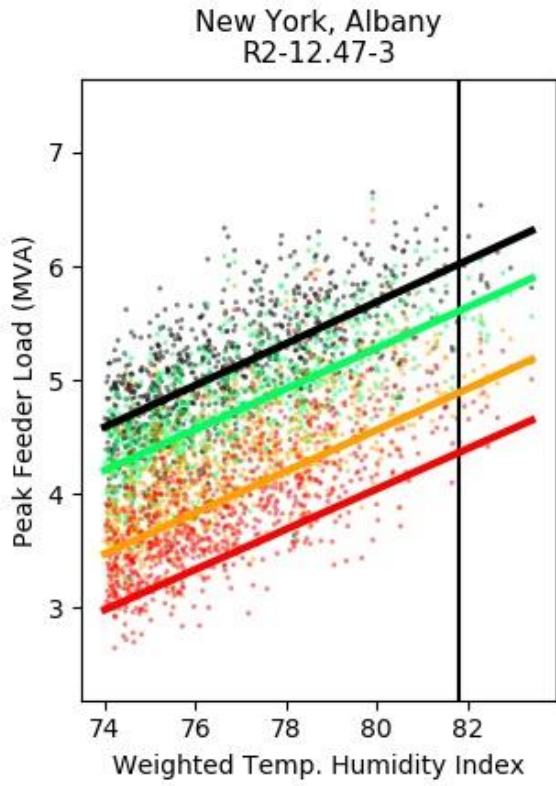
**Figure S1:** Transformer load factor and hotspot on New York Feeder R2-12.47-3. High penetrations of solar result in frequent overloads but overall, transformer aging caused by high hotspot temperatures is the same with and without solar.

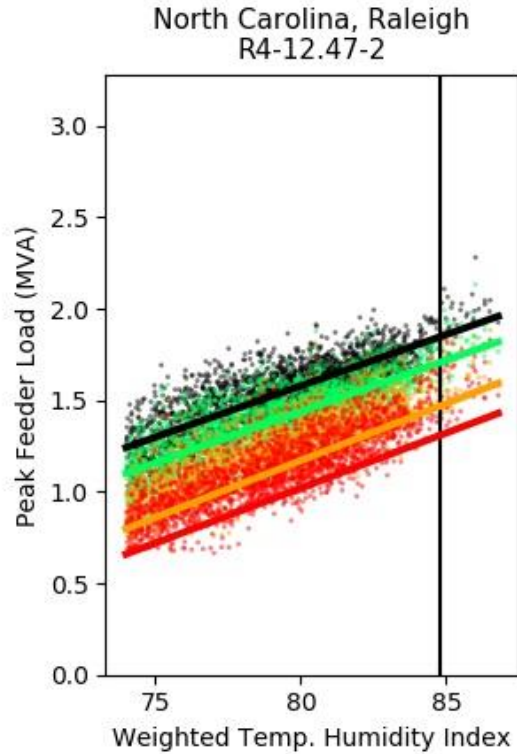
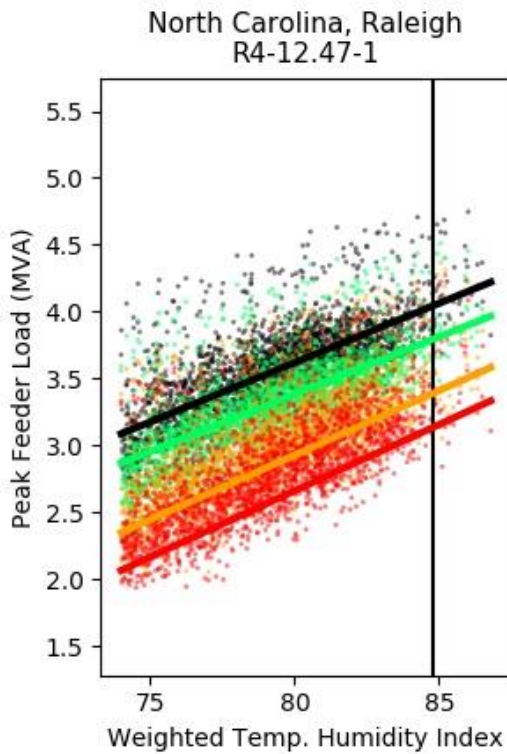
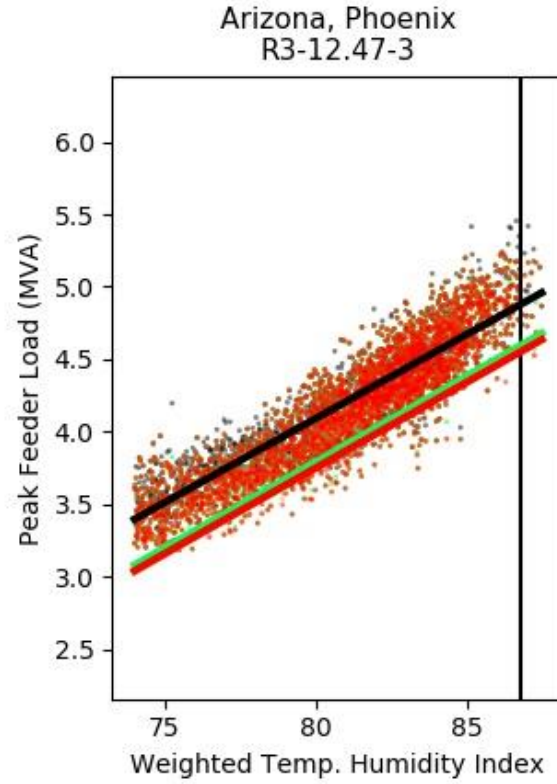
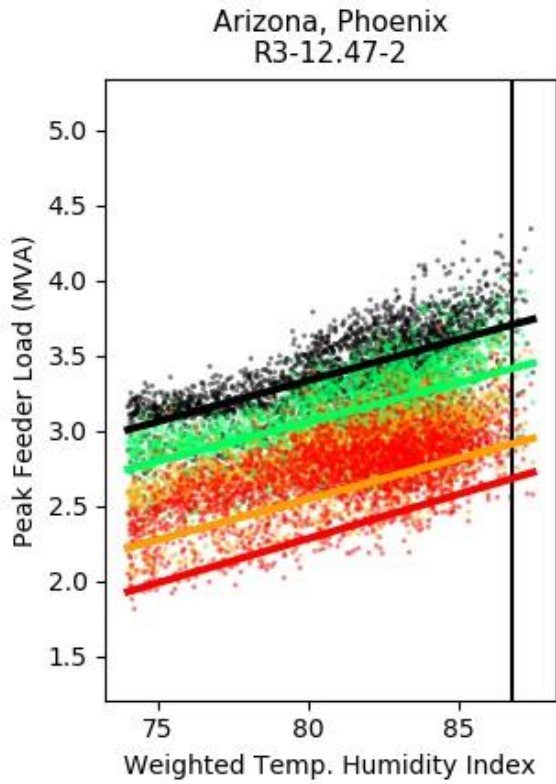
4. Weather Normalization Results

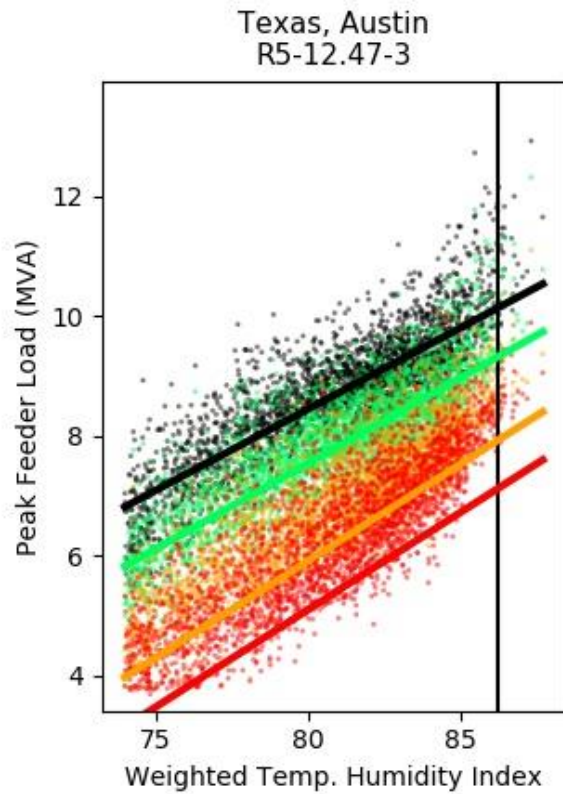
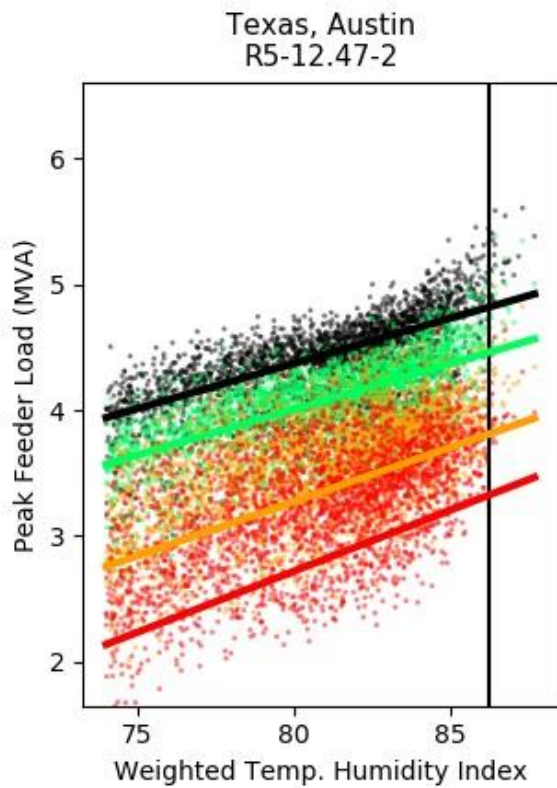
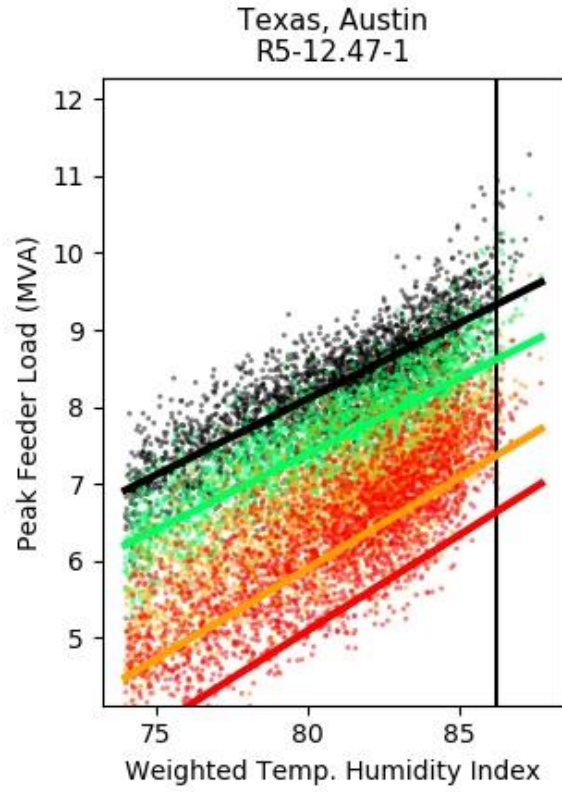
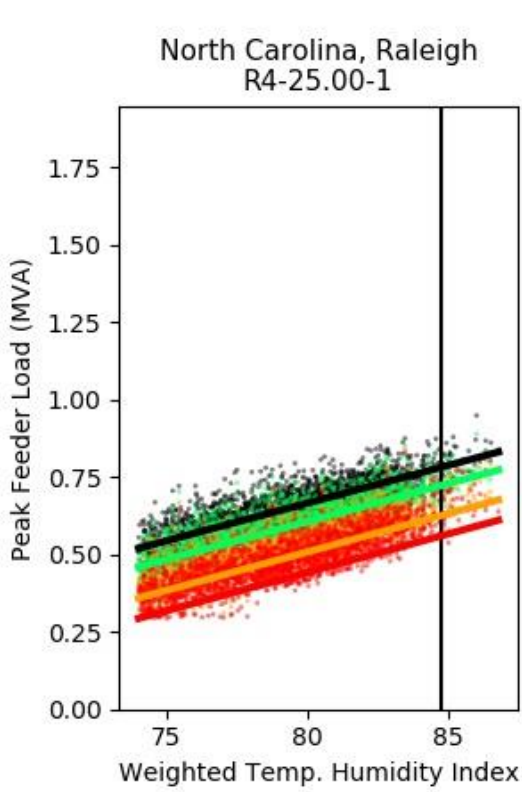


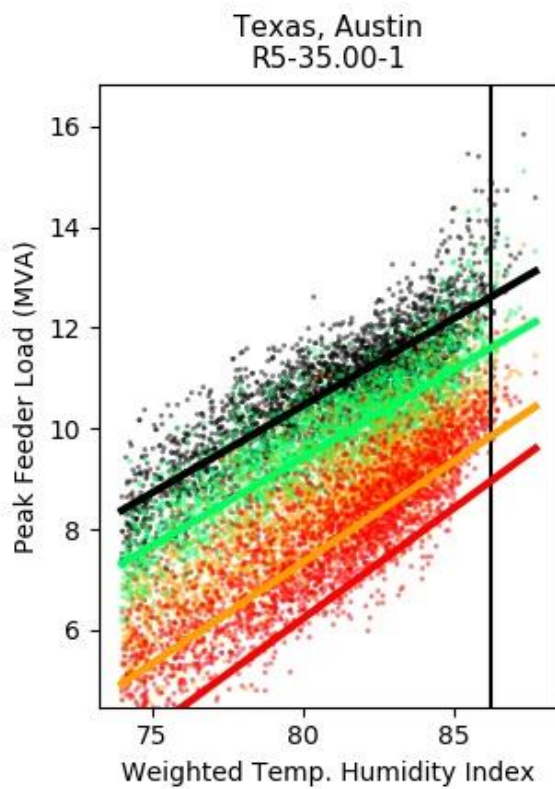
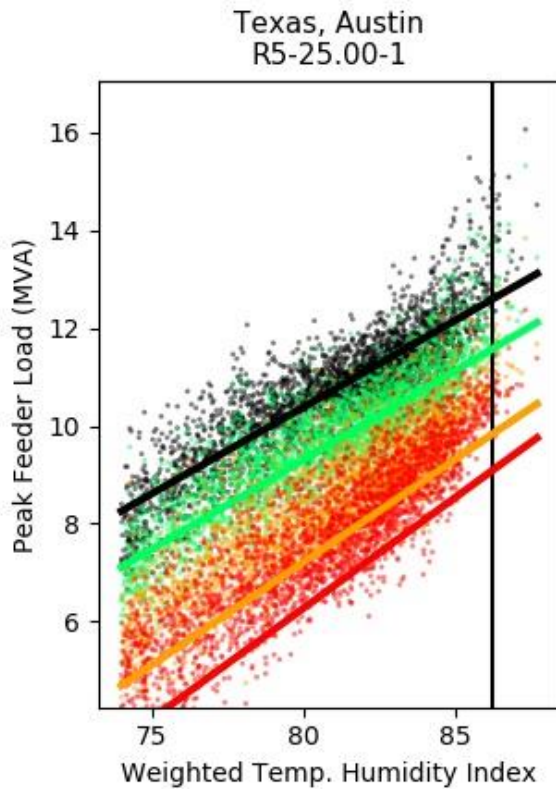
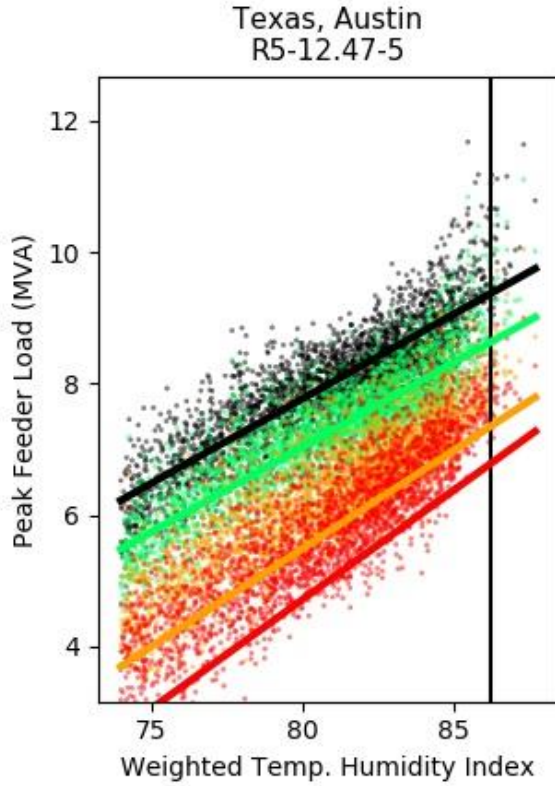
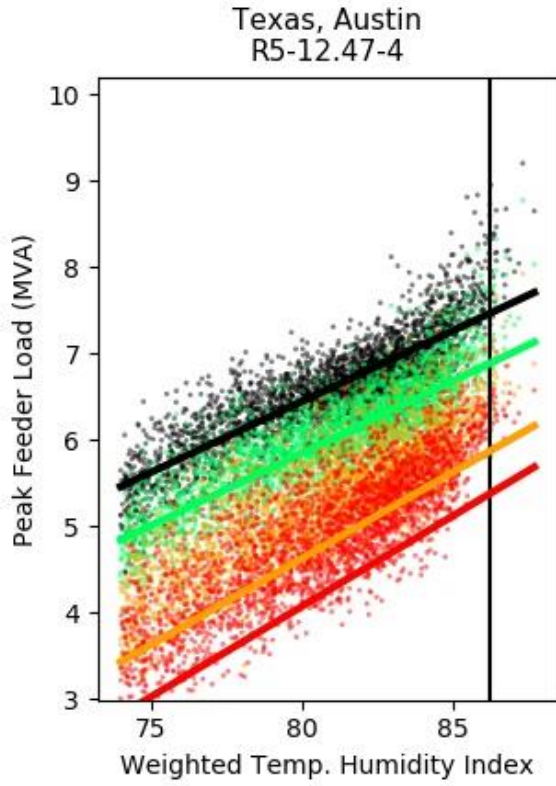












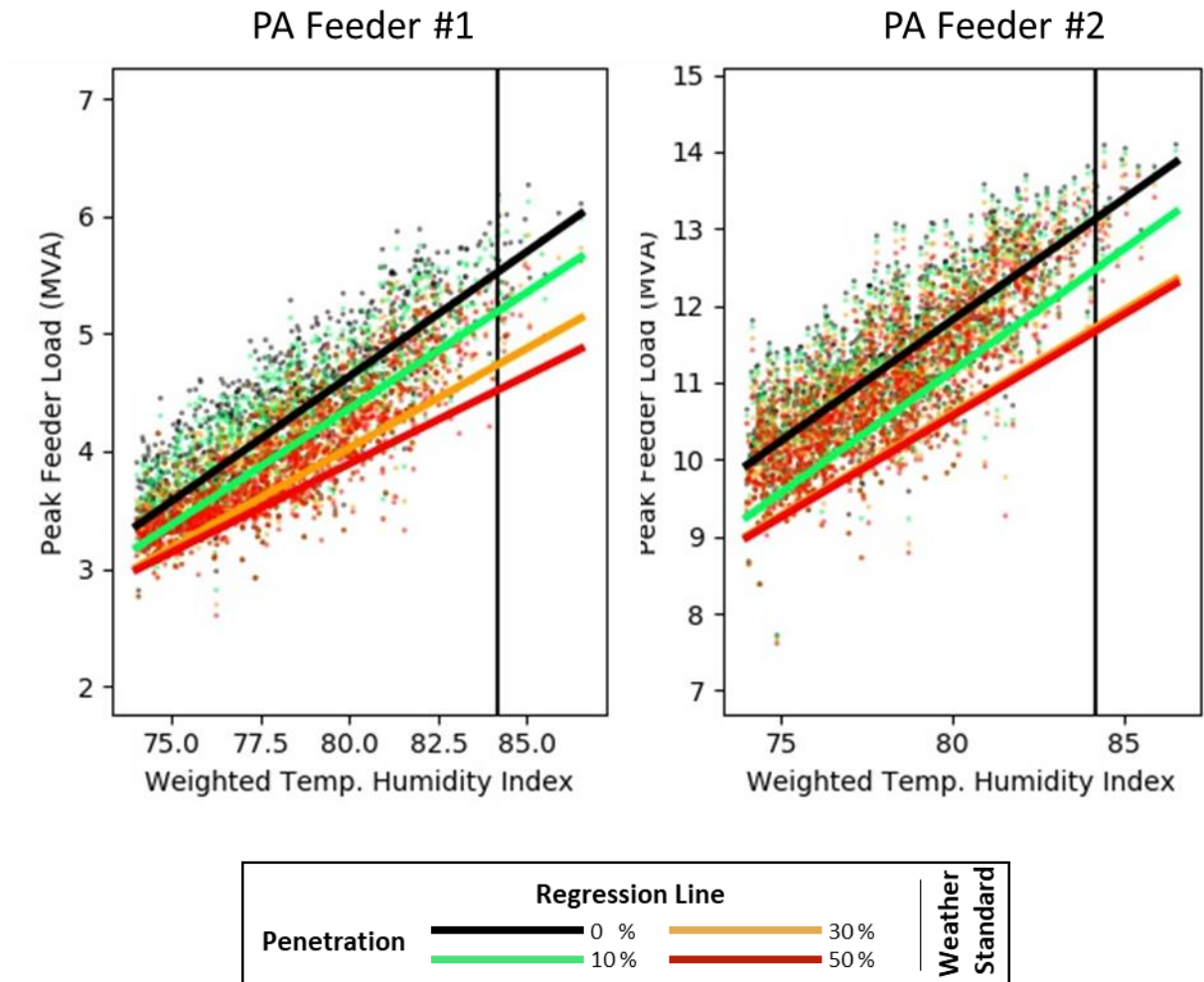


Figure S2: Weather Normalization of feeder taxonomy loads. Weather normalization regresses peak load events on weather indices and solves the resulting equation at an extreme weather event to estimate capacity requirements. The amount of overloading risk is quantified by the points that fall above the intersection of the regression line and the weather standard.

5. Peak Hour by Location, Feeder, and penetration

Table S2: Peak Hour for each location, feeder and penetration. The peak hour is not strongly related to the penetration.

Location	Penetration							
	0	0.01	0.05	0.1	0.2	0.3	0.4	0.5
California, Sacramento: R1-12.47-1	13	13	13	13	13	16	16	11
California, Sacramento: R1-12.47-2	13	13	13	13	11	11	11	11
California, Sacramento: R1-12.47-3	13	13	15	15	15	16	16	16
California, Sacramento: R1-12.47-4	13	13	13	13	16	16	17	17
California, Sacramento: R1-25.00-1	14	14	14	14	14	16	16	16
Minnesota, Saint Paul: R2-12.47-1	15	15	15	15	14	15	15	15
Minnesota, Saint Paul: R2-12.47-2	13	13	13	16	16	14	14	14
Minnesota, Saint Paul: R2-12.47-3	14	14	14	14	17	17	14	14

Minnesota, Saint Paul: R2-25.00-1	14	14	14	17	17	17	17	18
Minnesota, Saint Paul: R2-35.00-1	13	13	13	13	14	14	14	14
New York, Albany: R2-12.47-1	12	12	12	12	15	11	11	11
New York, Albany: R2-12.47-2	14	14	11	11	11	11	11	11
New York, Albany: R2-12.47-3	11	11	11	11	11	11	11	11
New York, Albany: R2-25.00-1	14	11	11	11	11	11	11	11
New York, Albany: R2-35.00-1	11	13	11	11	11	11	11	11
Arizona, Phoenix: R3-12.47-1	14	14	16	16	16	16	16	16
Arizona, Phoenix: R3-12.47-2	14	14	14	14	14	15	15	15
Arizona, Phoenix: R3-12.47-3	14	14	14	20	20	20	20	20
North Carolina, Raleigh: R4-12.47-1	12	12	12	14	14	14	14	18
North Carolina, Raleigh: R4-12.47-2	12	12	12	12	12	14	14	15
North Carolina, Raleigh: R4-25.00-1	6	6	6	6	6	6	6	6
Texas, Austin: R5-12.47-1	14	14	14	14	14	14	14	16
Texas, Austin: R5-12.47-2	14	14	14	14	14	14	14	16
Texas, Austin: R5-12.47-3	14	14	14	14	14	14	14	14
Texas, Austin: R5-12.47-4	14	14	14	14	14	14	14	14
Texas, Austin: R5-12.47-5	13	13	14	14	14	14	14	14
Texas, Austin: R5-25.00-1	14	14	14	14	14	14	14	14
Texas, Austin: R5-35.00-1	14	14	14	14	14	14	14	14
Pennsylvania Feeder #1	17	17	17	17	17	17	17	17
Pennsylvania Feeder #1	18	18	18	18	18	19	19	19

6. Supplementary D-ELCC Results

Marginal Distribution-Effective Load Carrying Capability

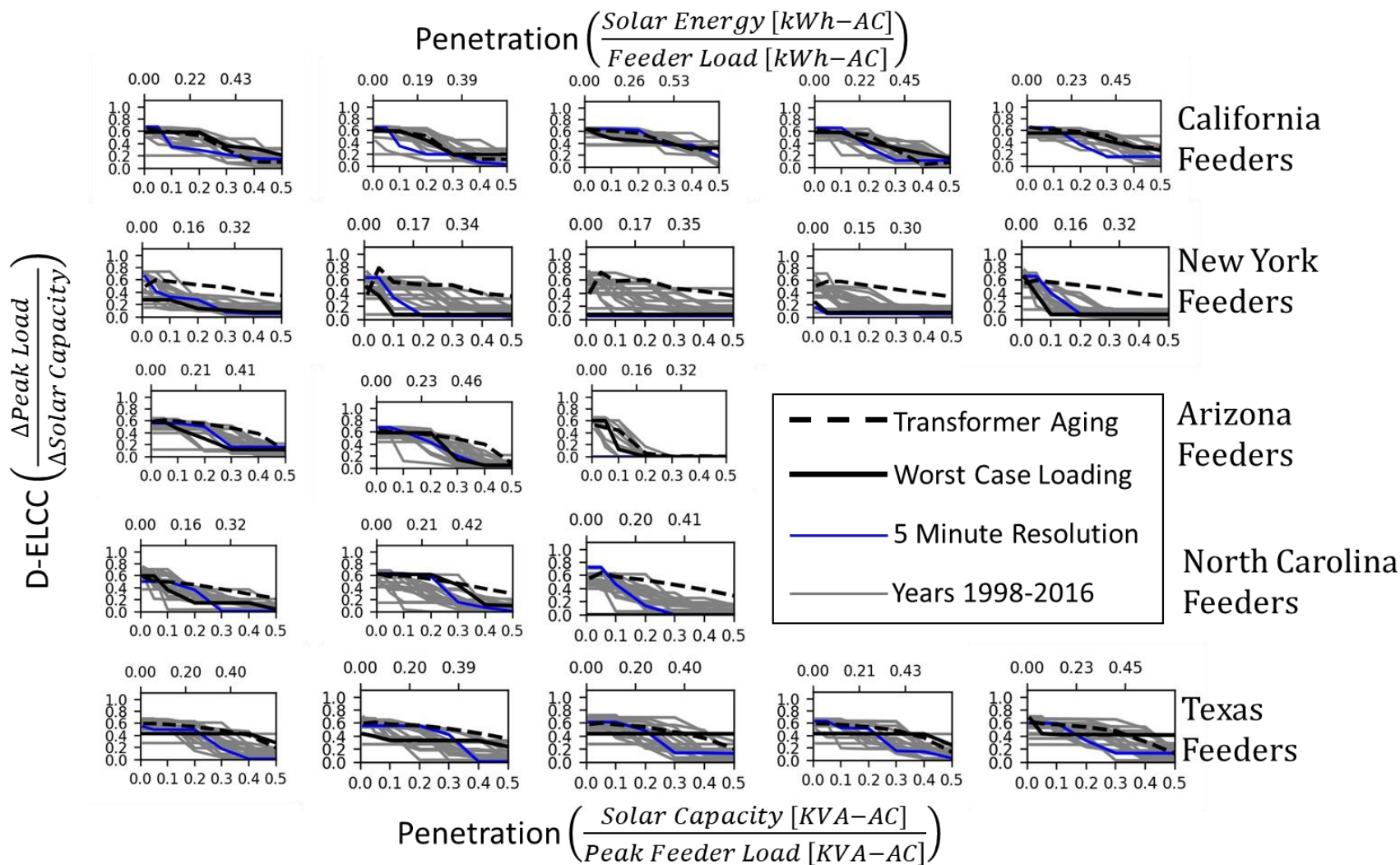


Figure S3: Marginal Distribution-Effective Load Carrying Capability for the PNNL Feeder Taxonomy. Columns show the taxonomy feeders in order from left to right. California Feeders: R1-12.47-1, R1-12.47-2, R1-12.47-3, R1-12.47-4, R1-25.00-1. New York Feeders: R2-12.47-1, R2-12.47-2, R2-12.47-3, R2-25.00-1, R2-35.00-1. Arizona: R3-12.47-1, R3-12.47-2, R3-12.47-3. North Carolina Feeders: R4-12.47-1, R4-12.47-2, R4-25.00-1. Texas feeders: R5-12.47-1, R5-12.47-2, R5-12.47-3, R5-12.47-4, R5-12.47-5.

Average and Marginal D-ELCC for Texas and Minnesota

The following D-ELCC plots were not in the main body of the chapter due to space constraints.

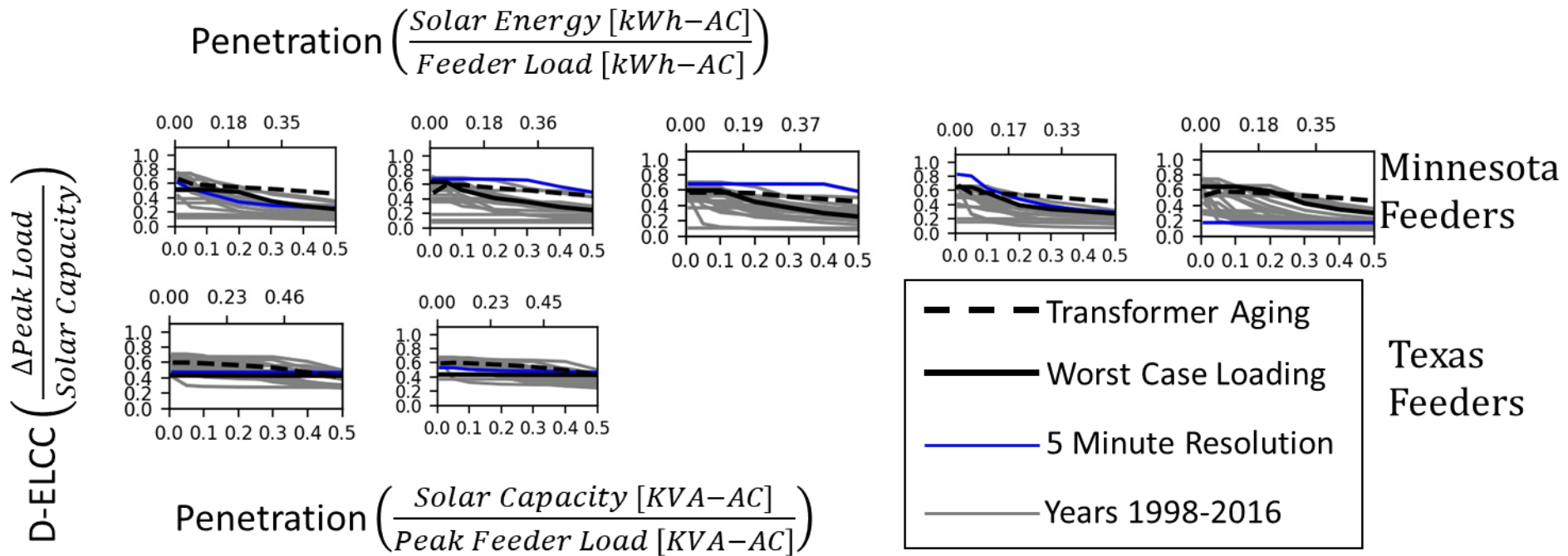


Figure S4: Average Distribution Effective Loading Capability (additional feeders). Columns show the taxonomy feeders in order from left to right. Minnesota Feeders: R2-12.47-1, R2-12.47-2, R2-12.47-3, R2-25.00-1, R2-35.00-1. Texas Feeders: R5-25.00-1, R5-35.00-1

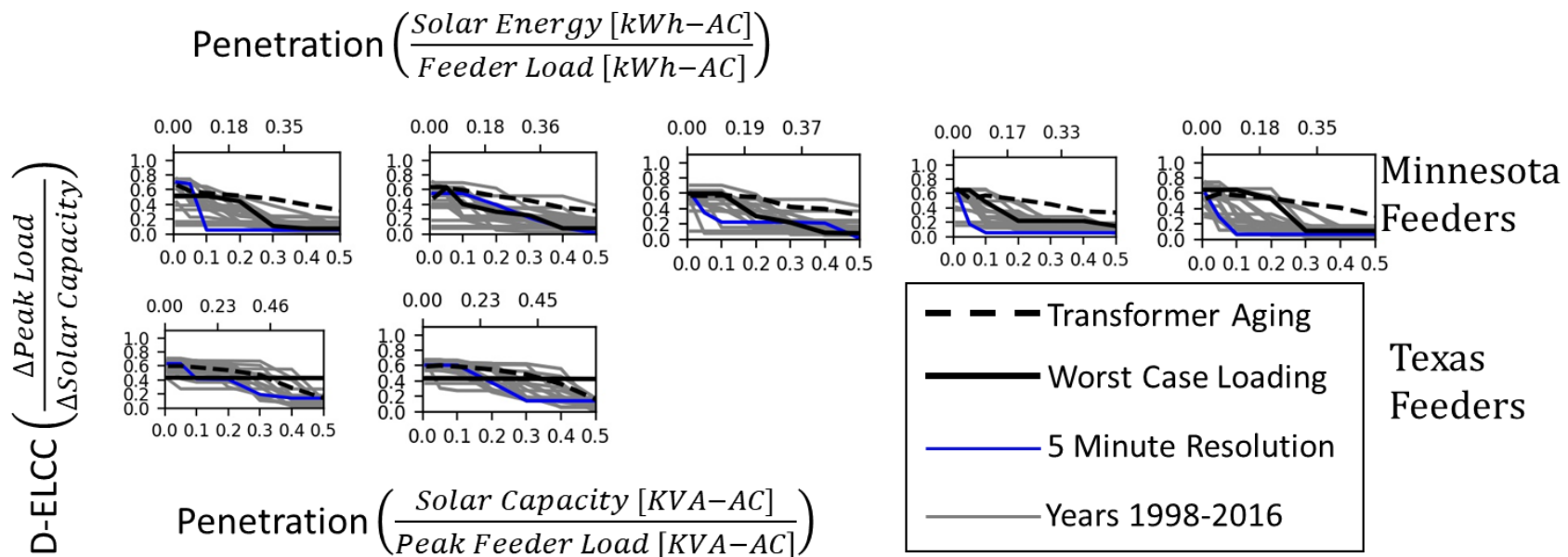


Figure S5: Marginal Distribution Effective Loading Capability (additional feeders). Columns show the taxonomy feeders in order from left to right. Minnesota Feeders: R2-12.47-1, R2-12.47-2, R2-12.47-3, R2-25.00-1, R2-35.00-1. Texas Feeders: R5-25.00-1, R5-35.00-1

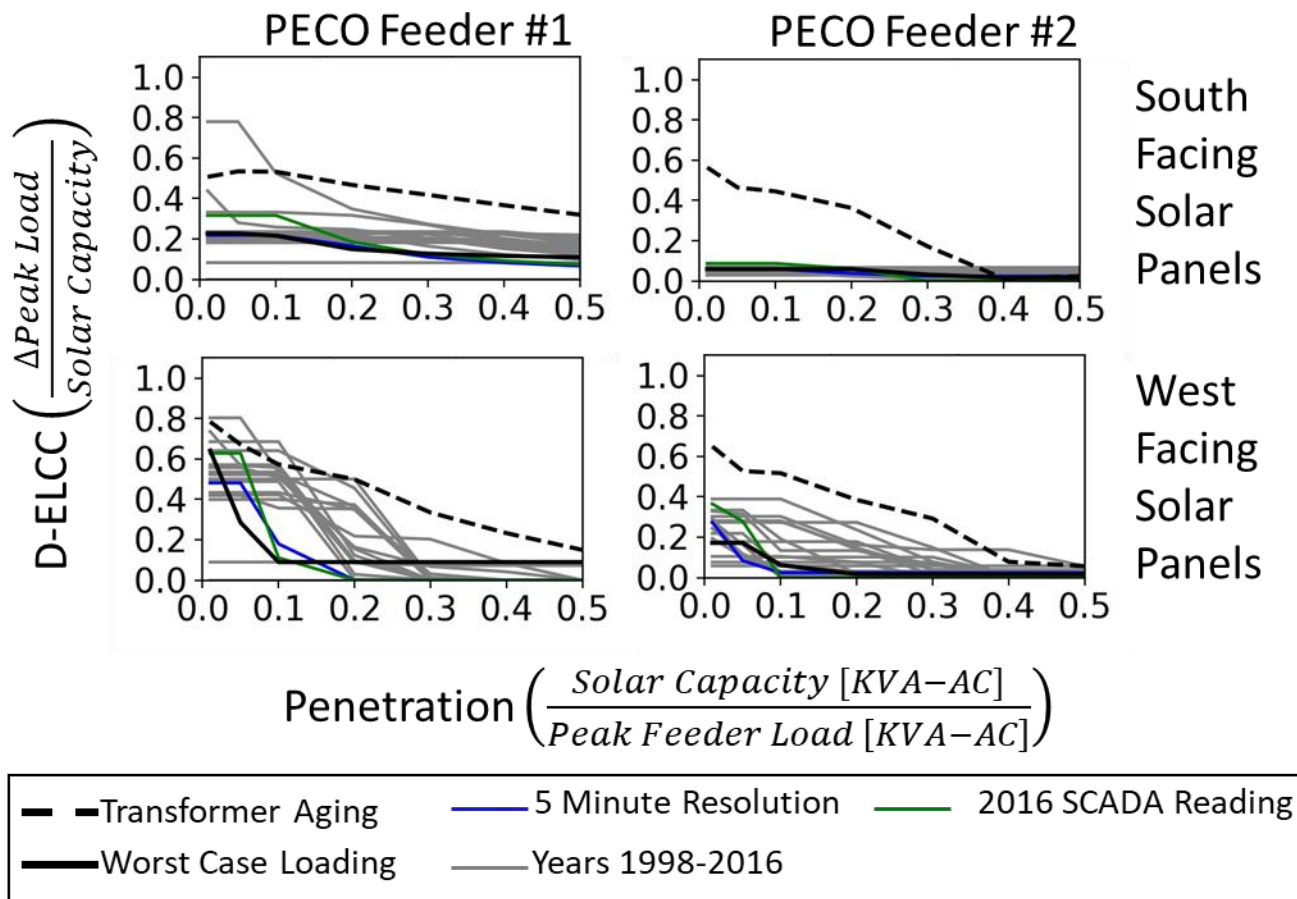
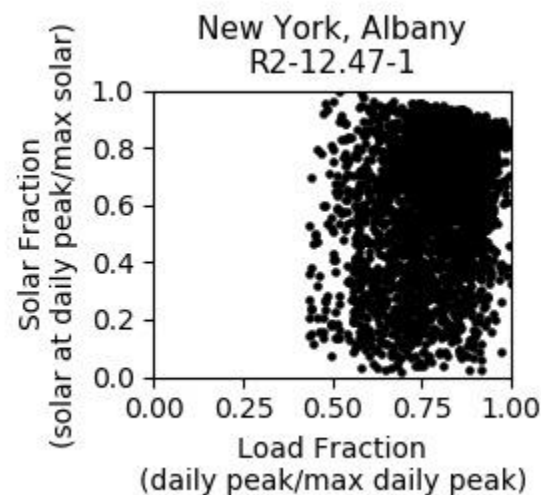
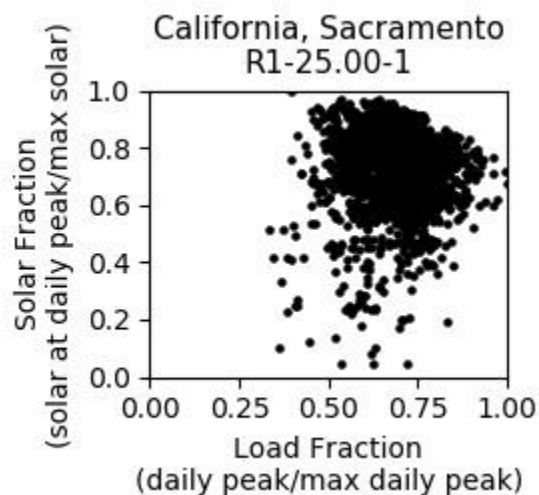
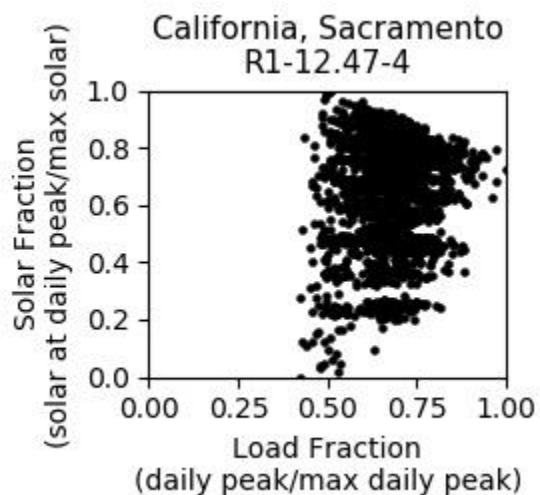
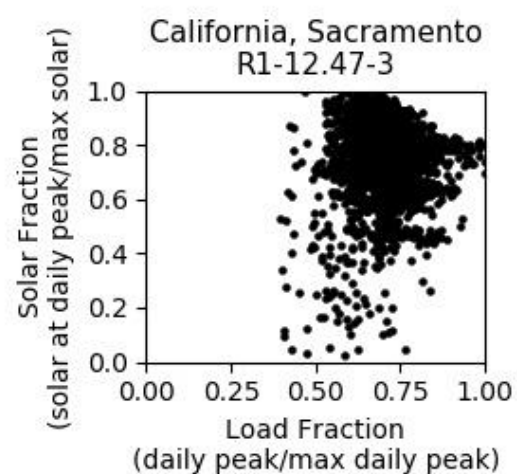
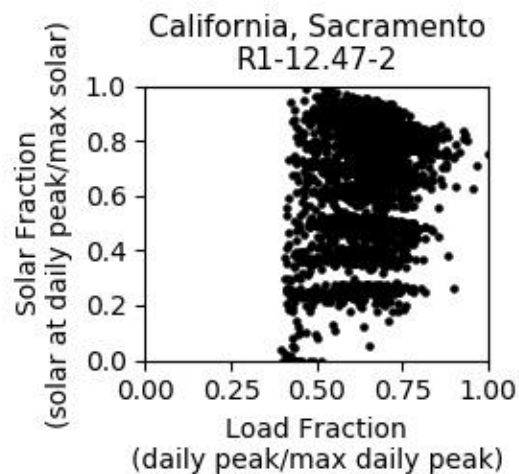
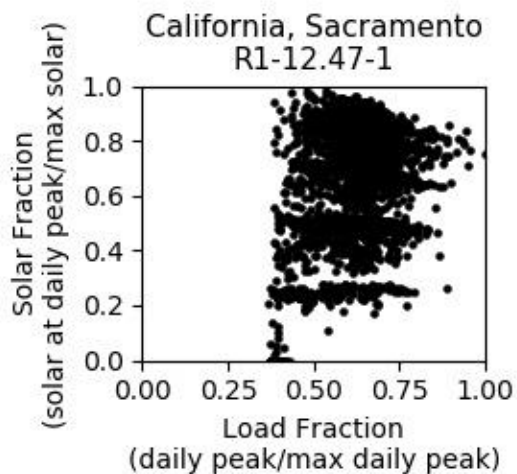
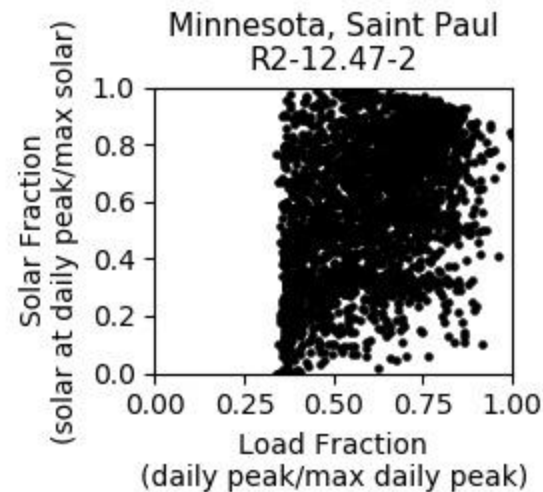
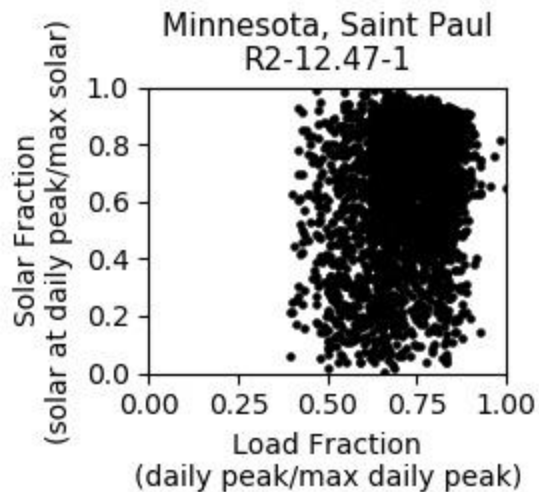
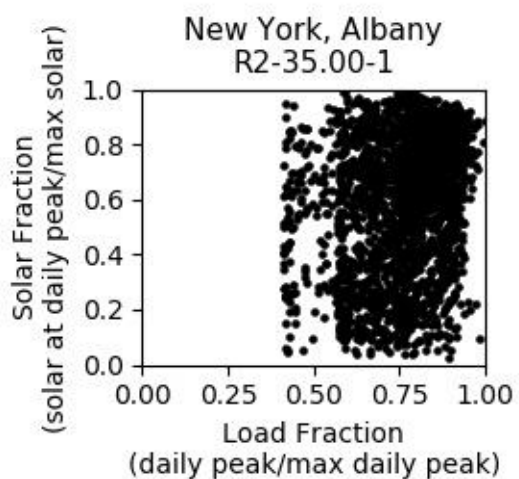
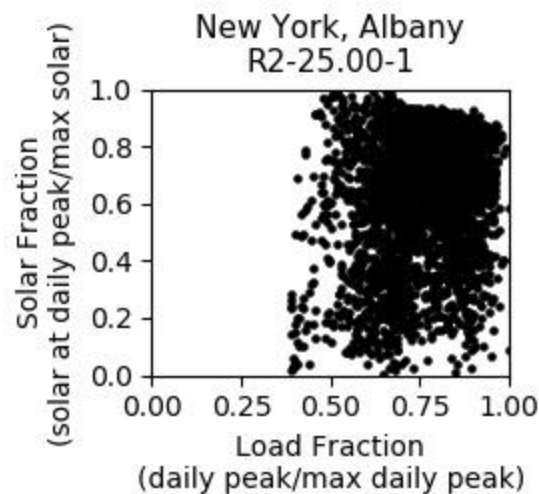
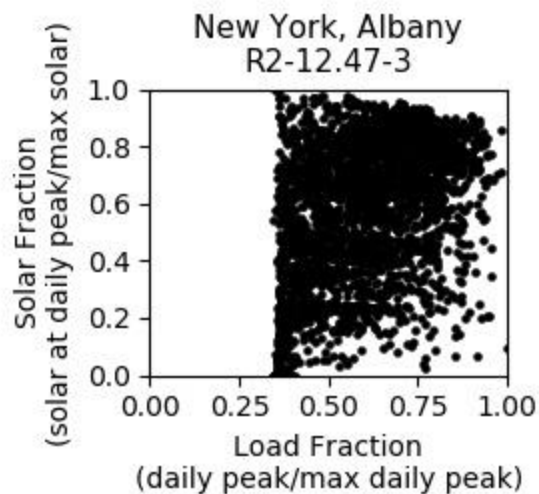
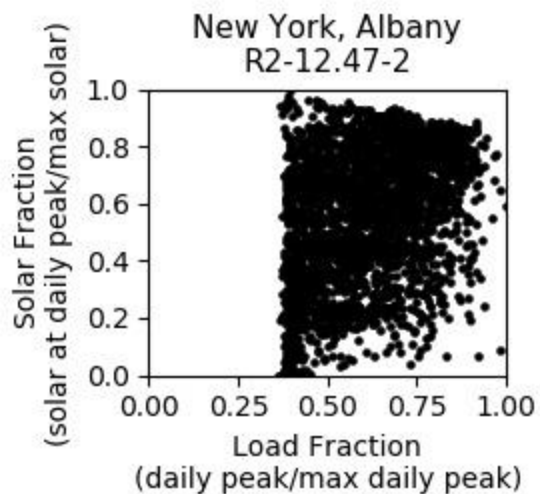
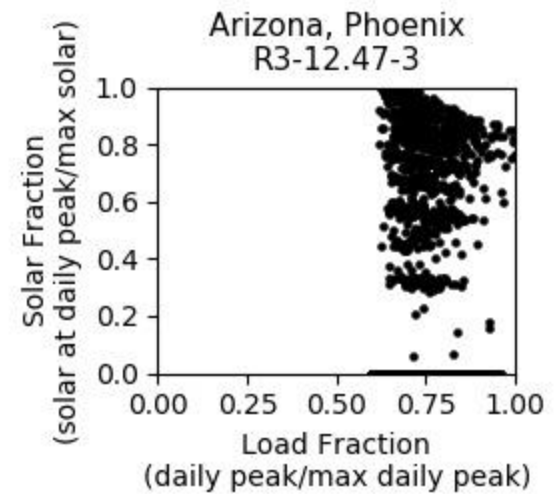
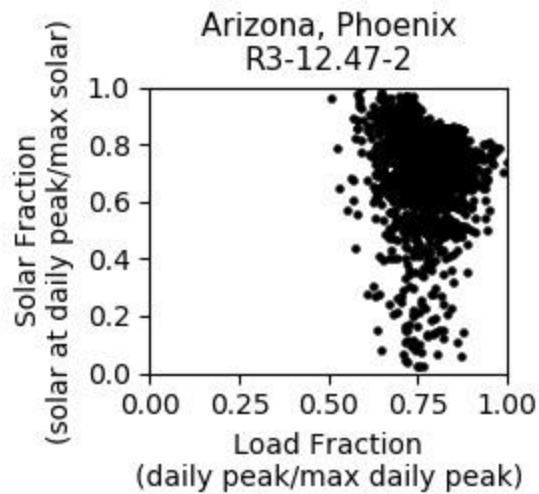
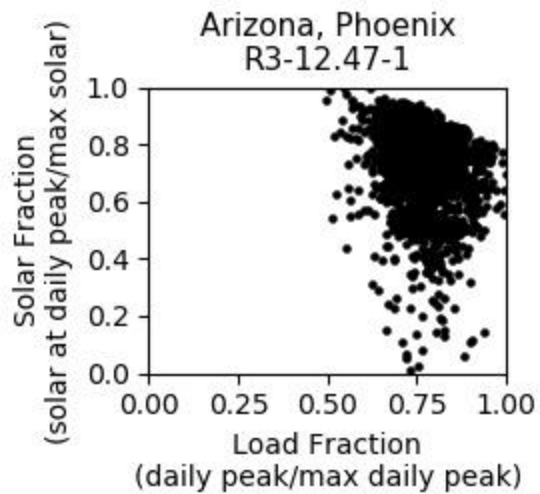
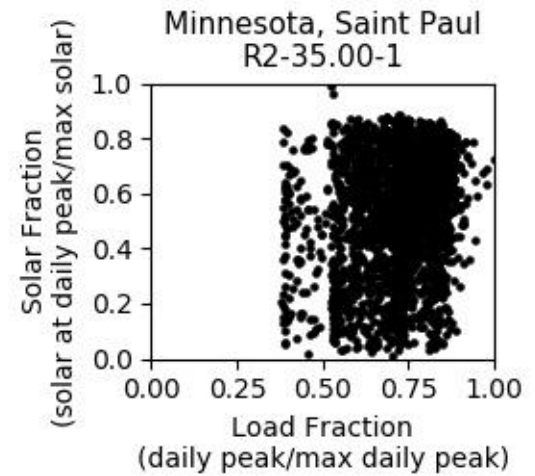
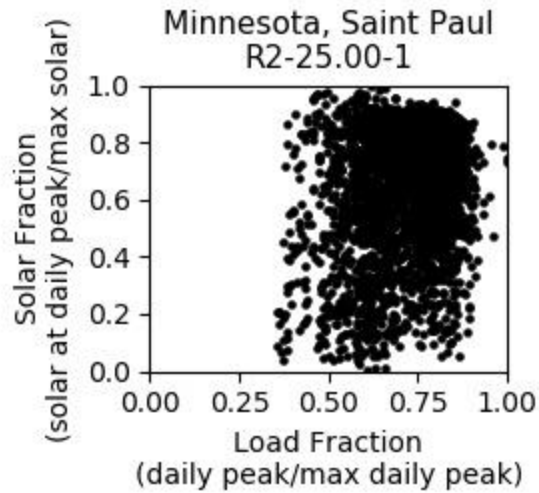
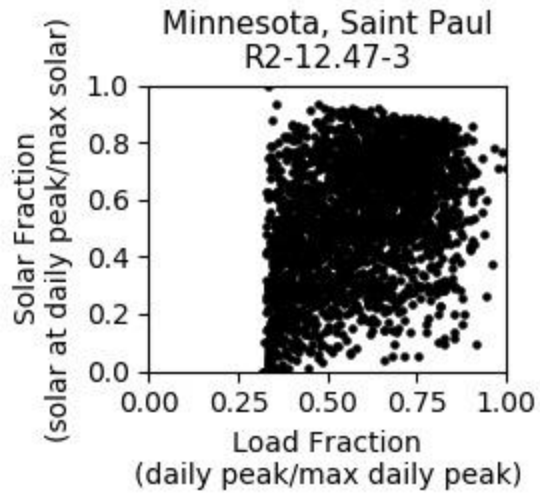


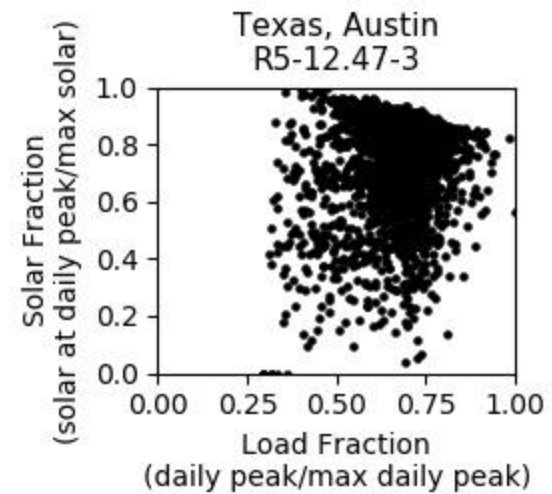
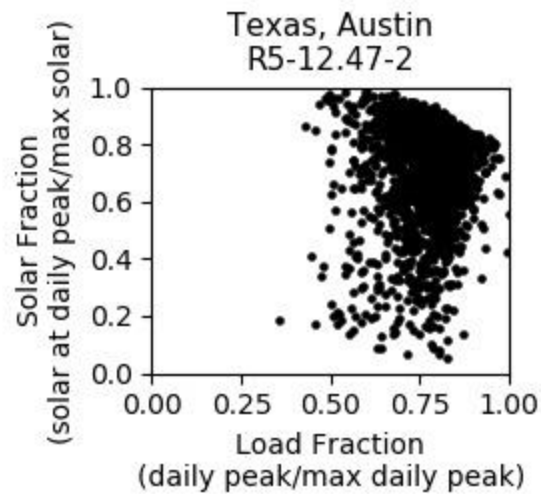
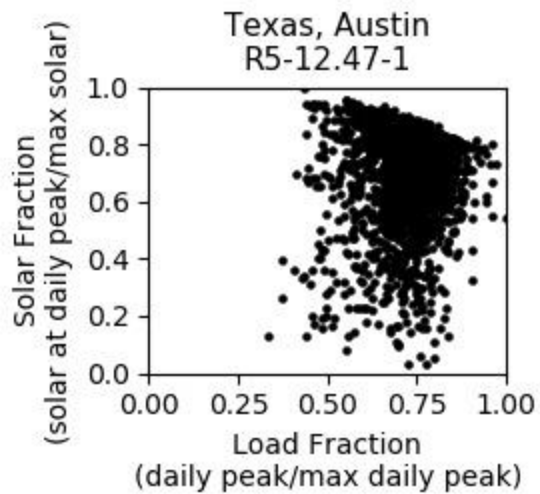
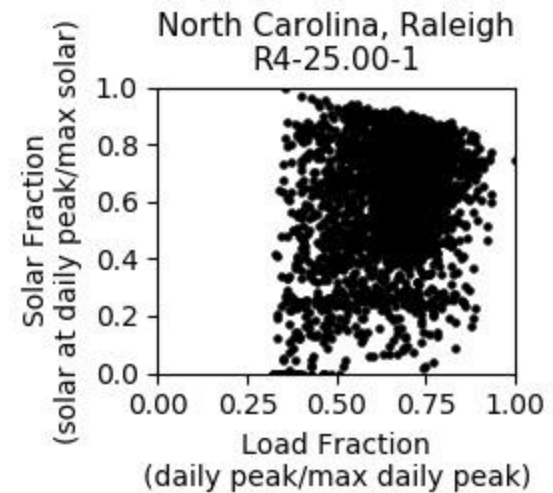
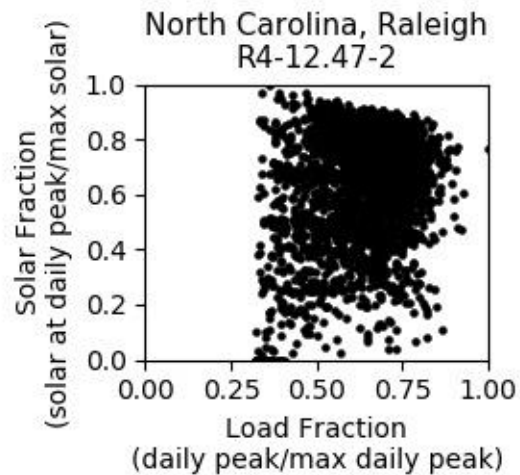
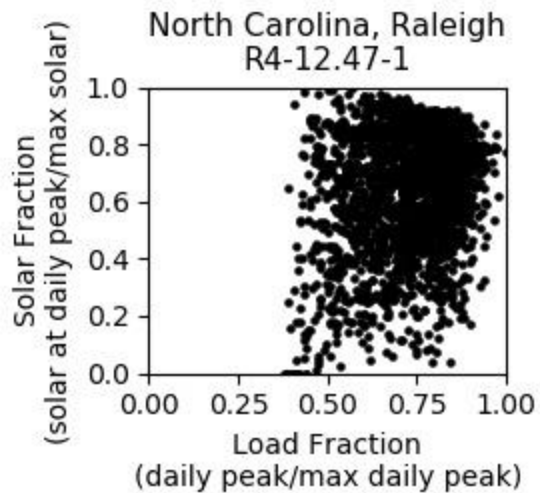
Figure S6: Marginal Distribution Effective Load Carrying Capability for Pennsylvania Feeders.

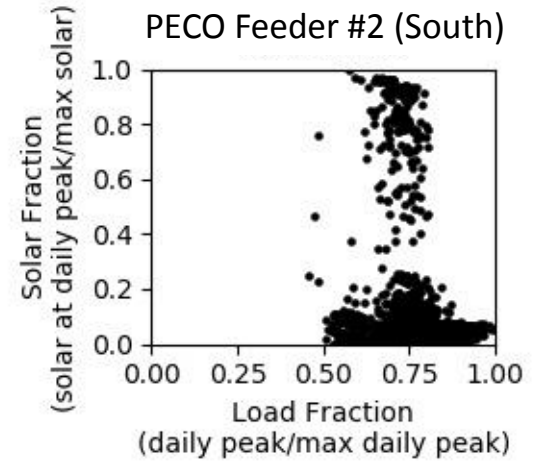
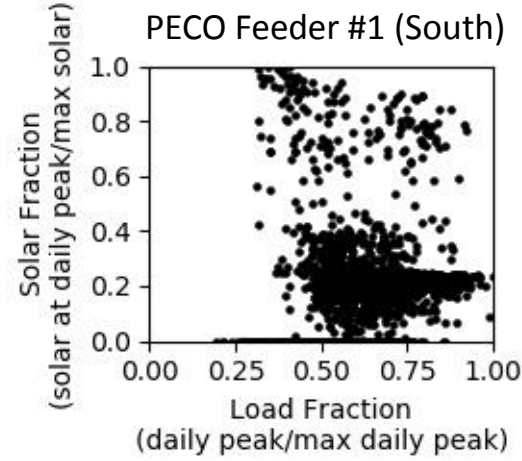
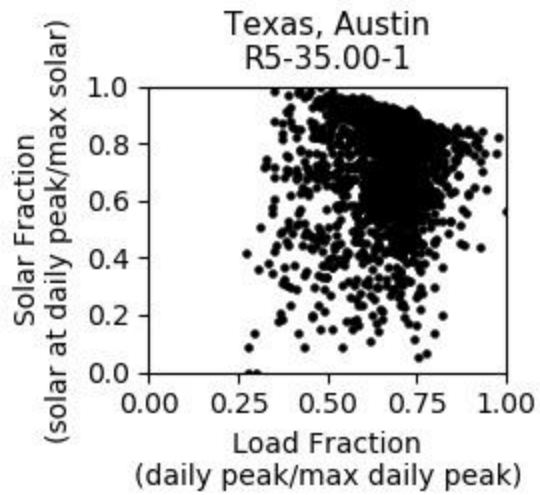
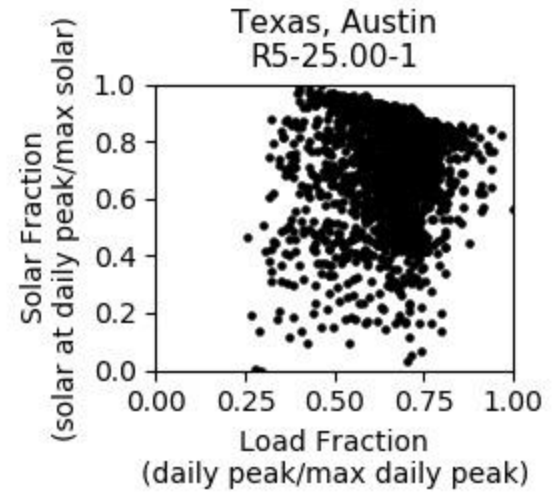
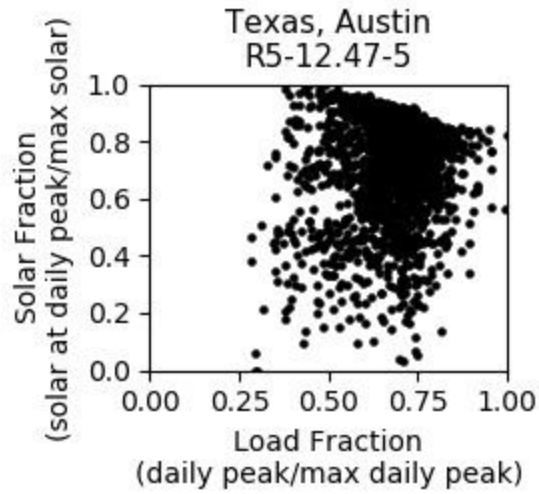
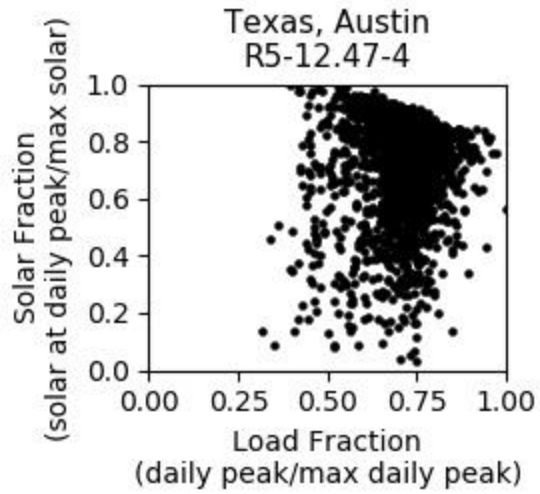
7. Solar Performance Scatterplots











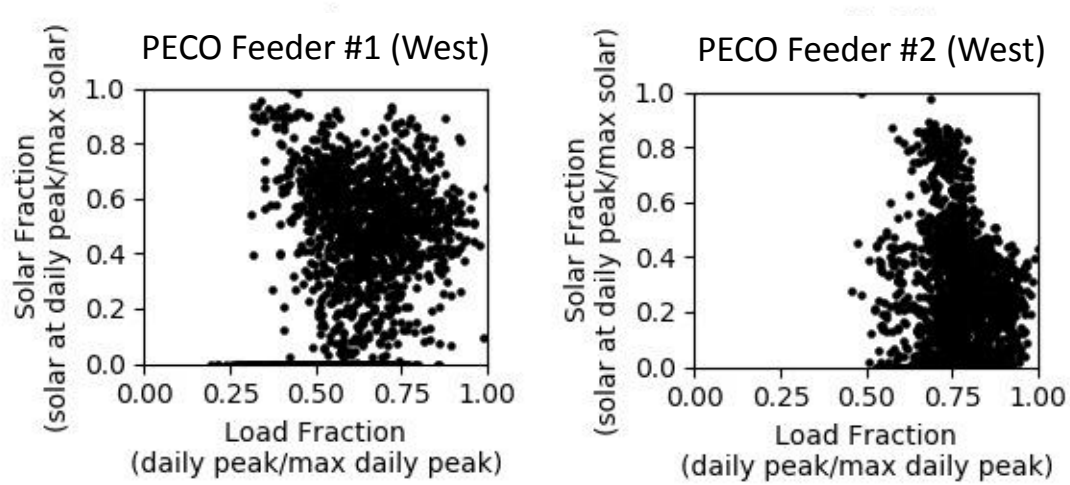
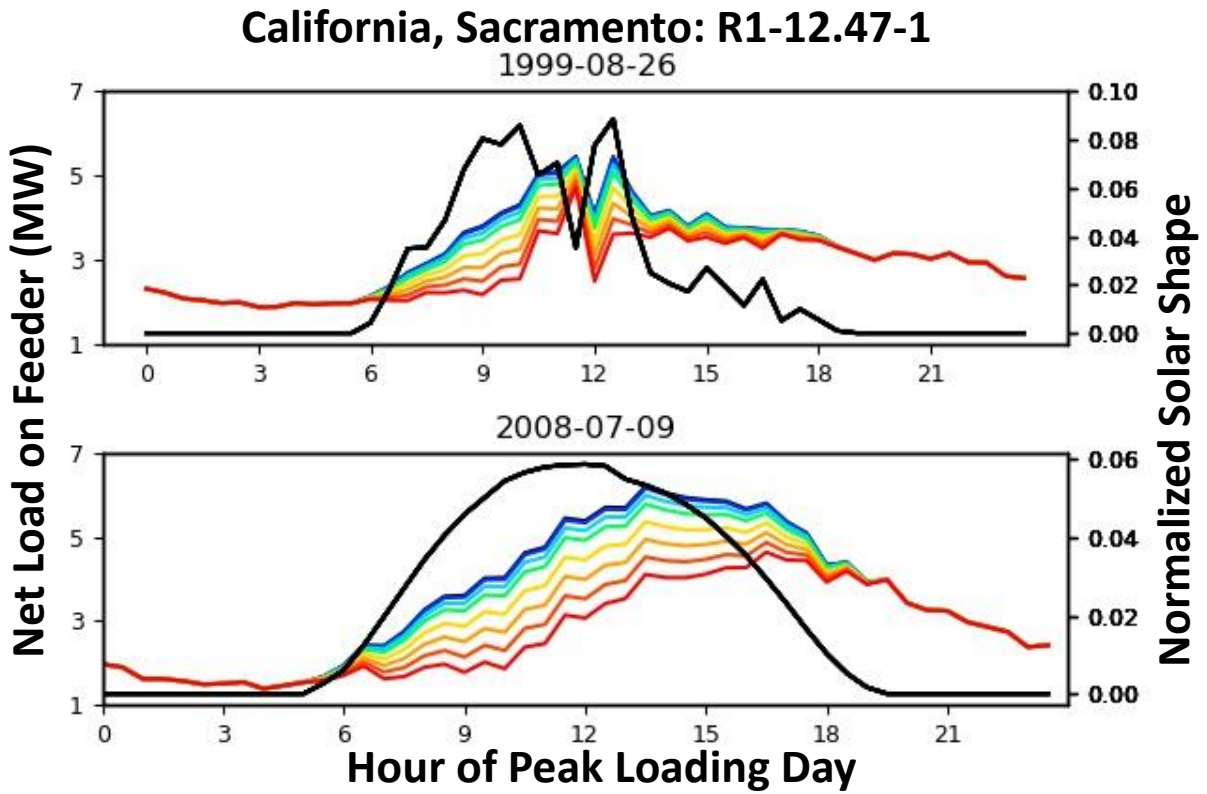
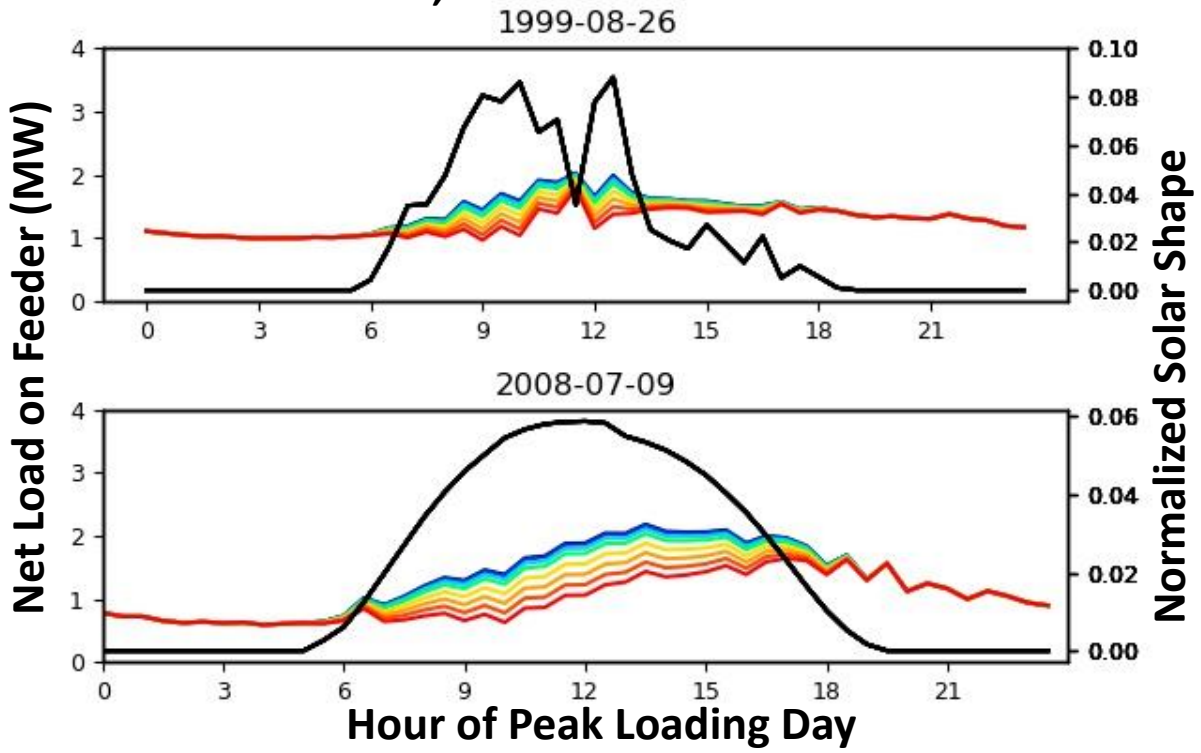


Figure S7: Solar Performance Scatterplot. The solar performance scatterplots show a trend towards greater solar output during peak load events.

Net Load on Peak Days

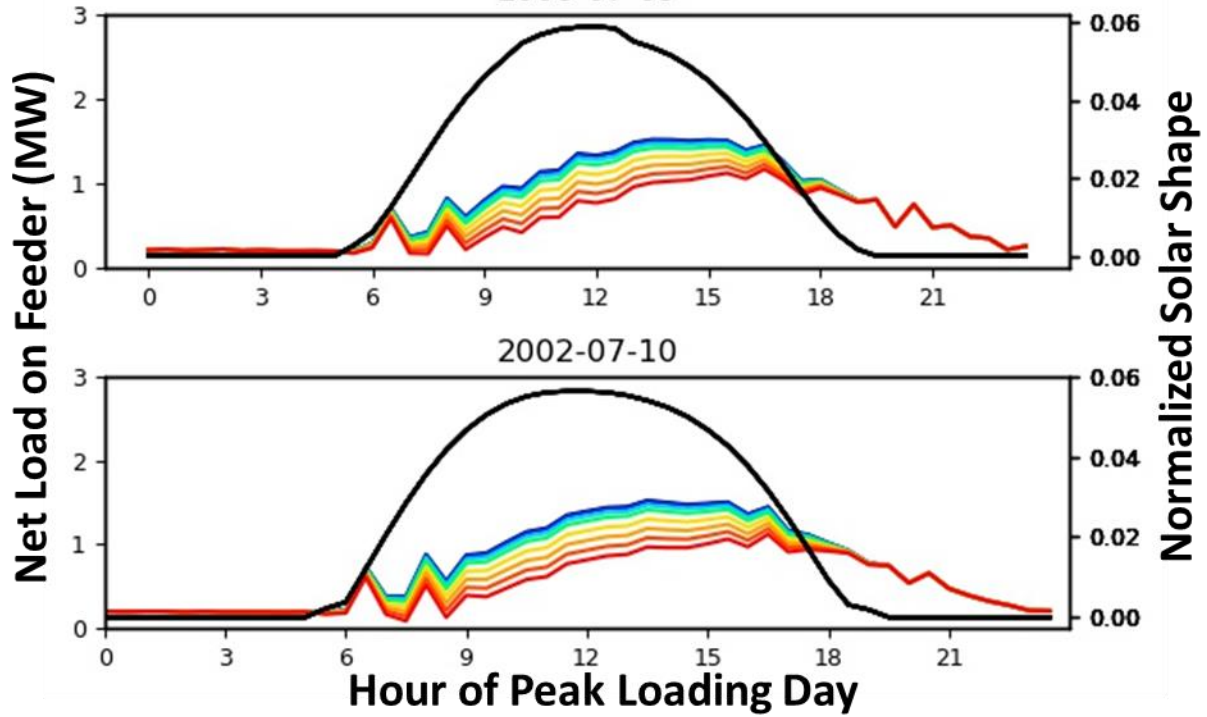


California, Sacramento: R1-12.47-2



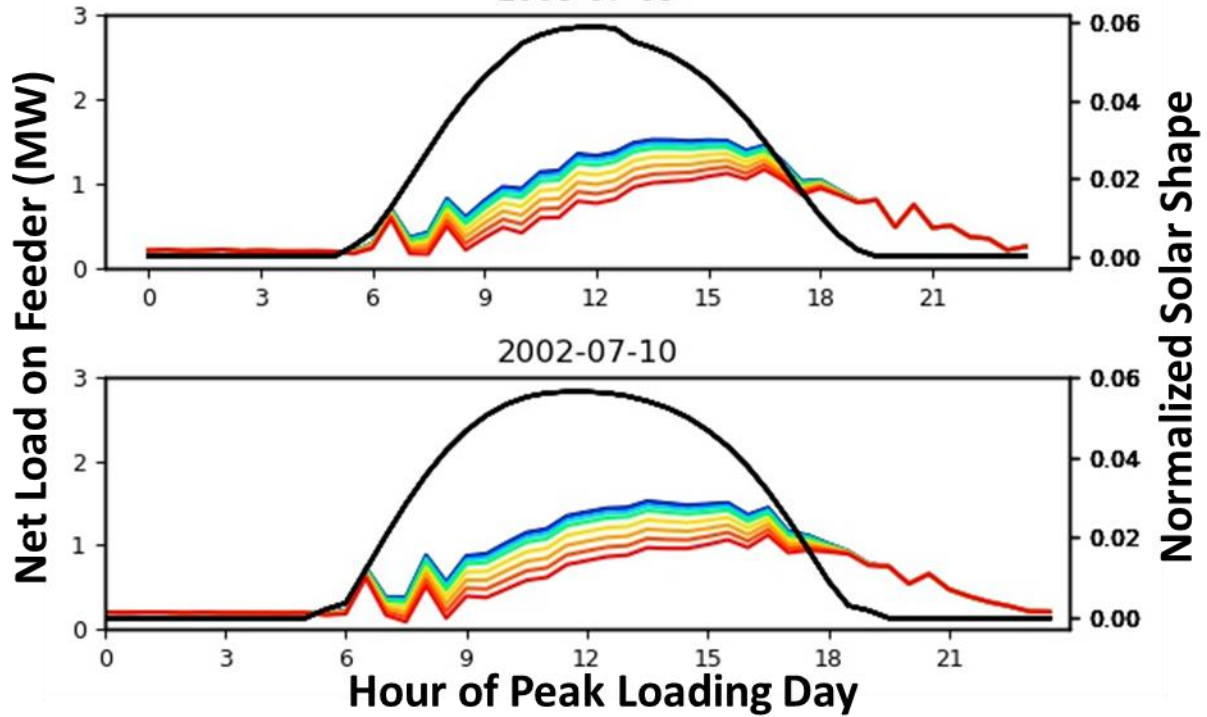
California, Sacramento: R1-12.47-3

2008-07-09



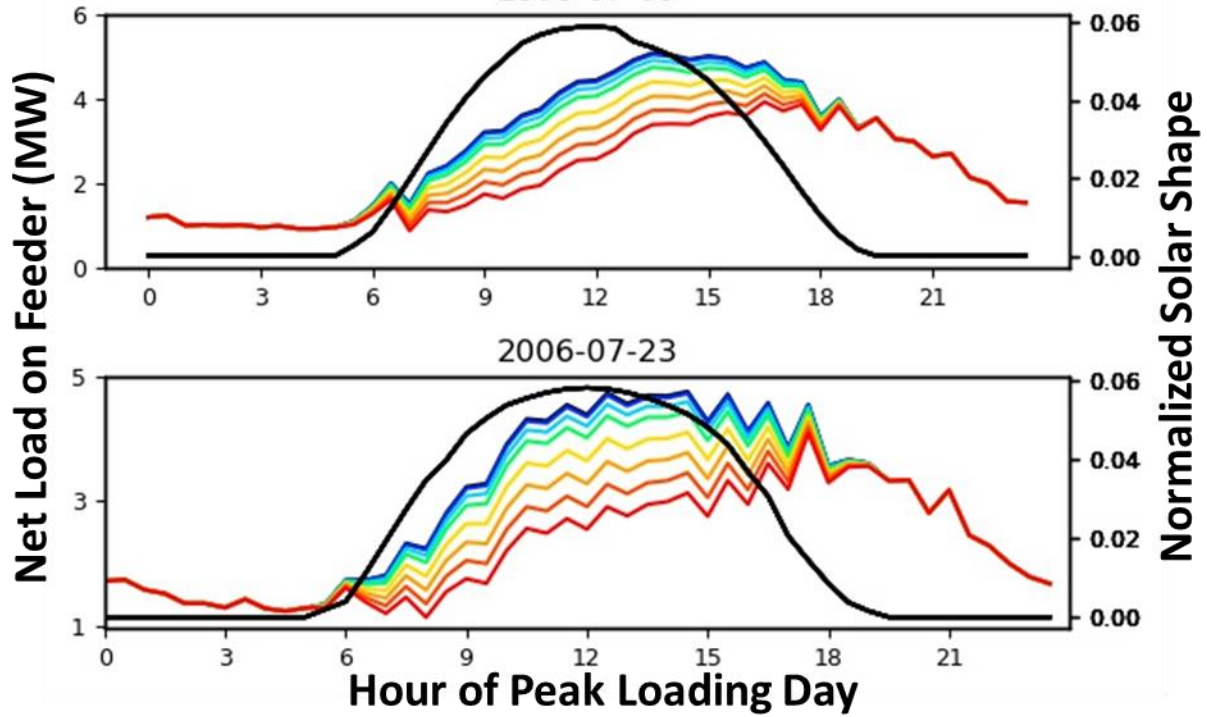
California, Sacramento: R1-12.47-3

2008-07-09



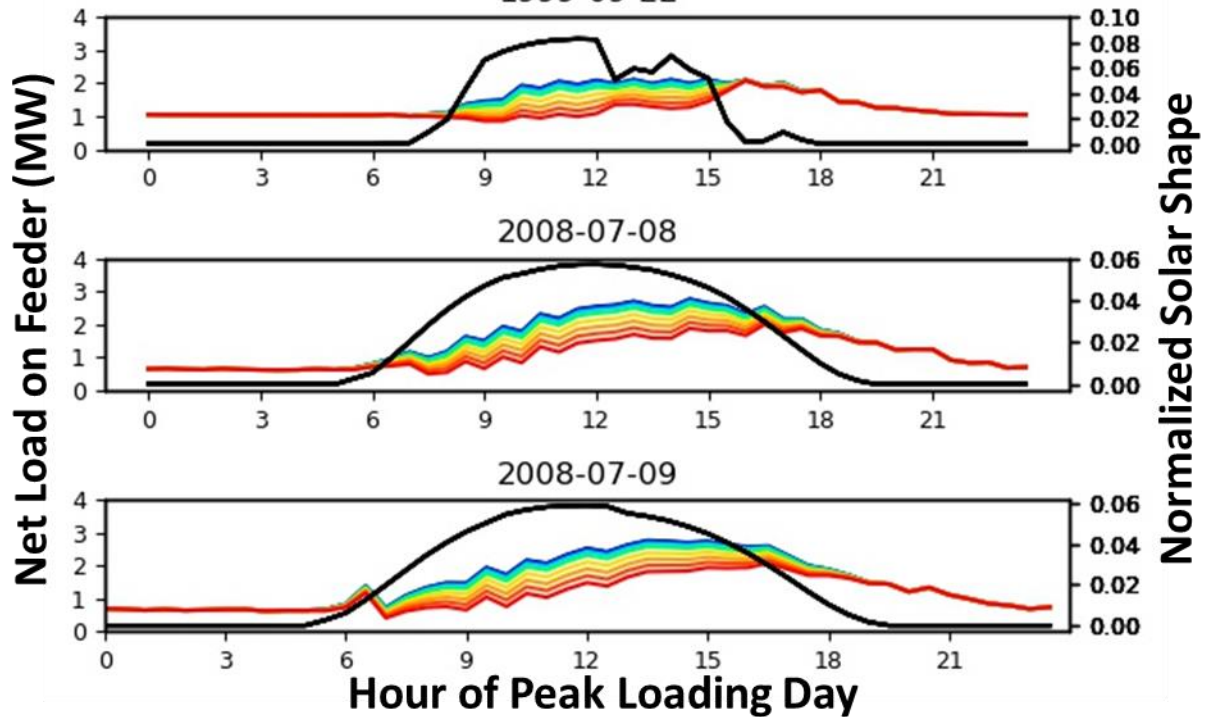
California, Sacramento: R1-12.47-4

2008-07-09



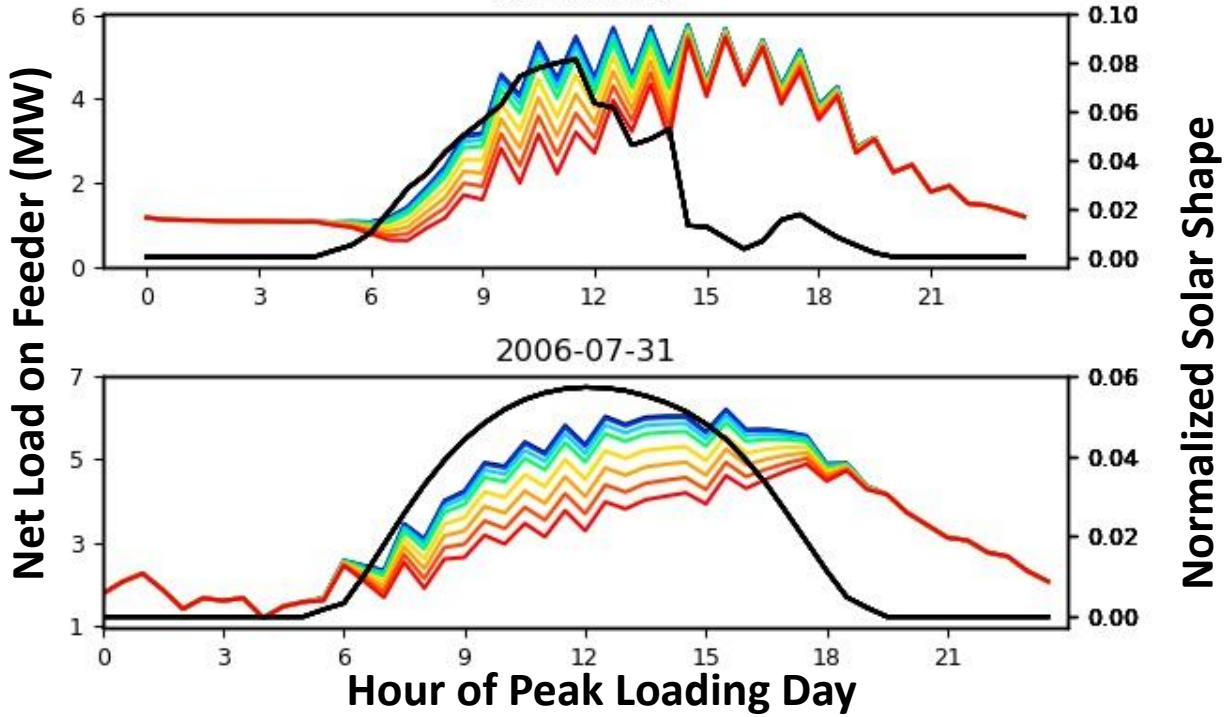
California, Sacramento: R1-25.00-1

1999-09-22



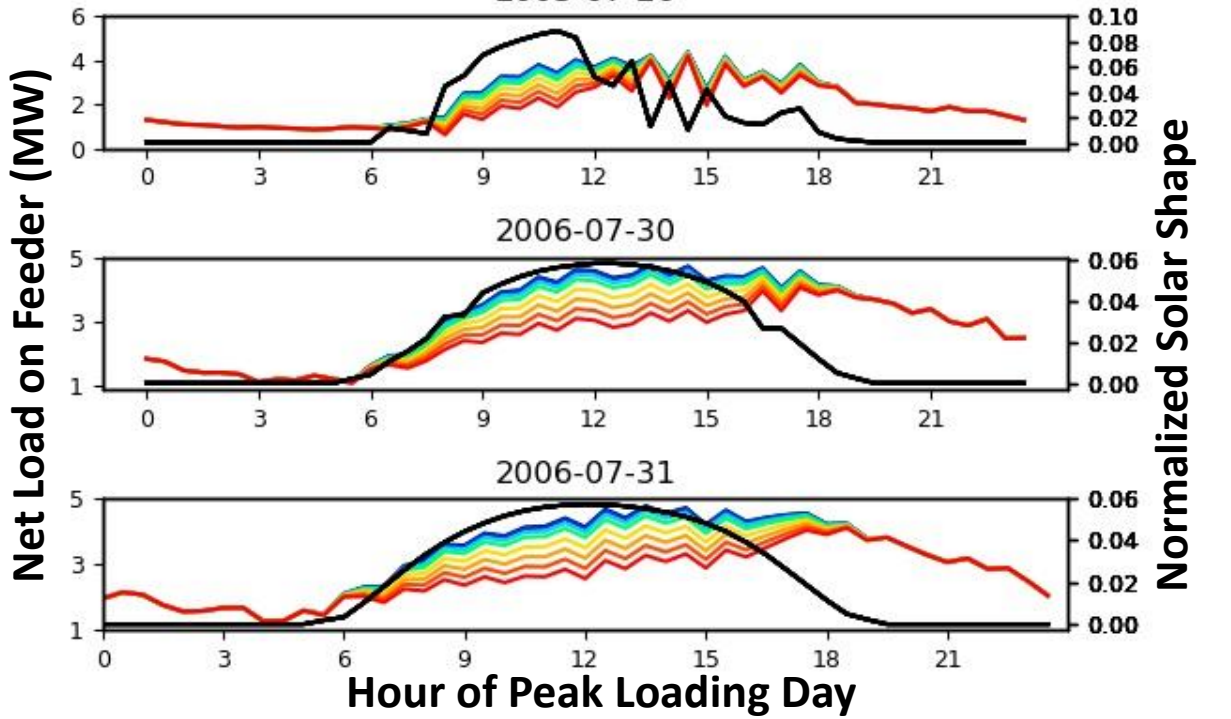
Minnesota, Saint Paul: R2-12.47-1

2016-06-10



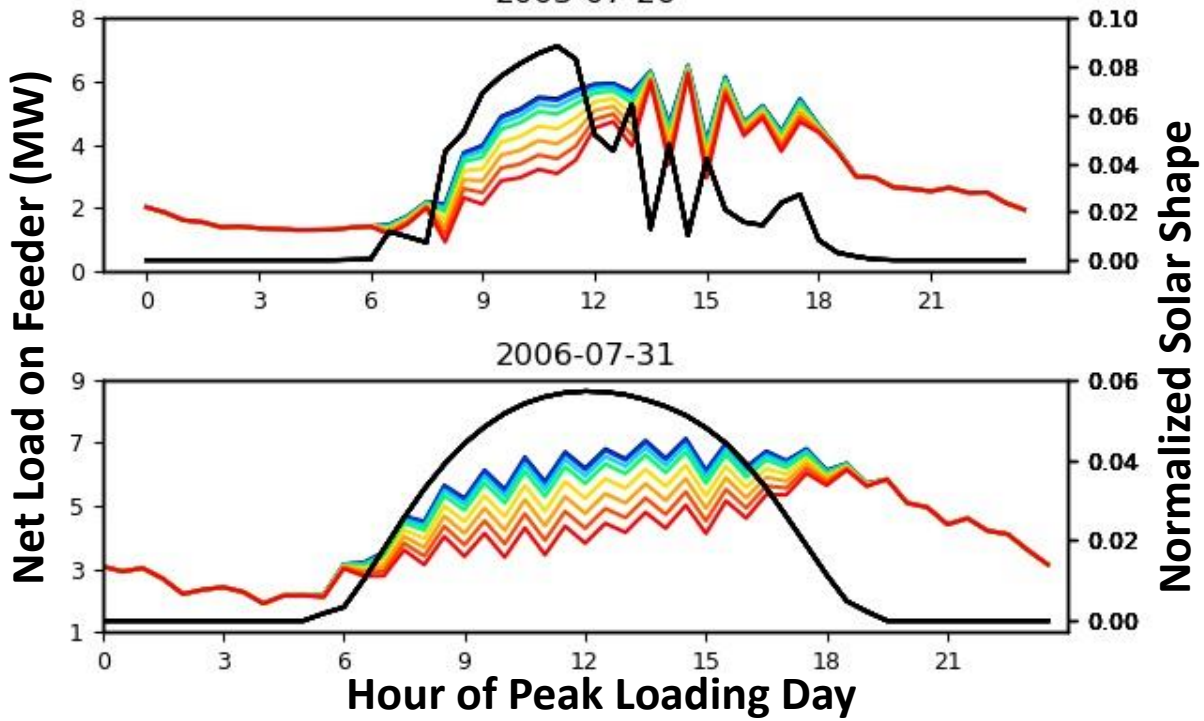
Minnesota, Saint Paul: R2-12.47-2

2003-07-26



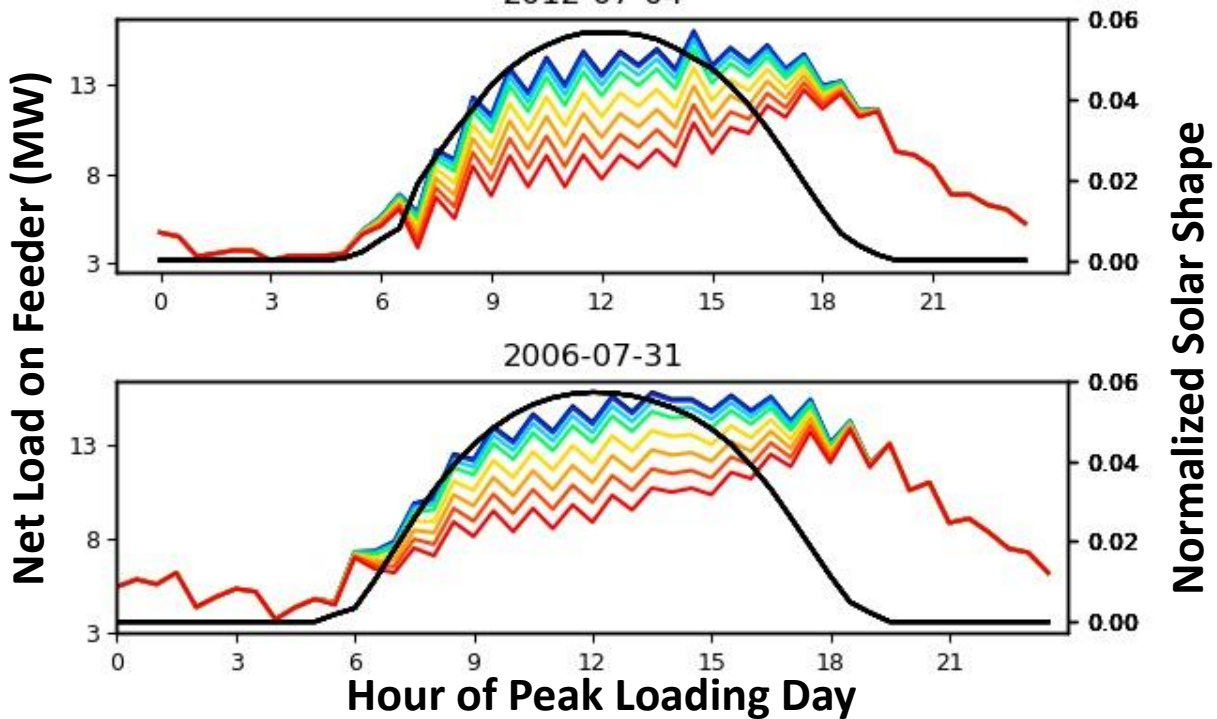
Minnesota, Saint Paul: R2-12.47-3

2003-07-26



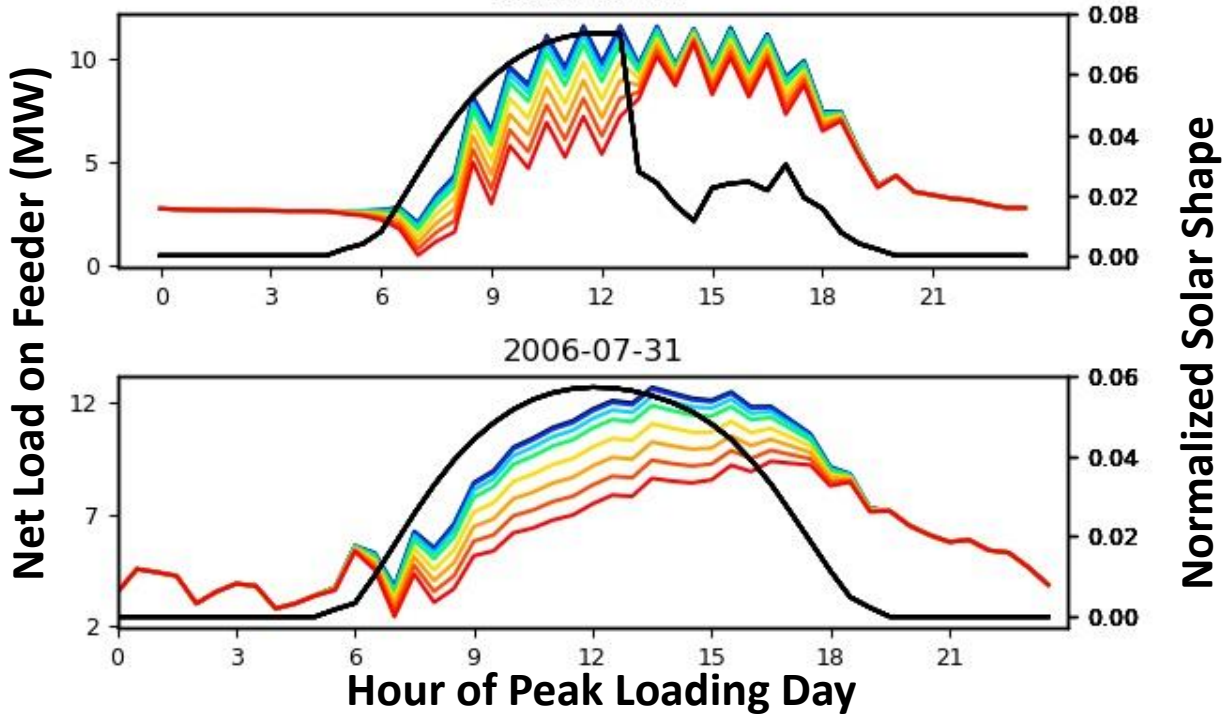
Minnesota, Saint Paul: R2-25.00-1

2012-07-04



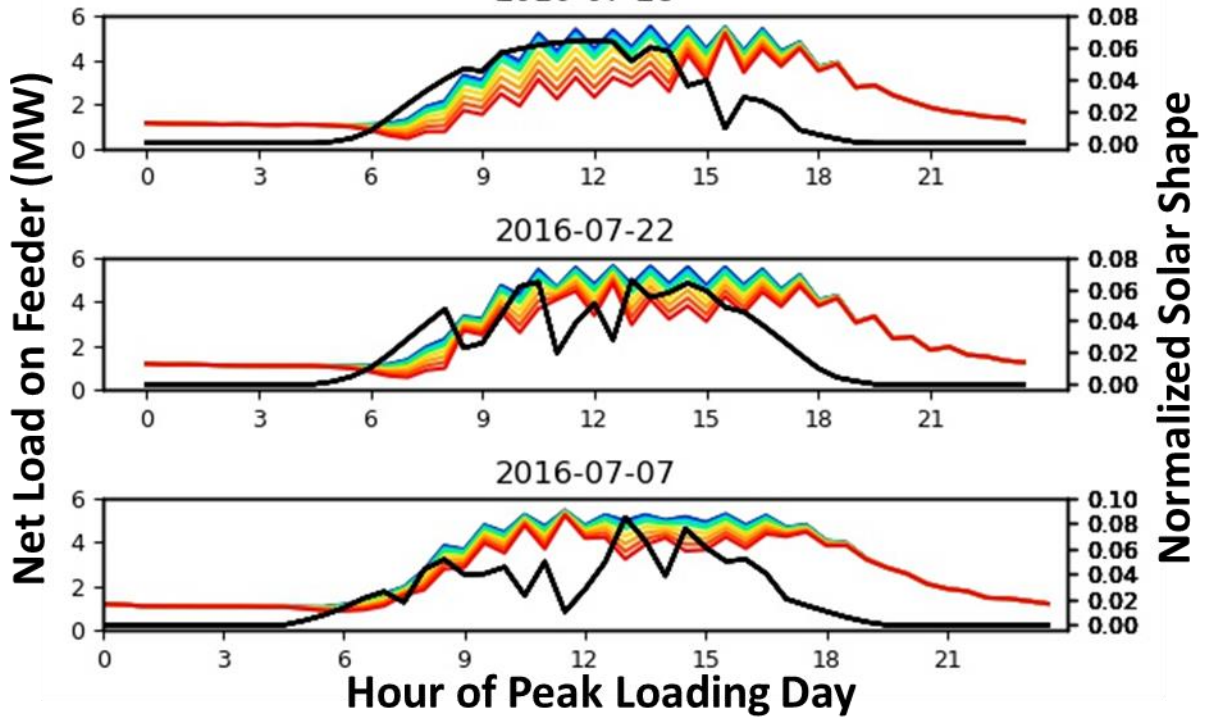
Minnesota, Saint Paul: R2-35.00-1

2009-06-23

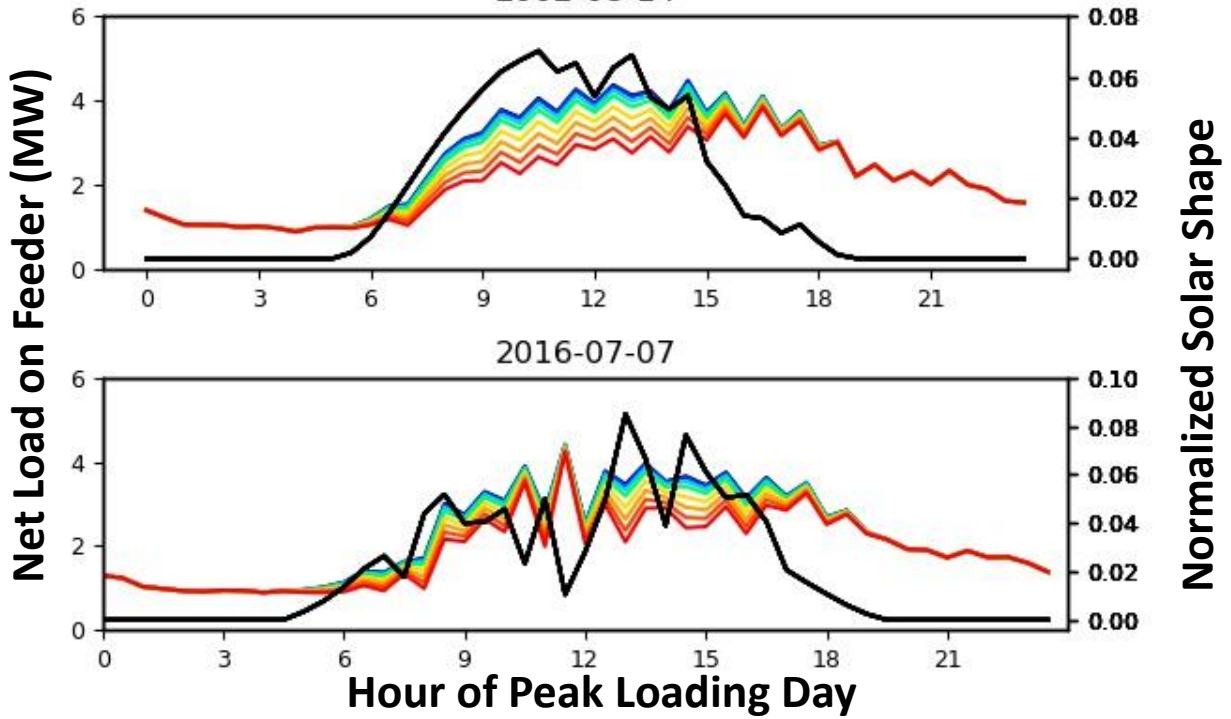


New York, Albany: R2-12.47-1

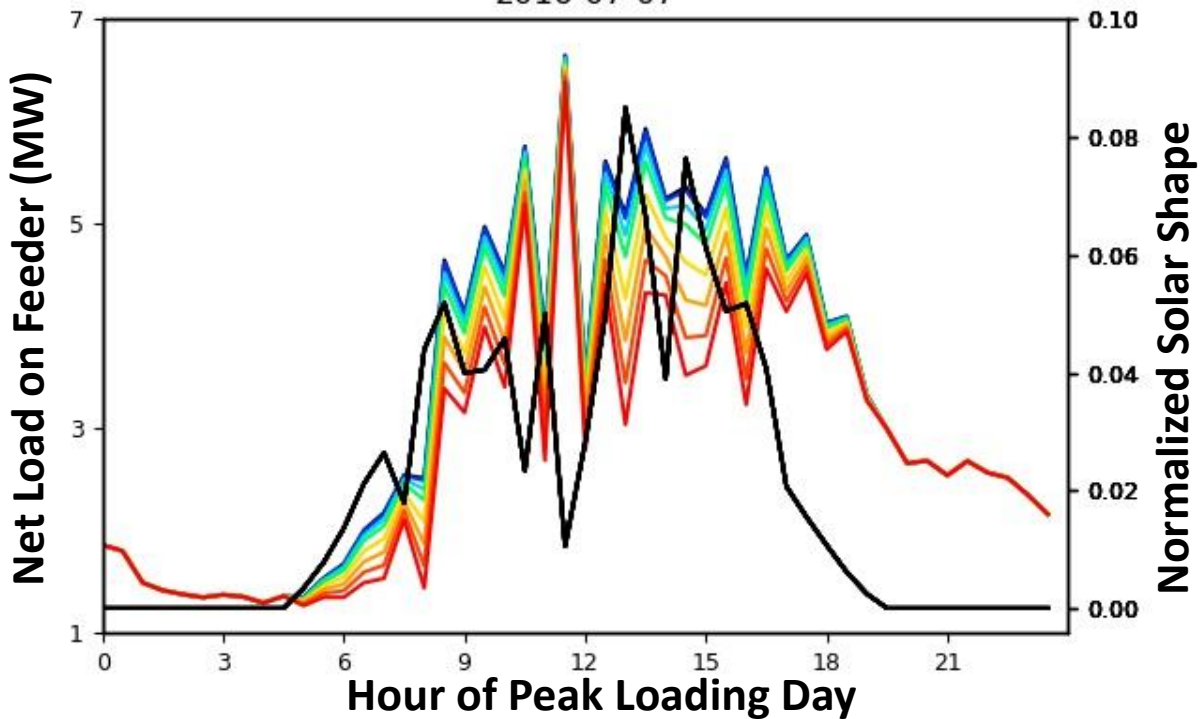
2010-07-28



New York, Albany: R2-12.47-2
2002-08-14

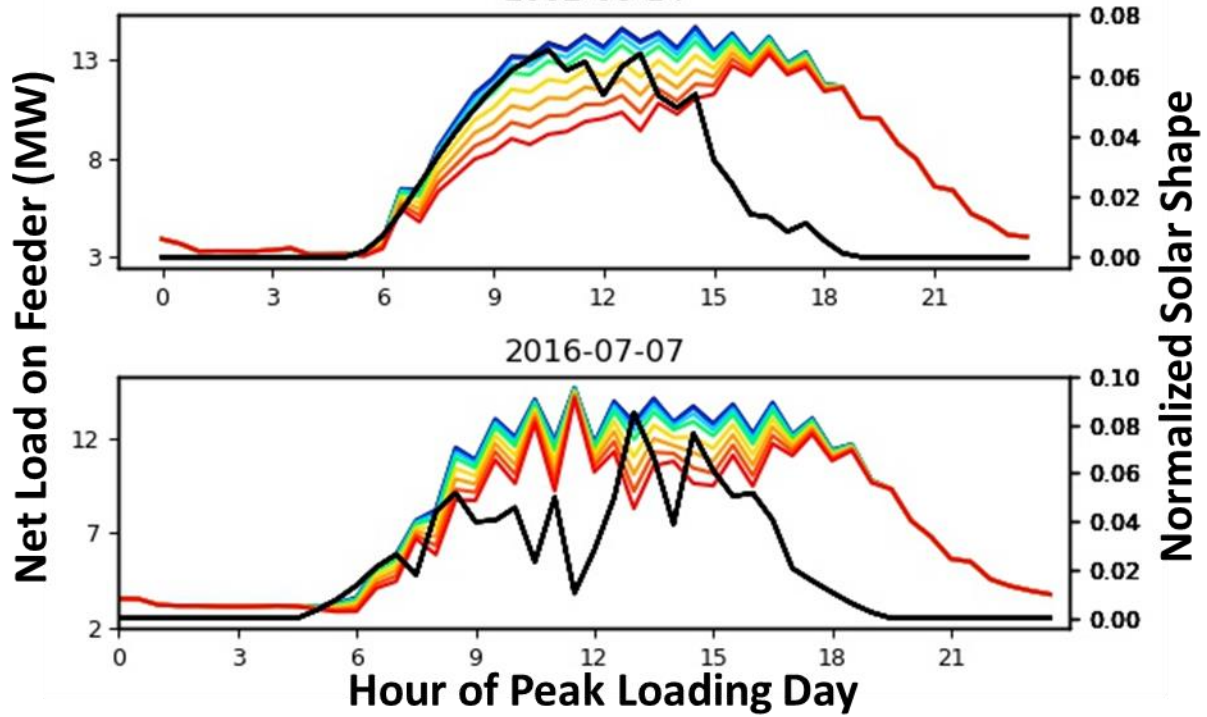


New York, Albany: R2-12.47-3
2016-07-07



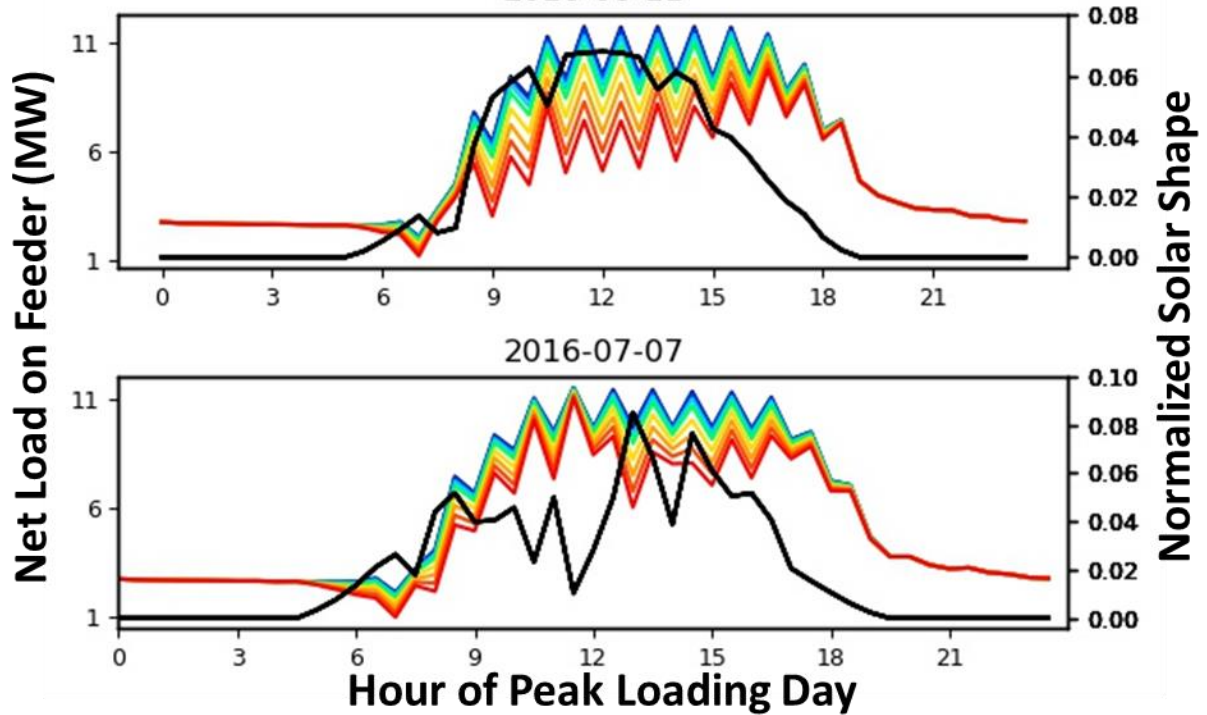
New York, Albany: R2-25.00-1

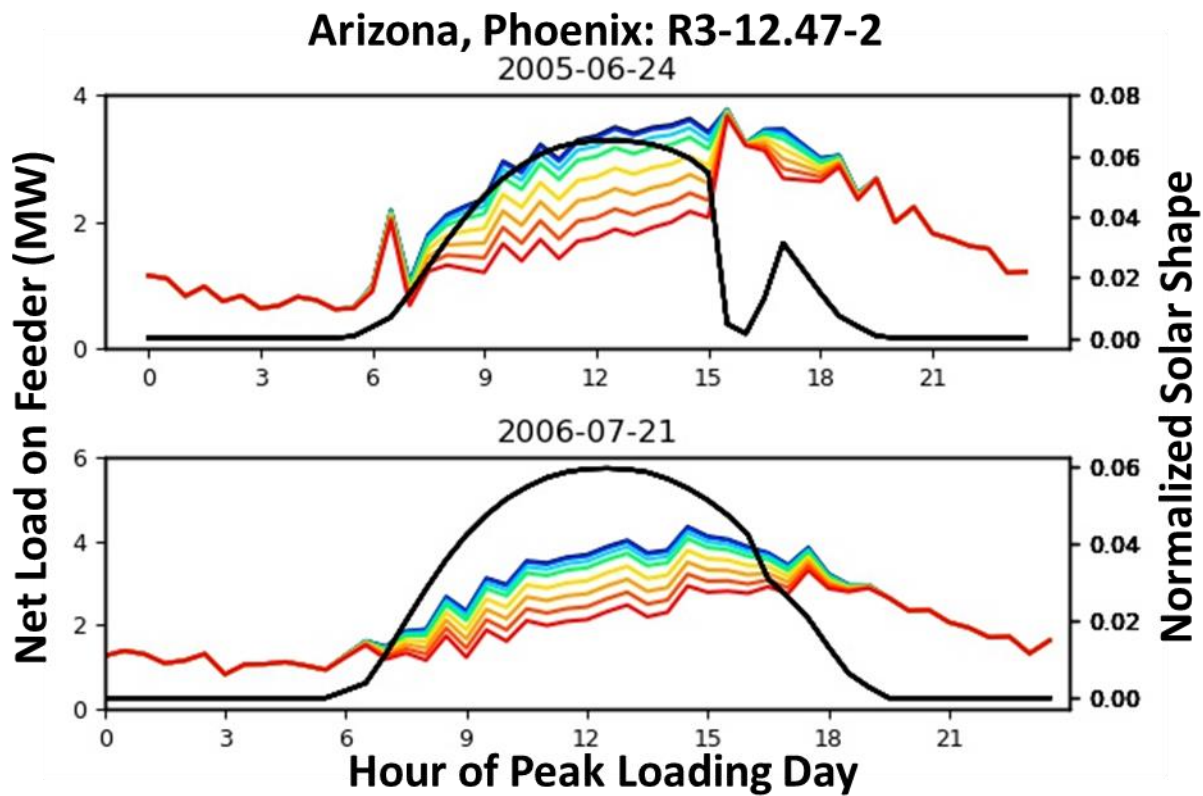
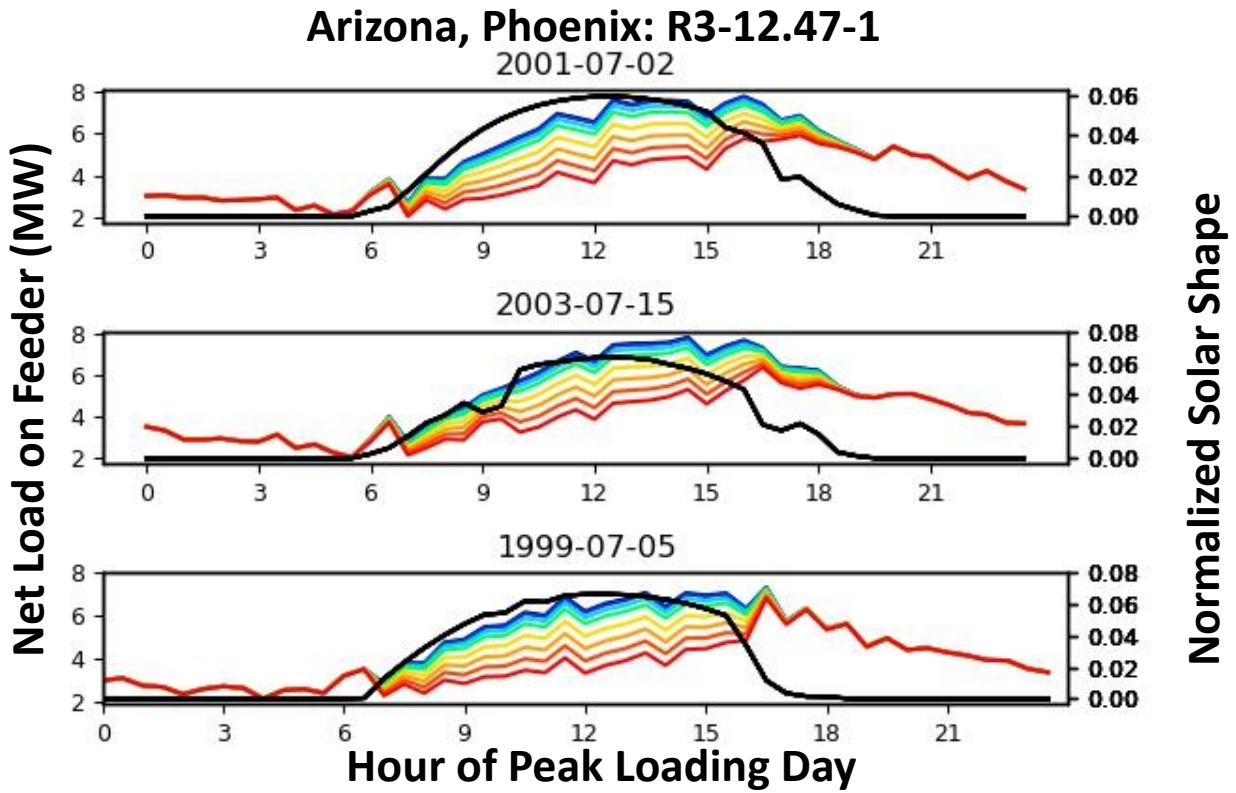
2002-08-14

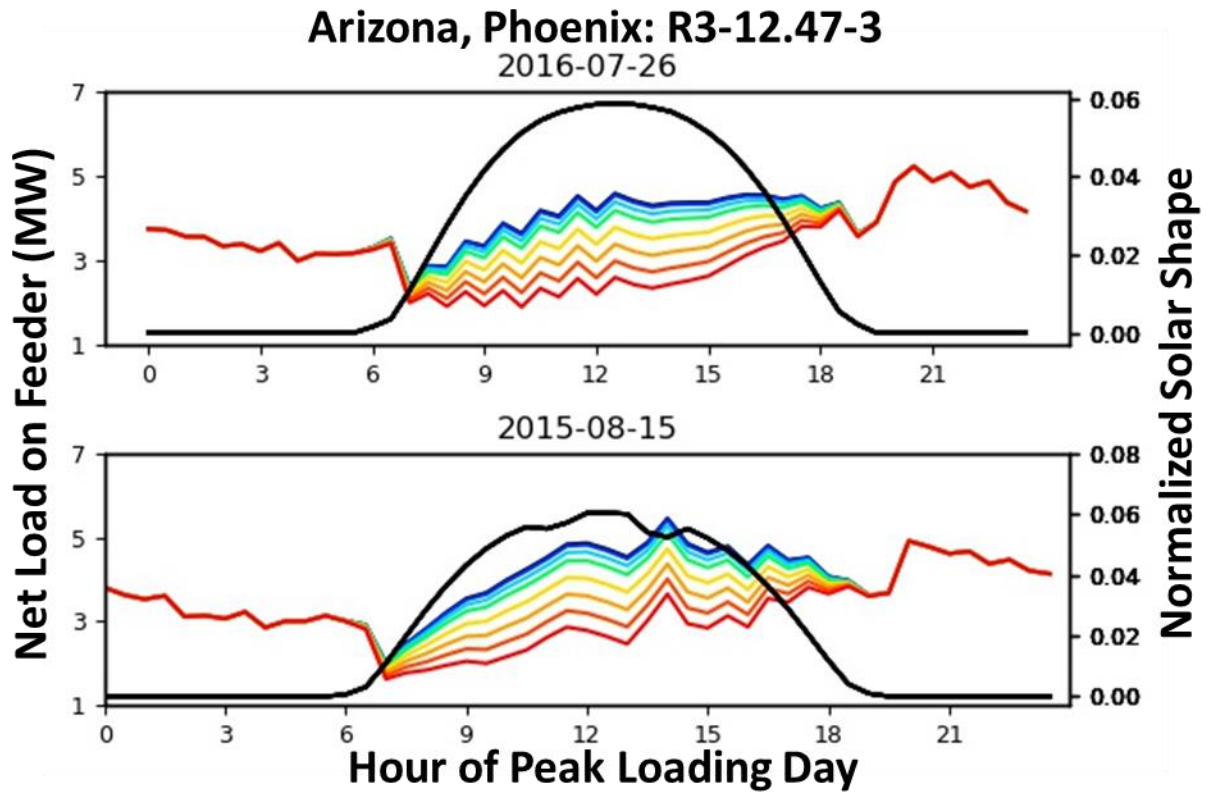


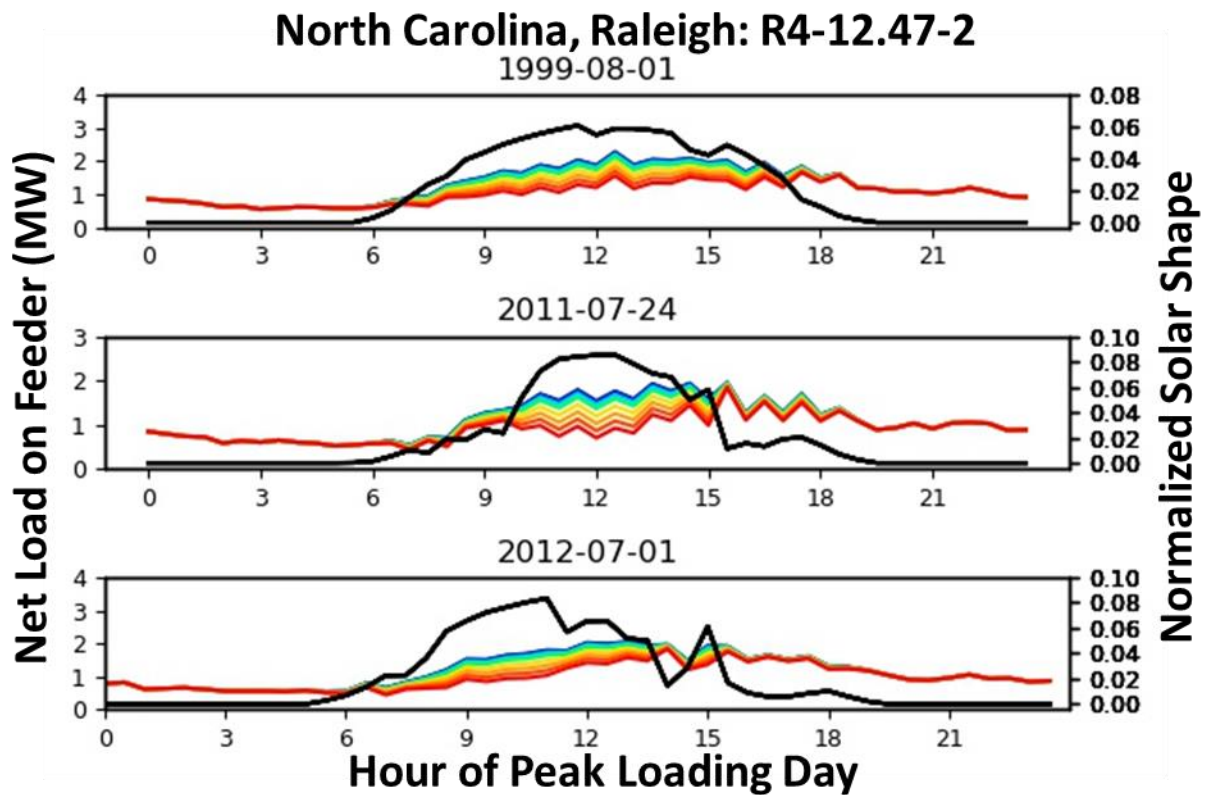
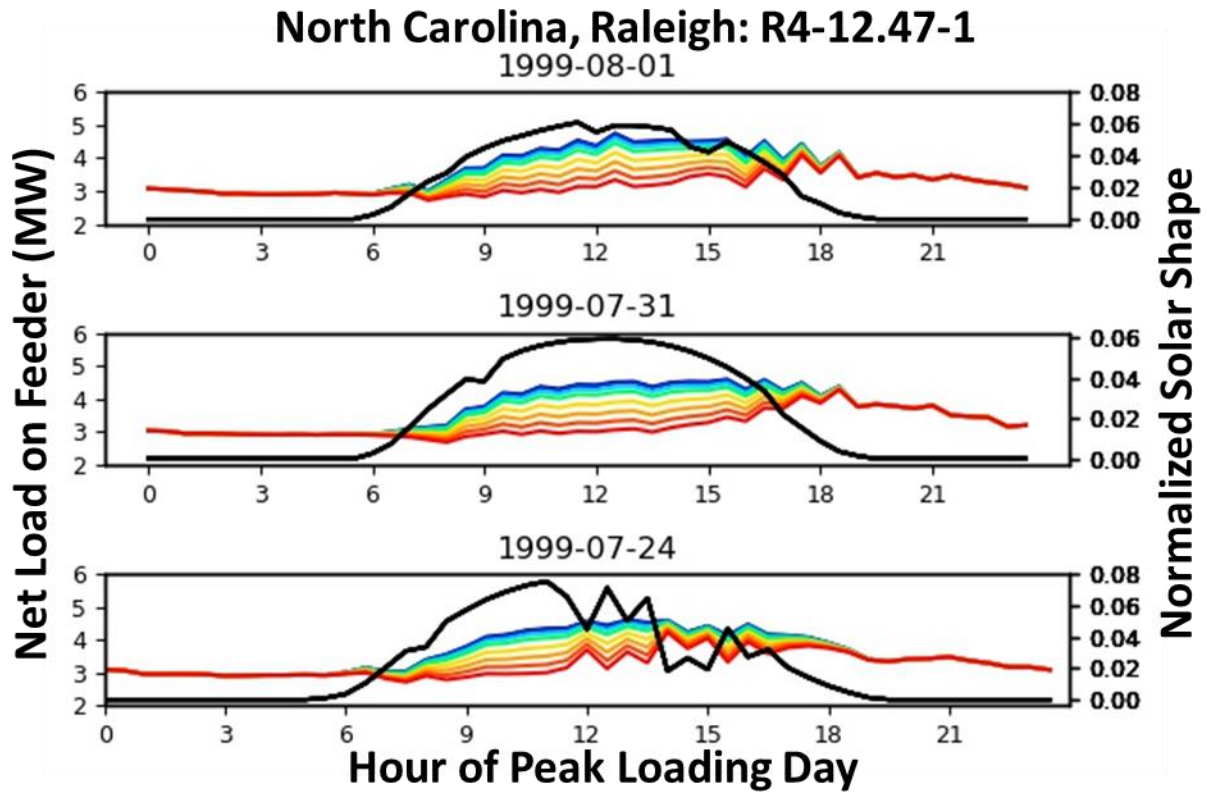
New York, Albany: R2-35.00-1

2016-08-11

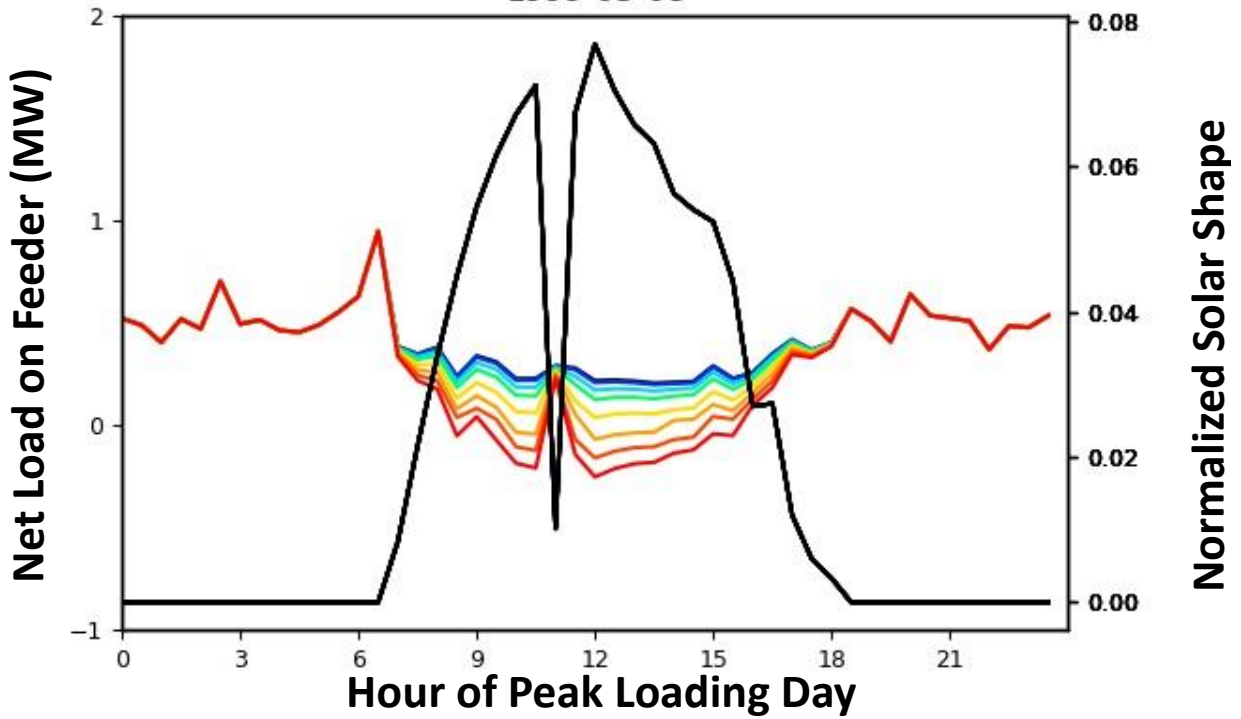




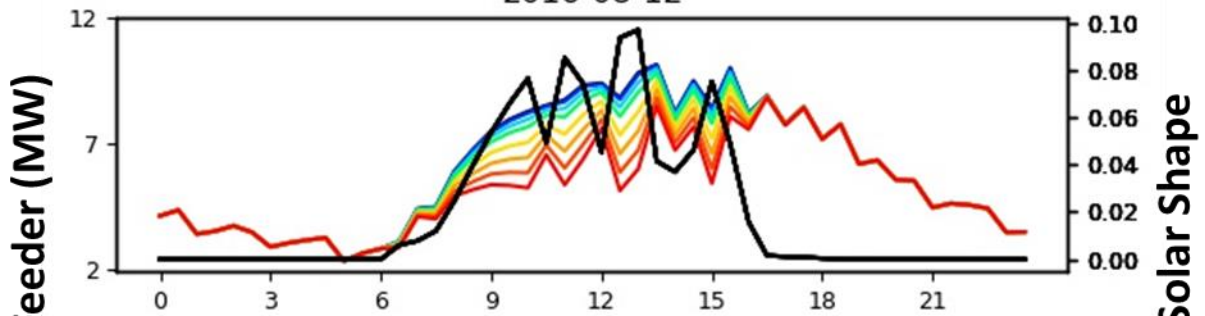




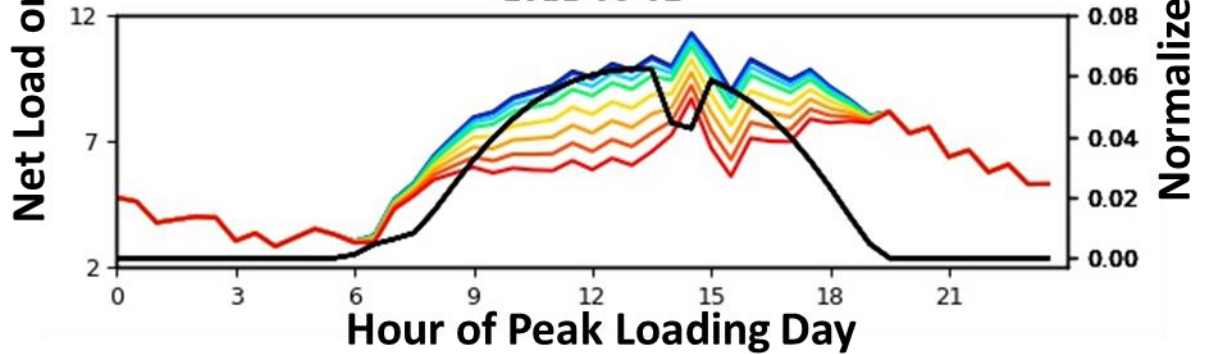
North Carolina, Raleigh: R4-25.00-1
1999-03-08

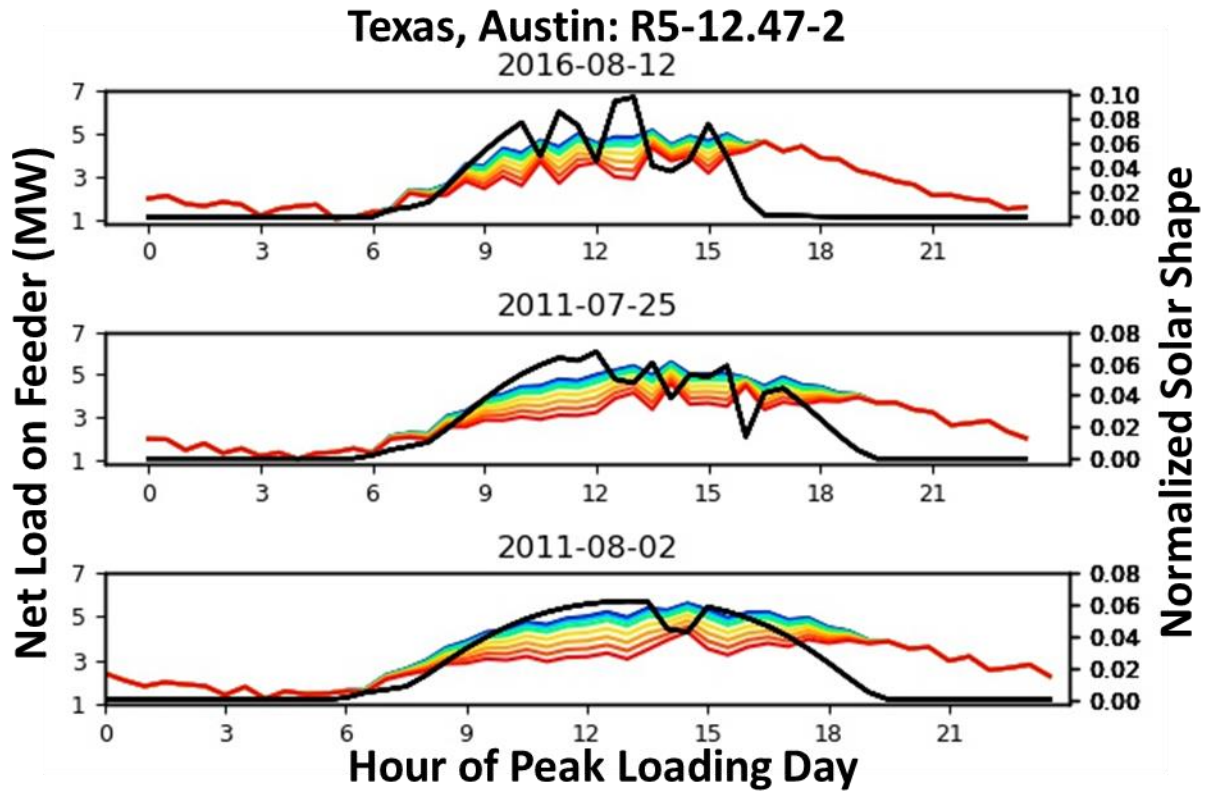


Texas, Austin: R5-12.47-1
2016-08-12

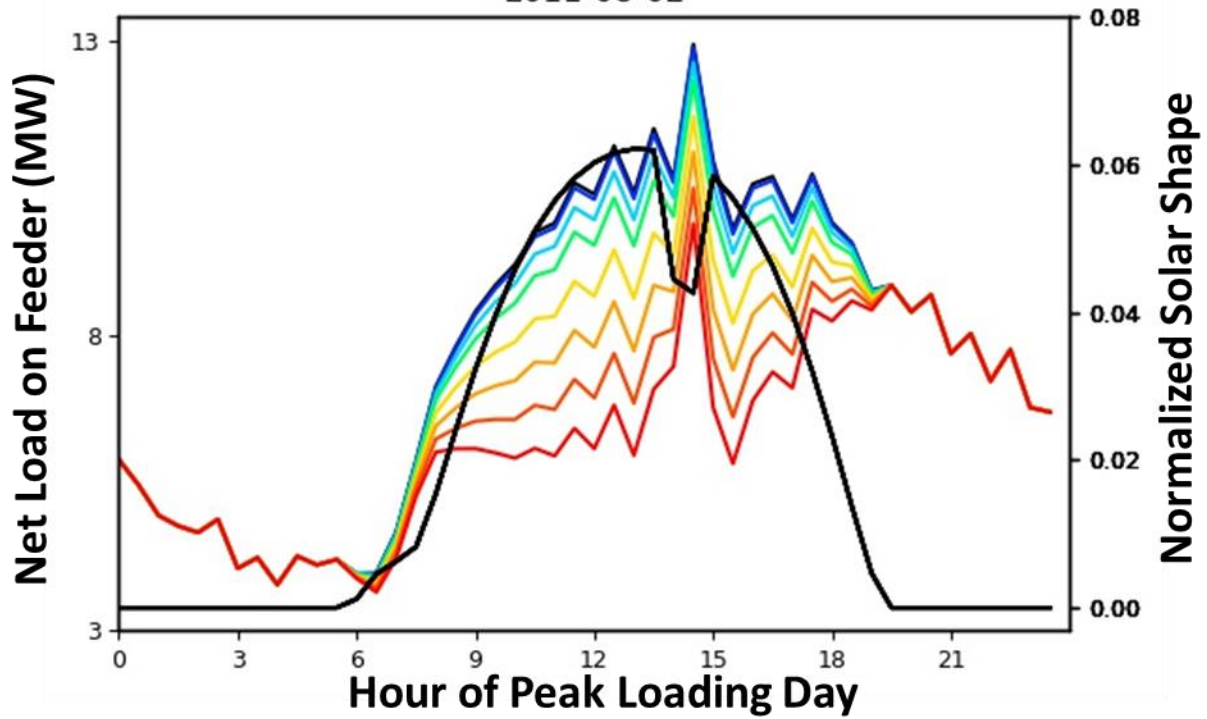


2011-08-02

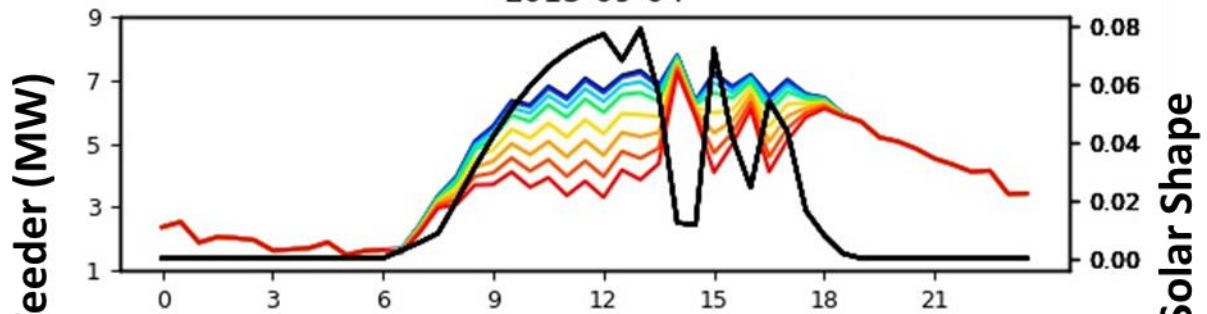




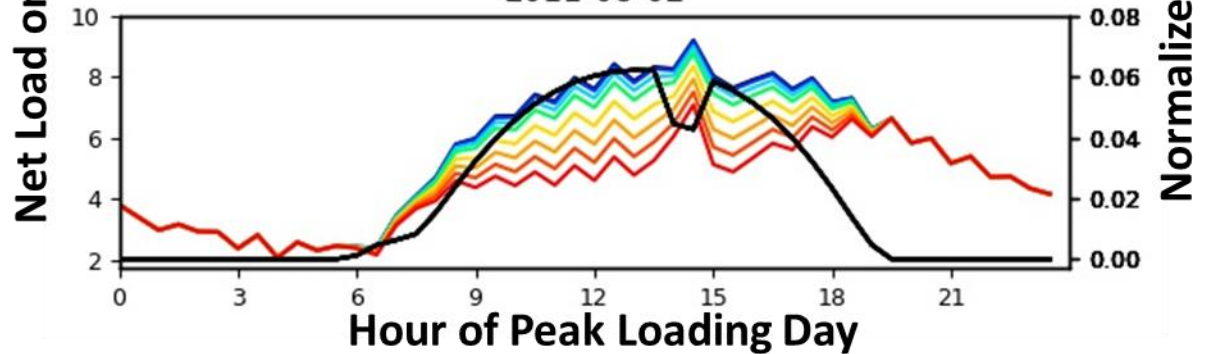
Texas, Austin: R5-12.47-3
2011-08-02



Texas, Austin: R5-12.47-4
2013-09-04

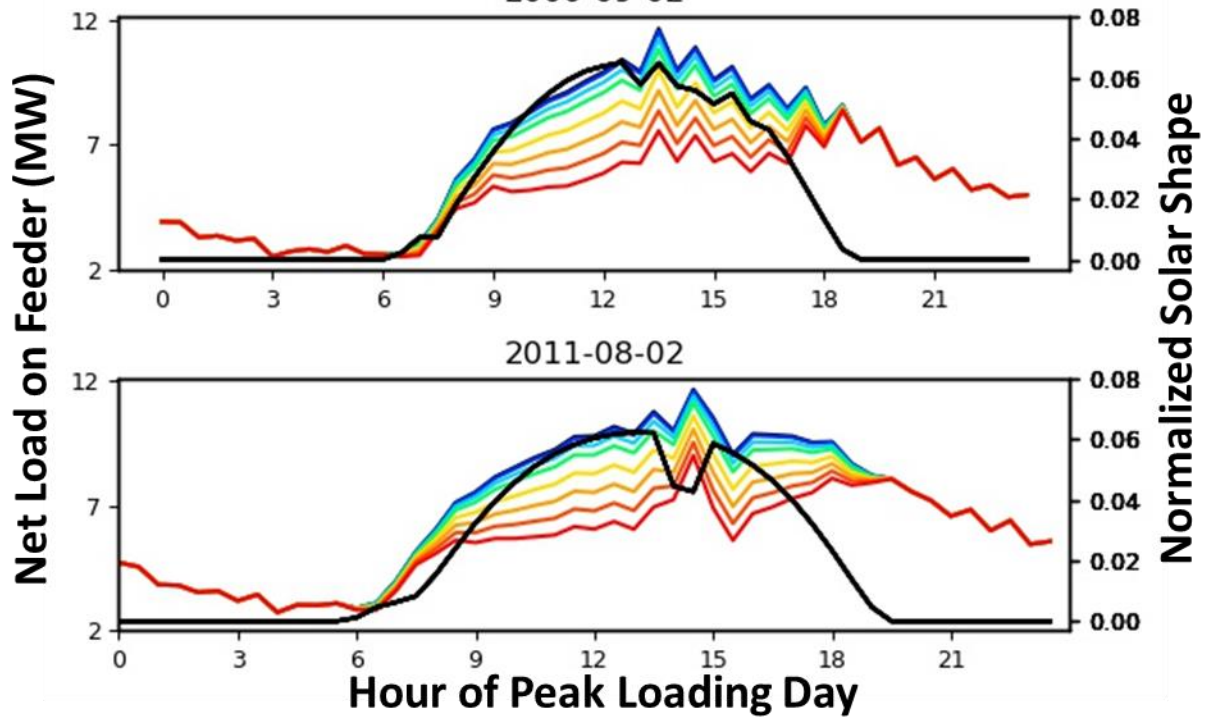


2011-08-02



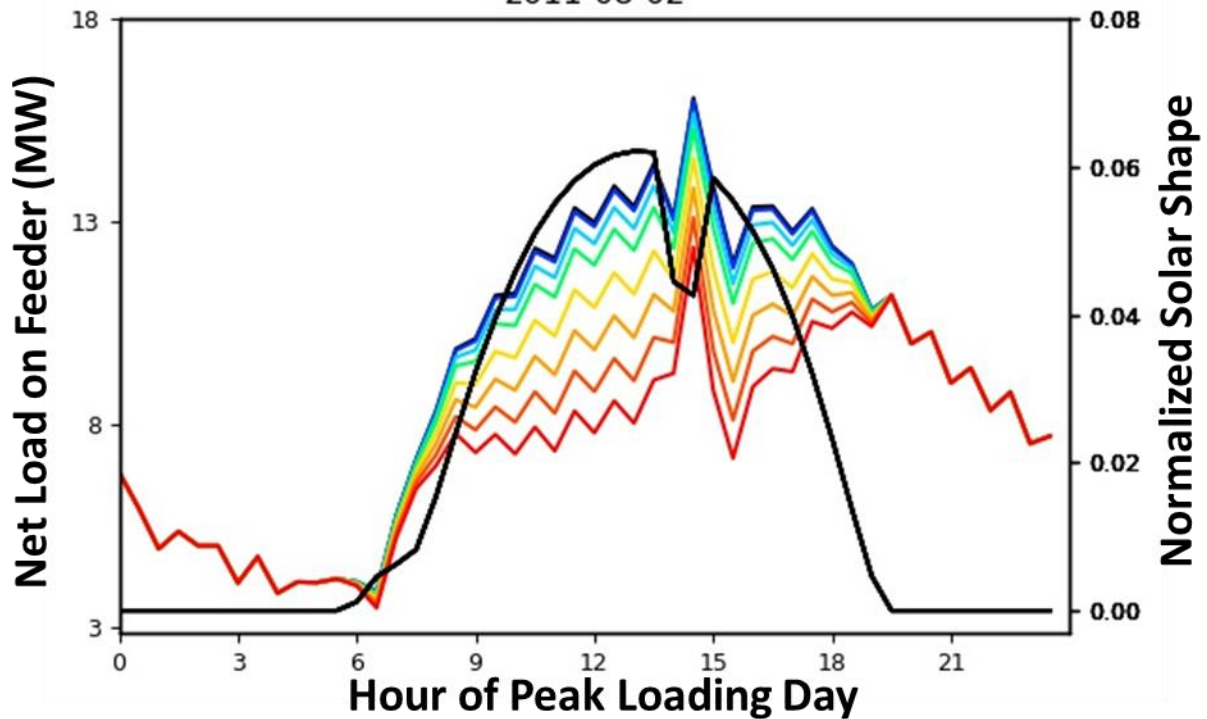
Texas, Austin: R5-12.47-5

2000-09-02

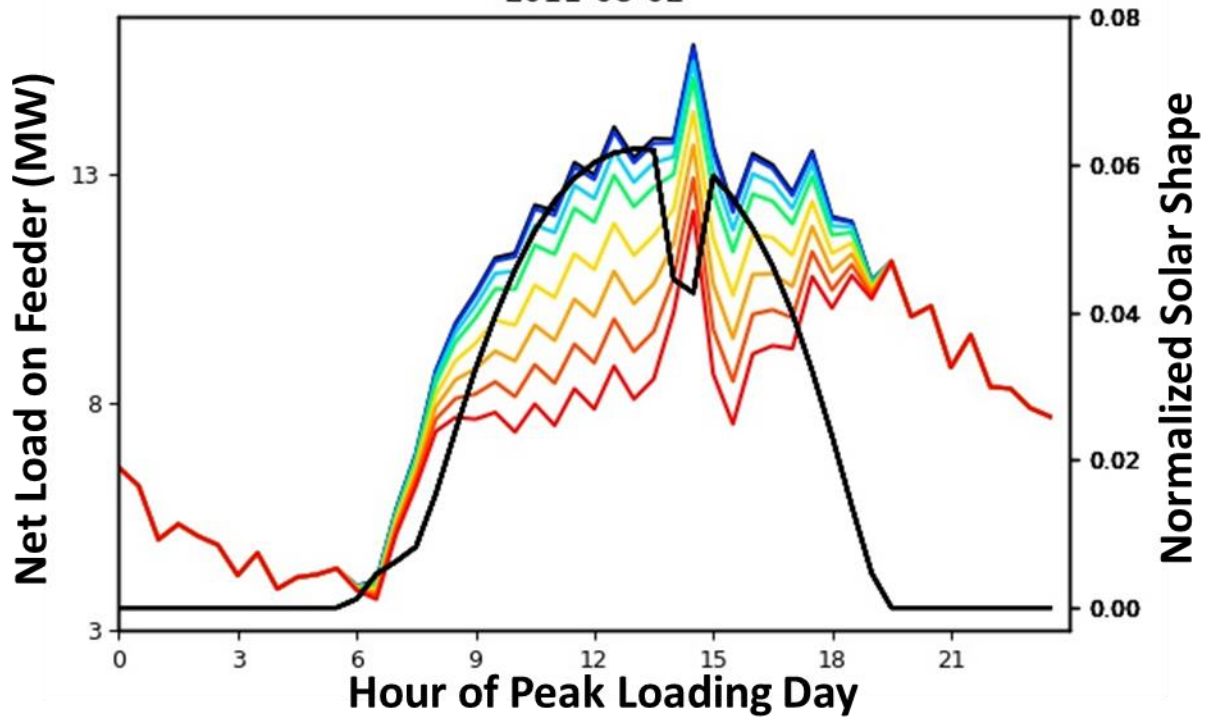


Texas, Austin: R5-25.00-1

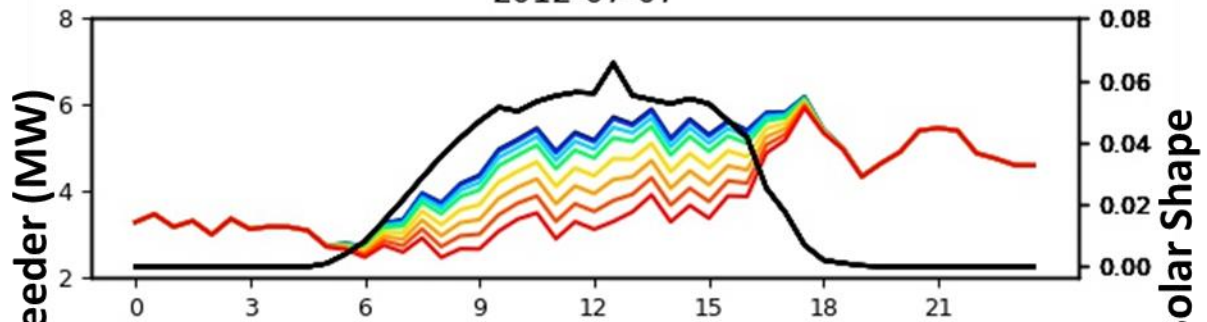
2011-08-02



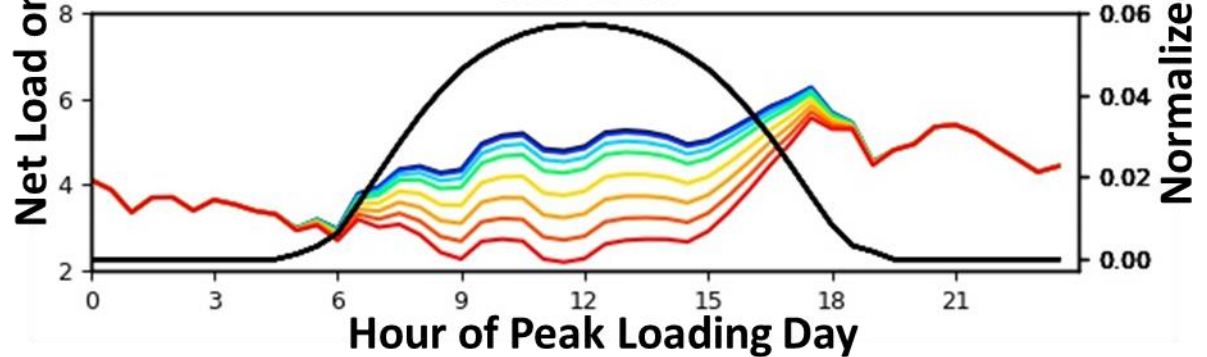
Texas, Austin: R5-35.00-1 2011-08-02

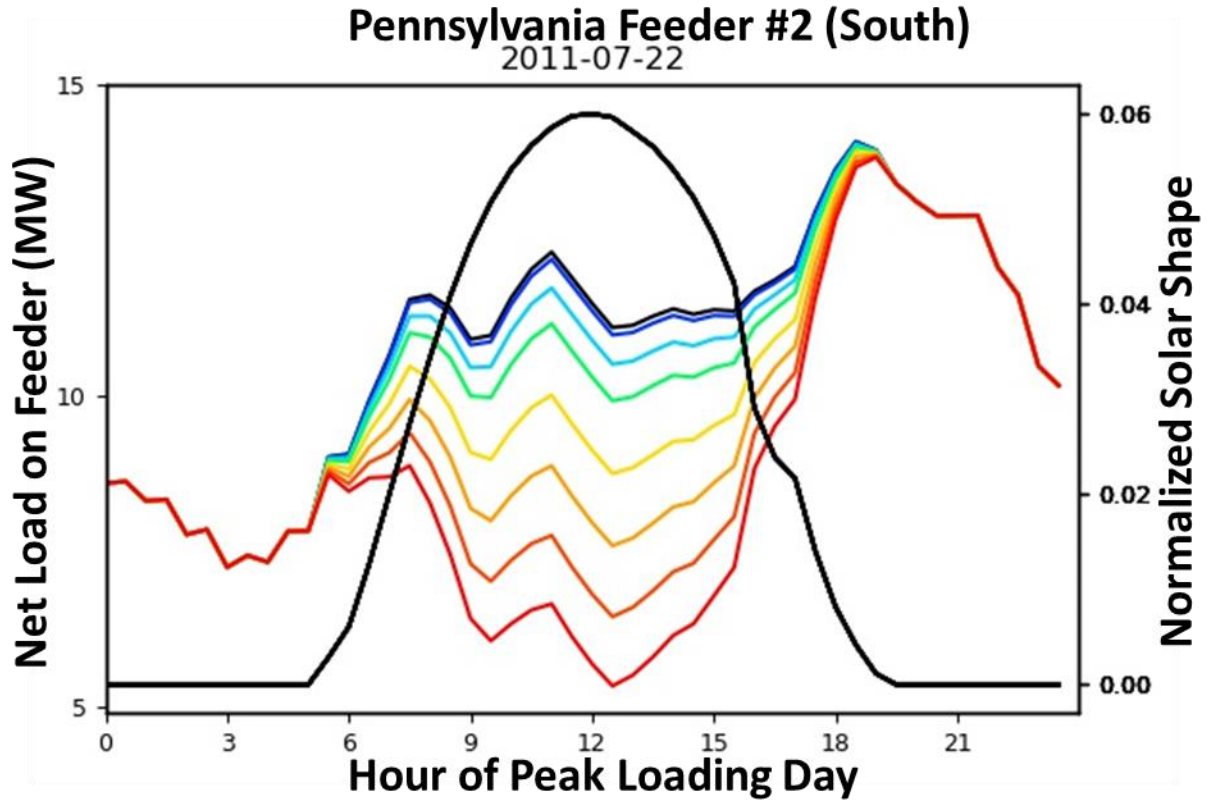


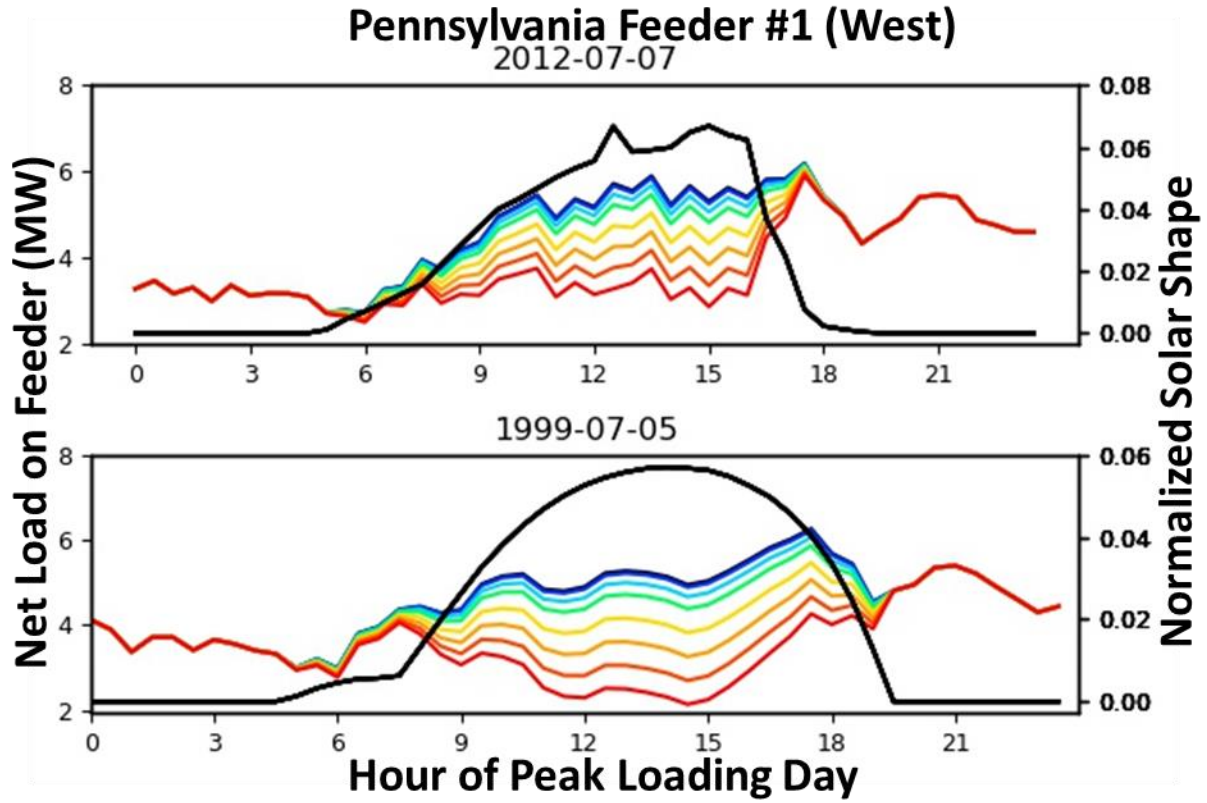
Pennsylvania Feeder #1 (South) 2012-07-07



1999-07-05







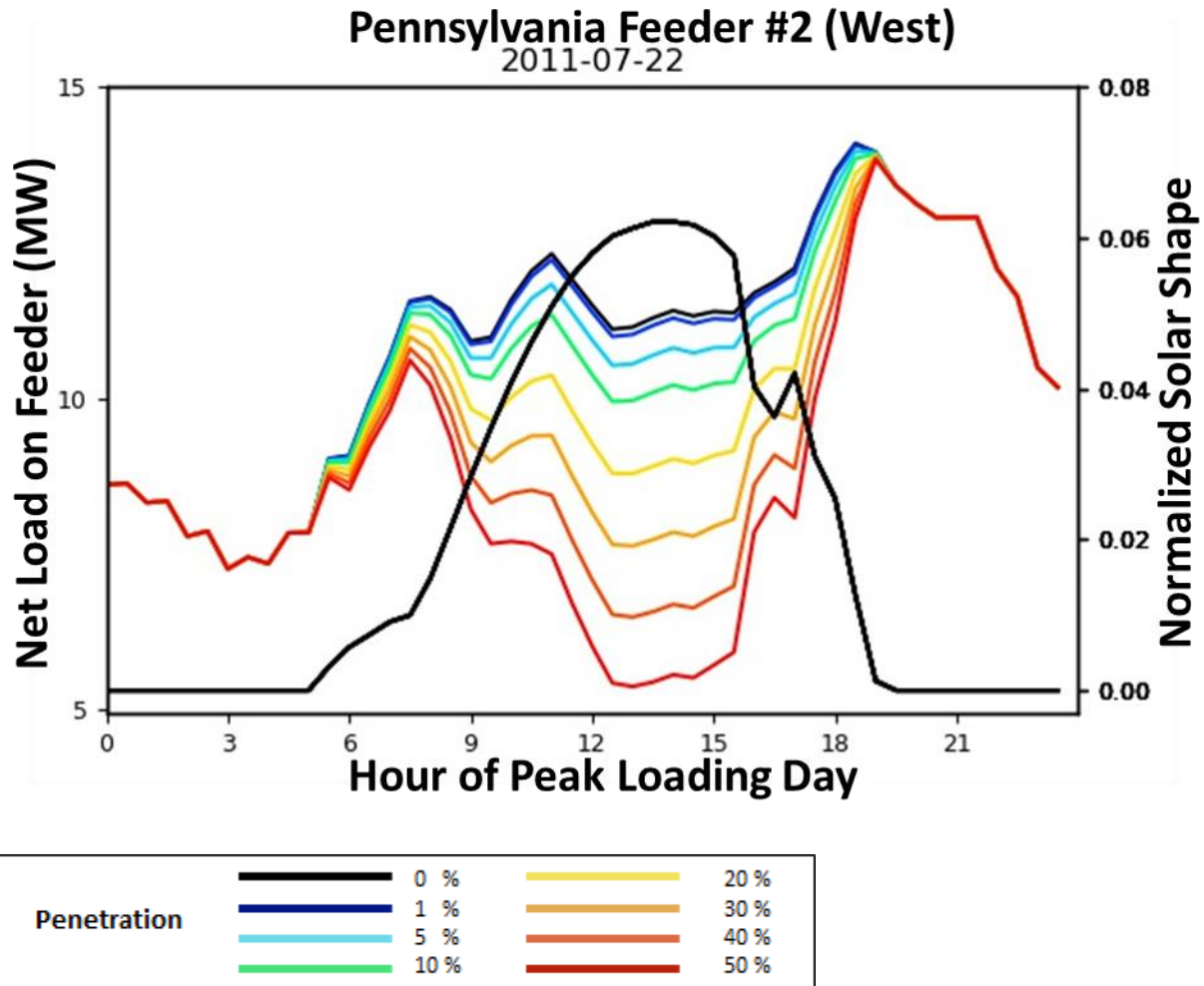


Figure S8: Feeder Net Load on Peak Days. Feeder loads are shown without solar (0% penetration) and for varying amounts of solar. Plots include every day where a peak load event occurred over all penetrations. For example, Pennsylvania feeder #2 experiences a 14 MW peak on July 22nd 2011, July 5th 1999 and July 6th 1999. Solar reduces the load on each of these days. On Feeder #1, cloud events reduce solar's performance on July 7th 2012.

References

- IEC. 2005. "Power transformers-Part7: Loading guide for oil-immersed power transformers (60076-7:2005)." <https://webstore.iec.ch/publication/605>.
- IEEE. 2012. "IEEE Guide for Loading Mineral-Oil-Immersed Transformers and Step-Voltage Regulators (IEEE Std C57.91™-2011)." March 7. <https://ieeexplore.ieee.org/document/6197686>.
- PJM. 2017. "PJM Manual 19: Load Forecasting and Analysis, Revision 32." <https://www.pjm.com/~media/documents/manuals/m19.ashx>.
- Schneider, K P, Y Chen, D Chassin, Dave E, and S Thompson. 2008. *Modern Grid Initiative Distribution Taxonomy Final Report*. Pacific Northwest National Laboratory. http://www.gridlabd.org/models/feeders/taxonomy_of_prototypical_feeders.pdf.